CAPACITY OF AN INFOSTATION SYSTEM

BY JOAN BORRÀS-CHIA

A dissertation submitted to the

Graduate School—New Brunswick

Rutgers, The State University of New Jersey

in partial fulfillment of the requirements

for the degree of

Doctor of Philosophy

Graduate Program in Electrical and Computer Engineering

Written under the direction of

Roy D. Yates

and approved by

New Brunswick, New Jersey

January, 2000

ABSTRACT OF THE DISSERTATION

Capacity of an Infostation System

by JOAN BORRÀS-CHIA

Dissertation Director: Roy D. Yates

An Infostation system consists of a network of wireless ports providing discontinuous coverage. In these coverage zones, the conditions for communication are such that transmission at high bit rates is possible. Consequently, we may be able to download large amounts of information even if the mobile terminals spend little time within coverage.

In this dissertation we define several models for an Infostation system and evaluate the performance in terms of capacity, throughput, and delay. The models we consider are the periodic model, the single-Infostation model, and cellular models.

The periodic model studies the case where Infostations are regularly spaced, such that a probability distribution for the distance mobile-Infostation can be found. With this distribution it is possible to derive the power control policy to maximize the average capacity in the information-theoretic sense, or similarly to maximize the BPSK cutoff rate.

The single-Infostation model looks at what is the maximum amount of data that can be transmitted to an isolated Infostation. We find the throughput when continuously adapting the symbol rate, and the optimum rates and coverage radii

when restricting to a finite number of rates. We also study the effect of varying the modulation scheme.

In the cellular models, we locate the Infostations in a cellular layout, both in one and two dimensions. We find what is the worst-case SIR as a function of coverage and determine possible operating points according to modulation and frequency-reuse cluster size. Next, we model the Infostation as a queueing system with reneging and study throughput and delay. The results show that for one dimension the best choice is the highest level modulation with the smallest cluster size (which gives the smallest coverage area). For two-dimensions there is a trade-off, such that for small loads a fuller coverage is preferred.

We also consider the introduction of Infostations in an existing cellular system, taking advantage of unused excess capacity.

Still using a cellular layout, we analyze the uplink for a static situation, in which the load perceived by the Infostation depends on the area covered. We derive the optimum coverage radius for a given data rate and a maximum throughput constraint. Then we extend the result to the case of two data rates, solving for the corresponding optimum radii that define the coverage areas in which we should use each rate.

Acknowledgements

I am highly indebted to my advisor Prof. Roy D. Yates for letting me participate in long discussions on many topics in wireless communications that have broadened my knowledge on this area. His open mind has changed my whole idea of what research means. I would like to express my deep appreciation also for his guidance, accessibility and patience.

I want to thank my committee members, Prof. David J. Goodman, Prof. Narayan B. Mandayam, and Prof. Christopher Rose of the Department of Electrical & Computer Engineering at Rutgers University, and Prof. Stephen S. Rappaport of the Department of Electrical & Computer Engineering at State University of New York. Their suggestions and comments have helped improve the thesis in content and presentation.

The research environment at WINLAB has been superb, and its human face makes my experience at WINLAB one that I shall really cherish. I want to thank all WINLAB staff, professors and students. Special thanks to Pi-Chun Chen, Paul Hatrack, and Mark Wehle for their encouragement, help and friendship.

I finally thank "la Caixa" fellowship program for giving me the opportunity to study in the United States of America, funding my first two years at Rutgers.

Dedication

To Eulàlia

Table of Contents

List of Tables

List of Figures

Chapter 1
Introduction

1.1 Infostation Concept

Cellular systems today bring with them the promise of "anytime, anywhere" communications. But this ubiquitous availability may become a burden. Voice messaging, email and fax are alternatives that return some control of time and place to the user, which may account for their dramatic growth. Recently, an array of isolated wireless ports called **Infostations** has been proposed [1]. This system is characterized by isolated pockets of high bandwidth connectivity. This "many-time many-where" communication is well suited to messaging and can offer a wide range of useful and economical services. Its high bit-rate connections can deliver information that would be impractical using a voice system with ubiquitous coverage. Unlike voice systems, where the payload is a low delay, constant bit-rate service, such messaging and information systems can often tolerate significant delays. Therefore the payload of interest is often a quantity of bits rather than a bit-rate. This suggests service that is frequent and predictable, though without the need for continuous connectivity. Finally, while voice systems are generally equal in their uplink and downlink traffic, for data and messaging the downlink is likely to be predominant [2–5]. The above considerations lead to a system with isolated pockets (or core areas) of high bandwidth that caters to the mobility and information requirements of users.

Ubiquitous coverage in cellular systems usually is based on statistical criteria. Typically, systems are designed to provide an adequate signal-to-interference ratio (SIR) in most locations (e.g., SIR > 18 dB with probability 0.9). As a result, many locations (typically at the core of each cell) have a channel quality that exceeds this criterion, sometimes by a significant margin. Current systems reduce this "excess quality" through power control, or treat these core areas as a grid of overlaid microcells with reduced channel-reuse distance. Another way to capture this excess capacity would be to increase the data rate, while using the same channel bandwidth. One example of such a utilization could be to switch to a higher order modulation scheme in the core areas. While there has been little incentive for this approach in voice-only systems, messaging applications may justify future consideration of this possibility. A simpler alternative would be to use a portion of the available spectrum to provide high bit-rate services in core locations, using a separate radio and channel. Figure 1.1 illustrates such core areas which could be used to deliver large files quickly with high spectral efficiency and low cost. In the following, we will refer to an Infostation system in general as a wireless communication system characterized by discontinuous coverage and high data rate transmission. The system is composed of fixed radio stations, which we call Infostations, and mobile radio terminals, referred to as mobiles. This definition is very broad and allows a full range of design solutions to adapt the system to different environments and services.

As was pointed out in [1] and [3], these pockets of high bandwidth connectivity could be spaced along roadways, in building entrances, at airports, and in other predictable, accessible locations. Relating them to the "fast food" paradigm, such access options were characterized in [1] as being "drive-through, walk-through and sit-through" with different ranges of Infostation coverage. In absence of "anytime-anywhere" constraints, we show in this dissertation that capacity is maximized by using small pockets of coverage. With proper spatial separation and reduced coverage, the interference conditions are improved, such that universal frequency reuse and higher level modulations become possible. These two characteristics combine, resulting in much higher data rates than those achievable with cellular systems. This spectral efficiency will allow significant transfer of information (e.g. fax, e-mail, voice

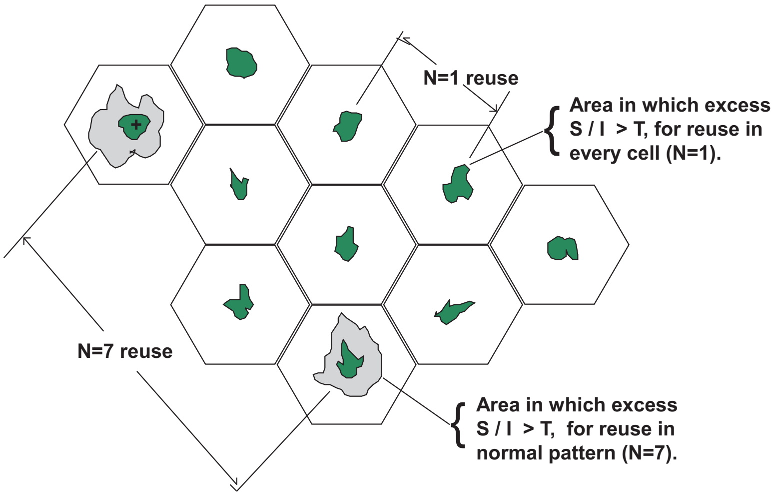

Figure 1.1: Core areas in which excess capacity allows information transfer at a higher rate

messages and large data files) to take place in a few seconds.

Infostations can be relatively simple devices and might be organized in different ways (see Figure 1.2). Individual Infostations on highways, streets and in airports, for example, might function independently, providing specialized gateways to the Internet and accessing remote servers for information and messages. The access between the Infostation and gateway could be wired or dial-up, depending on traffic and latency demands. In particular, the high-mobility application raises issues of latency in retrieving the desired information from the network, and of having time to deliver large files. Along highways, one could enhance the system architecture with "upstream" Infostations at which the vehicle registers and requests information, and "downstream" Infostations which can complete long file transfers and correct errors. Such auxiliary Infostations might possibly communicate with the main Infostation over the radio path, thus avoiding additional connections to the network [6–8]. These possibilities are illustrated in Figure 1.3.

One may consider cases in which Infostations would be integrated into, or coordinated with a ubiquitous, low bit-rate service such as cellular, or with paging or

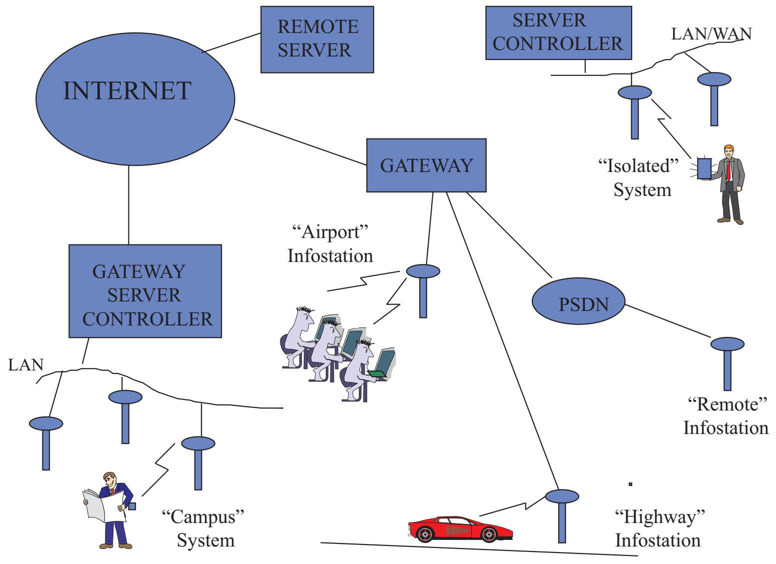

Figure 1.2: Infostation system architecture

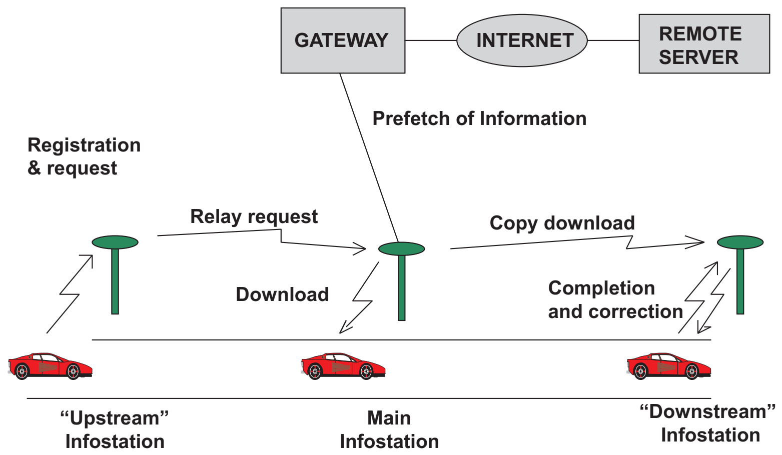

Figure 1.3: Architecture for high-speed application

even wireline services. In addition to the configurations in which the Infostations are independent access ports to the Internet, geographic clusters of Infostations could home on local controller/servers, which would provide "campus" services in addition to Internet access.

Similarly dispersed or clustered groups of Infostations could be organized into "isolated" systems, with controller and server functions, but without Internet access. Applications in this category include physical security (e.g. building access), financial security (e.g., ATM and credit card transactions), access to private LANs, and location dependent services (e.g., maps and advertising). The very high bit rates (and low cost per bit) of Infostations could create opportunities to deliver new wireless information services, and a single set of equipment and protocols would provide different applications in different environments [6, 9].

While radio resource management in cellular systems has received a lot of attention, this new system concept of isolated wireless ports requires renewed and possibly different approaches. Key issues that arise in designing Infostations for supporting high-mobility users include multiple access technologies, radio design, coverage and layout, guarantee of achievable payloads, and algorithms for power control and handoffs. In this thesis, we want to identify and analyze those issues that are crucial to the successful design of a system of Infostations.

1.2 Issues in Radio Design for Infostations

Due to the high data rates and the low-cost terminal envisioned, our primary focus is on an Infostation radio channel separate from cellular or conventional PCS channels. Mobile terminals costing few dollars could foster new mass markets for applications delivered by wireless credit cards, electronic badges and other small devices capable of short range wireless communications. Advances in cost, miniaturization and power consumption will be required to realize the full potential of simple wireless terminals

[7]. We also anticipate that Infostations will serve high-end mobile terminals such as laptop computers, facsimile terminals, etc.

For all applications, the radio transmission system from the Infostation to the mobile will have to be capable of transporting variable data rates up to several megabits per second. Under the premise that in many situations the mobile user is not a source of large amounts of information, the communications from the mobile to the Infostation can be at a lower data rate. This suggests that a radio system with asymmetric transmission rates may be a good candidate for the family of simple terminals. A possible approach is to use time division duplex transmission with a simple amplitude modulated downlink and an uplink using modulated reflection, also known as *backscatter* [10–12].

To adapt to multiple situations, Infostations may provide rings of coverage having different data rates. Data rate and framing issues also include the need to transmit large files quickly for the "drive-through" case, allow multiple access for the "sit-through" case and conserve energy for a "badge" configuration. The available bit rate on the downlink channel will depend on the distance between the terminal and the Infostation, increasing as distance decreases. As an illustration, we show, in Figure 1.4, the case where several bit rates may be available for transmission.

In addition to the radio transmission technique, Infostations require new designs throughout the protocol hierarchy. This requires study of all OSI layers, from the application layer to the physical layer, and the introduction of procedures for the different modes of operation discussed above ("drive-through, walk-through and sit-through"). Issues in the physical layer include identifying minimum bit-rates for system ID and synchronization, and allowing terminals to select appropriate bit-rates depending on the file sizes to be transmitted, the mobility of the terminal, the network environment, and the latency constraints of the application. The choice of MAC protocols will depend on the type of Infostation. The "drive-through" Infostation typically deals with very few simultaneous users within the Infostation's range

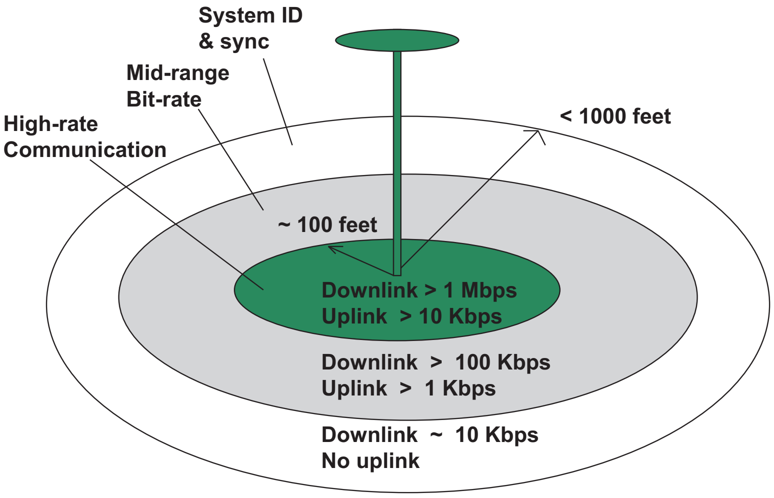

Figure 1.4: Illustrative ranges and bit-rates for Infostation zones

while a "sit-through" situation is closer to a wireless LAN environment. In addition, there may also be a need to prioritize users depending on their mobility, such as in an airport terminal where there may be both "walk-through" and "sit-through" users. Further, since user requests may require the Infostation to access remote servers (and incur additional delays), there may be a need for an upstream registration and request, and a downstream completion process. This requires coordination among groups of Infostations.

Issues in the data link layer deal with framing, flow control and connection management from the time when the terminal first senses the Infostation's presence to the time when the terminal leaves the coverage area. The design must reflect varying bit-rates transmitted during passage through an Infostation coverage area like the one illustrated in Figure 1.4. Even in coverage areas near a base station, high terminal velocity poses challenges to efficient, reliable information transfer. Variations in vehicle speed influence the rate and duration of radio fades [13]. Consequently, it would be useful to adopt protocols that modify packet sizes and modes of error correction in order to match the data link protocol to the changing properties of the transmission path [6]. Challenges in the transport layer design include deferred and intermittent connections and limited capacity to transmit acknowledgments from terminals with simple radios incorporating backscatter transmitters. Issues in the application layer call for handling interactions between the client and server when a communication session consists of sporadic intervals of high bandwidth connectivity. When a file cannot be received in its entirety from the current Infostation, the remaining portion will have to be made available at the next Infostation the terminal encounters. This requires prefetching information from remote servers and local caches to reduce latency [8,14]. In addition to data-on-demand, there may also be other modes of data dissemination such as publishing [15], which require clients to filter relevant information locally.

Our goal in this dissertation is the definition of several models for an Infostation system and the performance evaluation in terms of capacity, and in some cases delay, using different approaches of adaptive power control, modulation and coding schemes. The motivation is to set a ground of theoretic results to help in the design of future prototypes.

1.3 Models

The definition of an Infostation system gives plenty of room for design choices to tailor the system to different environments and services. That is why we will consider several models with varied characteristics. For each of them, performance measures like capacity or throughput will be used to identify the best design choices. We now describe several parameters which are important in choosing appropriate models.

- **One or Two dimensional.** A first classification comes from considering the movement of the mobile to be either one-dimensional (1D) or two-dimensional (2D). 1D models are simpler to analyze and, although they greatly constrain the possibilities of mobile terminal movement, they can faithfully represent real cases, such as cars on a highway passing through toll booths, exit ramps, or traffic signals, where the Infostations might be located.

2D models are more accurate for those cases when the mobile terminals are not constrained in their movements. This kind of model uncovers more clearly several problems of network management like false registrations (the mobile registers but leaves coverage right away) or multiuser operation (several mobiles registered at a given time).

- **Single user/Multiple users.** A single user model will avoid the problems of user division and fairness in resource distribution, allowing us to concentrate on the effect of other system variables. Although it may seem highly idealized, a single user model is appropriate when there is a marked physical spatial division between the users.

  The multiple user case introduces several problems. One problem is how to handle the mobile's registration: what kind of random access to use, how often to register, or whether to use in-band or out-of-band signaling. Another problem is how to schedule data transmission to the mobiles once they are registered, and how to distribute the power. The solutions will depend on the mobility model and user density. We will have to take into account both the performance and the complexity of these solutions. A new concept of fairness will have to be used, as giving equal service to everyone is not the premise anymore.

  The multiple access scheme of choice will probably be time division, since there is negligible interference with neighboring Infostations and therefore no need for frequency reuse nor for spread spectrum signal separation for multiaccess. In spite of this, the use of moderate processing gain spreading may be advisable if we use an unlicensed band. Spreading in this case is not for user separation but for interference reduction.

- **Mobility model.** Depending on the real situation we are trying to represent, we can consider different mobility models. The analytical complexity also has to be taken into account. One important point in choosing the mobility model is whether the mobiles will be willing to approach the Infostation to get or improve service. As an alternative, mobiles may not care or even know about Infostation locations, resulting in a mobility process that is independent of Infostation locations.

  A simple one-way constant-speed model can be a starting point for modeling vehicles on a 1D highway. If we use simulation, more complex car-following models exist in the literature [16, 17].

  For 2D, we can consider a fixed (no mobility) multiple user location distribution (sit-through case). In this case, users not only go to the Infostation to obtain service but also stay for a while. Or we can use a single-user constrained mobility (for instance, linear) to see how to optimize coverage in the absence of interference. When we don't have any idea about the mobility, a multiuser random mobility model (Brownian motion or random walk) may be appropriate. We may also use more complex models for simulations, with user accumulation areas, where the Infostations should probably be located. A Manhattan model could represent an intermediate model that may be analytically tractable.

- **Downlink/Uplink/Both.** The basic service we want to consider is a downlink data transmission, with one or more relatively high rates, and a nominal uplink for registration purposes only. A more symmetric situation can also be considered, to account for the case when mobile power is not so scarce.

- **Adaptability.** We refer to adaptability in the sense of being able to change the power, modulation, bandwidth, and/or coding scheme responding to changing channel conditions. The most simple system will be fixed (non-adaptive), and as such it will have to be tuned to the best combination of parameters. Note that the uplink can be different from the downlink in all aspects.

Next, we can consider the effect of introducing adaptability in one factor at a time. The complexity of this feature needs to be compared with the performance gains. Also we can contemplate combining adaptive parts to approximate the ultimate bound given by capacity calculations.

In any case, adaptability will translate to different bit rates at different distances.

- **Mobile location and radio channel quality.** In practice, the mobile location is unknown to the Infostation. The mobile needs to register to access the Infostation and messages have to be exchanged indicating the measured link quality. Based on these measurements, it can be decided whether to transmit or to wait for better conditions. The process of registration and measurement, though, may complicate the analysis unnecessarily. It is usually convenient to assume, in theoretic models, that there is a perfect knowledge of location and that the channel quality is determined by distance attenuation. In this way, there is no need for registration and the Infostation will be able to decide when is the best time for transmission and what resources to allocate. This approximation can be later refined with more complex channel models and multiple access schemes. Nevertheless, the assumption that the position is known will give a bound on system performance.

- **Infostation location.** Another classification comes from considering either isolated Infostations or groups of them. If we are considering an isolated Infostation, we would like to maximize the data transfer through that Infostation. On the other hand, we can consider a "group" of an infinite number of Infostations, laid out periodically. In this case the fact of knowing that eventually a mobile will get to another Infostation may change the strategy of resource allocation.

Other classifications or simplifications of the models come from considering certain choices of modulation type, frequency band, power supply in the mobile terminal, mobile speed, Infostation coverage range, directive antennas, targeted services, and capture.

1.4 Performance Measures

In cellular systems the performance measure is usually the number of users the system can support with a specified quality of service. With the introduction of new services, the ability to deal with different rates and qualities of service is required, and the performance measures are not as straightforward.

In an Infostation, we may have the possibility of single-user operation. In this case the measure of performance will either be a payload (amount of bits per Infostation) or a data rate (bits per second). For data services, where delay is of secondary importance, a payload per Infostation crossing seems to be the best indicator of performance. Nevertheless, there are situations where a data rate (actually an average rate) is more suitable to make the results independent of mobile speed, as we will see in the models of Chapter 2. Also, a data rate will be the performance measure in a sit-through Infostation, in which the connection can take as long as the user is willing to stay under Infostation coverage.

In the multiuser case, we will add to the previous performance measures the delay in getting service once in the coverage area. Also we will have a certain outage probability, that is, probability of being within coverage but not being granted service before the coverage area is left. If the user has to visit several Infostations before the messages are completely delivered, we will have to account for delay from the time a message is created until it is finally delivered. Even though messaging services do not have stringent constraints on delay, we will want to upper bound this delay to ensure that the service is useful.

1.5 Scope and Organization of the Dissertation

In this dissertation we will study the following models:

1. **Periodic model** (Chapter 2). In this one-dimensional model, we assume a single-user with a constraint on average power that moves with constant speed along an infinite line. Infostations are distributed periodically along this line. We find the optimum power allocation that achieves capacity in the information-theoretic sense. We also consider the optimum power allocation that maximizes the BPSK cutoff rate.

2. **Single Infostation model** (Chapter 3). This a two-dimensional model that nonetheless is seen as having only one dimension because the single user moves in a straight line. We determine the maximum amount of data that can be transferred to a user passing near the Infostation when symbol rate adaptation is used. We also calculate the best single rate and the best three rates in terms of maximum data download, and the corresponding associated coverages. Next we account for the effect of having two dimensions by assuming a random minimum distance to the Infostation. We close the chapter by looking at the effect on coverage and throughput of having several modulation schemes available.

3. **Cellular models** (Chapters 4, 5 and 6). These models use a cellular layout for locating Infostations. The motivation for these models is to allow Infostations to take advantage of existing cellular infrastructure. Unlike cellular systems, though, they don't have ubiquitous coverage. The following cases have been studied:

    - **Infostation Overlays in Cellular Systems** (Chapter 4). We first analyze the downlink SIR as a function of coverage radius to cell radius ratio, both in one and two dimensions. Then we model the Infostation as a queueing system with reneging, and we analyze the system performance in terms of throughput and delay, for specific mobility models.

- **Cellular Excess Capacity for Infostations** (Chapter 5). We show how to deploy an Infostation system reusing cellular frequencies. Infostations' locations and power levels are chosen to generate tolerable interference to the cellular system, thus allowing the simultaneous operation of both systems. Infostations may then pool the available frequencies to provide high data rate transmission.

- **Uplink Access** (Chapter 6). A static situation is assumed, with users accessing the Infostation through a random access algorithm. The access load is controlled by adjusting the coverage radius (only users within a certain area will try to access). We first find the SIR expressions for uplink, and then calculate the optimum coverage given a single data rate and a constraint on the maximum load. We also show the improvement when having the possibility to use two data rates, with two concentric coverage rings.

Chapter 2
Periodic Model

There are situations in which the mobiles have no alternative but to pass through the Infostation core coverage area. One possibility is to locate the Infostations in places where the mobiles would pass anyway. This is the case of Infostations in highway toll booths or in building entrances. In these situations, we can see the mobile trajectory as being locally linear, and a one-dimensional (1D) model will suffice. Using this paradigm, further simplifications or assumptions help us analyze the system. The periodic model comes from assuming an infinite number of Infostations on a line, at regular intervals. A highway with an Infostation every few miles inspires this case. The objective here will be the maximization of data rate given a certain average power constraint.

2.1 Model

The system model consists of an infinite line where there are an infinite number of Infostations, equally spaced one from the next by a distance $2r$ units. The Infostations are located at a height of h units. We assume $r \gg h$. We will see that an efficient design will result in coverage areas such that we can neglect the effect of interference from adjacent Infostations. Alternatively, we approximate a lightly loaded system by a single user model in which only one Infostation transmits at a time. Thus, we assume a single mobile terminal that travels from $-\infty$ and goes to ∞ at a constant velocity (see Figure 2.1). The mobile terminal antenna is considered to have a negligible height.

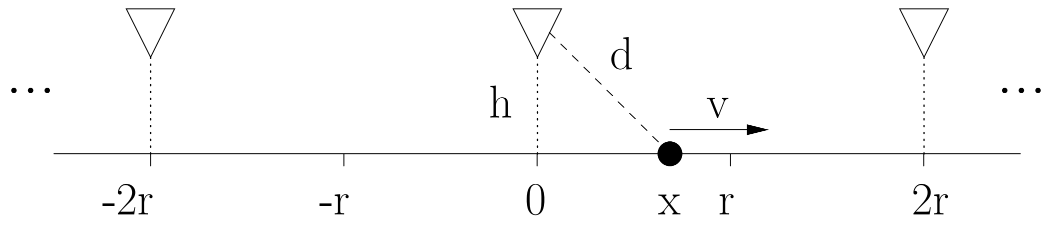

Figure 2.1: Infostation model

As the model is periodic, we can just consider a single period, say from $-r$ to r. Further, the conditions from $-r$ to 0 are identical to the ones from 0 to r, such that we can focus on half a period, say from 0 to r, with an Infostation located at point 0. We will call x the distance from the mobile to the bottom of the Infostation, and d the distance from the mobile to the top of the Infostation, where the antenna is located.

Given that the velocity of the mobile is constant, the position of the mobile at an arbitrary instant in time has a uniform probability distribution

$$\pi(x) = \begin{cases} 1/r & \text{for } 0 \leq x \leq r, \\ 0 & \text{otherwise.} \end{cases} \tag{2.1}$$

The Signal-to-Noise (SNR) ratio depends on the distance between the antennas and, assuming that h is fixed, it is a function of x. This SNR depends on such parameters like antenna gains, noise power, average transmitted power, and receiver design. To characterize all these parameters together and to focus on the effect of distance, we assume here that we know the value of SNR below the antenna ($x = 0$) when the transmitter is using power $\bar{P}$. We call this value α. The SNR at a certain distance when using constant power $\bar{P}$ is

$$\overline{\mathrm{SNR}}(x) = \alpha \left(\frac{h}{d}\right)^n = \alpha \left(\frac{h}{\sqrt{x^2 + h^2}}\right)^n \tag{2.2}$$

where n is the path loss exponent. Of course, $\overline{\mathrm{SNR}}(0) = \alpha$. If we don't specify otherwise, we assume a line-of-sight case with free-space propagation, and therefore we use a path loss exponent $n = 2$. Other cases can be considered obtaining similar results, although not necessarily with closed-form expressions. For $n = 2$, the SNR expression becomes

$$\overline{\mathrm{SNR}}(x) = \frac{\alpha h^2}{x^2 + h^2}. \tag{2.3}$$

Using this model, we will find the power allocation to maximize the average capacity. Anticipating the results, we will show that there is a certain *threshold distance* from the Infostation, beyond which no communication takes place. Therefore, the small coverage area of the Infostation is not a physical limitation given by propagation loss but a self-imposed limitation that allows the maximum average capacity to be attained. The interpretation of this fact is that power is saved for the epochs when the channel conditions are good (the mobile is near the Infostation), because in these epochs the reward in terms of capacity is much larger. This effect also appears when maximizing the BPSK cutoff rate instead of capacity, although the power profile is different. Finally, suboptimal solutions with an on-off power profile show that very good results are obtained with less complex policies if the idea of threshold distance is preserved.

2.2 Capacity and Optimal Power Gain

At a given distance x, we have an AWGN channel. The Shannon capacity therefore is given by [18]

$$C(x) = \frac{1}{2}\log_2(1 + \mathrm{SNR}(x)). \tag{2.4}$$

As the mobile can be at any position $x \in [0, r]$, capacity can be defined as the weighted sum (integral) of the capacities associated with every possible position. Hence, this average capacity is

$$C \triangleq \int_0^r C(x)\,\pi(x)\,dx. \tag{2.5}$$

In [19], this result is stated as a theorem and a proof is given that any rate $R < C$ can be achieved with arbitrarily small error probability if the state of the channel (in our case, mobile location) is known and adaptive coded modulation is used. The key requirement of the proof is that the variation of the radio channel be described by a renewal process. Note also that the average capacity is an asymptotic result. In our context, this means that the average capacity can be achieved after an infinite number of Infostation visits.

So far we have assumed a constant transmitted power. Let's further assume that the Infostation uses side information about the mobile position, x, to adjust its transmitted power, $P(x)$. Consider that this transmitted power is of the form

$$P(x) = \bar{P} \cdot g(x) \tag{2.6}$$

where $\bar{P}$ is the average power, which is fixed, and $g(x)$, which can be seen as a power gain, has a unit average. Now from equations (2.3) and (2.6), the expression for the SNR at position x becomes

$$\mathrm{SNR}(x) = g(x)\frac{\alpha h^2}{x^2 + h^2} \tag{2.7}$$

Note that here $\mathrm{SNR}(0)$ is not necessarily equal to α.

Accordingly, the capacity at distance x becomes

$$C(x) = \frac{1}{2}\log_2\left[1 + g(x)\frac{\alpha h^2}{x^2 + h^2}\right]. \tag{2.8}$$

The average capacity will be given by the maximum over all the possible choices of the power gain $g(x)$

$$C = \max_{g(x)} \int_0^r C(x)\pi(x)\,dx\,, \tag{2.9}$$

such that

$$\int_0^r g(x)\,\pi(x)\,dx = 1 \tag{2.10}$$

Finding the power gain $g(x)$ that maximizes the average capacity C is an optimization problem of a functional with equality and inequality constraints. The derivation can be found in Appendix A. The result is that the optimal power policy is

$$g(x) = \begin{cases} \dfrac{x_c^2 - x^2}{\alpha h^2} & \text{for } x \leq \min(x_c, r), \\ 0 & \text{otherwise,} \end{cases} \tag{2.11}$$

where x_c is a constant determined by the constraint in equation (2.10). For $r > r_{\min} = \sqrt{\frac{3}{2}\alpha h^2}$ we have that $x_c < r$. In this case x_c can be interpreted as a threshold distance for communication and can be expressed as

$$x_c = \left(\frac{3}{2}\alpha h^2 r\right)^{1/3}. \tag{2.12}$$

When $x_c > r$, the expression changes to

$$x_c = \left(\alpha h^2 + \frac{r^2}{3}\right)^{1/2}, \tag{2.13}$$

but then x_c has no physical interpretation because we have full coverage, with non-zero power gain up to r. For practical values of $\bar{P}$ and h, we will see that $r \gg r_{\min}$. Thus, we focus on the case $x_c < r$.

The average capacity for the case $x_c < r$ can be shown to have the closed-form expression

$$C = \frac{x_c}{r \ln 2} - \frac{h}{r \ln 2} \arctan\left(\frac{x_c}{h}\right). \tag{2.14}$$

Let's see some examples giving values to the parameters. Table 2.1 shows two examples for $r = 1000$ m and $h = 10$ m. The transmit power allocations are presented in Figure 2.2, as a function of the distance from the bottom of the Infostation. Note that the power is normalized by the average power $\bar{P}$, such that the area under the solid lines in Figure 2.2 is the same for the two cases, and is equal to the area under the dotted line, which represents a constant power allocation. We can also see in

α (dB)	x_c (m)	C (bits/symbol)
30	531	0.744
20	246	0.333

Table 2.1: Threshold distance and average capacity for $r = 1000$ m and $h = 10$ m

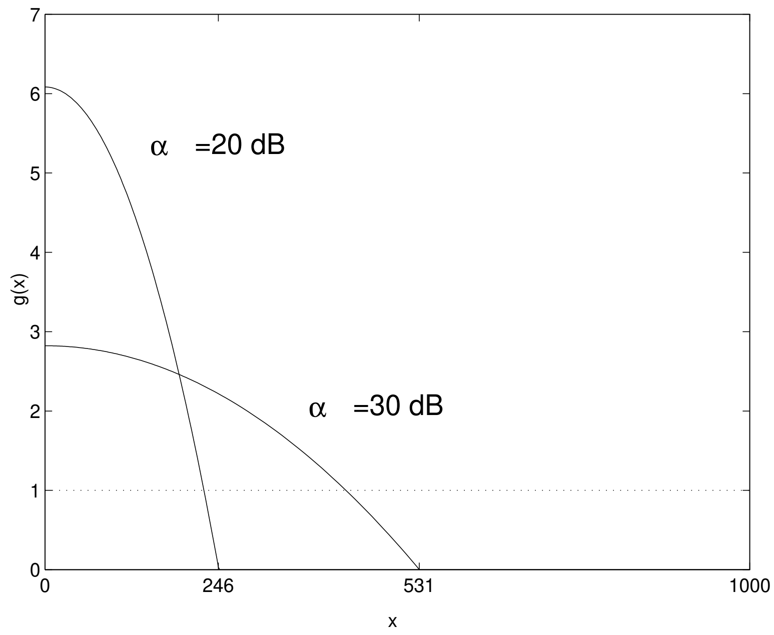

Figure 2.2: Optimal power allocation as a function of distance, for the Infostation model with parameters $h = 10$, $r = 1000$ and $\alpha = 20, 30$ dB

Figure 2.2 that the optimal power gain is maximum at $x = 0$, and then it decreases as x increases until it becomes zero at the threshold distance x_c.

Analogously, Table 2.2 and Figure 2.3 show two examples for $r = 10000$ m and $h = 10$ m. The longer cell radius results in a higher maximum power gain and relatively smaller threshold distances.

We have plotted in Figure 2.4 the "instantaneous" capacity versus the distance. As we can see, the spectral efficiency keeps decreasing to zero as we move away from the Infostation and approach x_c. If we are to approach capacity, a high-level modulation must be used. Otherwise, the modulation itself is not bandwidth-efficient

α (dB)	x_c (m)	C (bits/symbol)
40	2466	0.353
30	1144	0.163

Table 2.2: Threshold distance and average capacity for $r = 10000$ m and $h = 10$ m

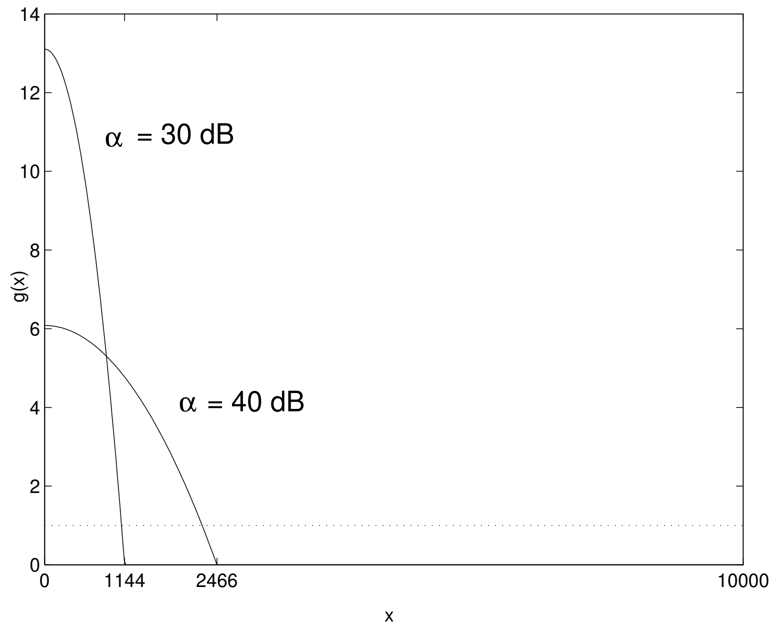

Figure 2.3: Optimal power allocation as a function of distance, for the Infostation model with parameters $h = 10$, $r = 10000$ and $\alpha = 30, 40$ dB

enough. For example, for $\alpha = 40$ dB, the spectral efficiency is around 8 bits/symbol at $x = 0$. Therefore, we need at least a 16-level modulation.

Figure 2.5 shows the dependence of the average capacity C with the Infostations' radius r for parameters $h = 10$ m and $\alpha = 40$ dB. Figure 2.6 shows the relation between threshold distance x_c and radius r. It can be appreciated that the percentage of area with coverage decreases very rapidly as r increases. We note again that x_c has no physical interpretation as a threshold distance when it is larger than r.

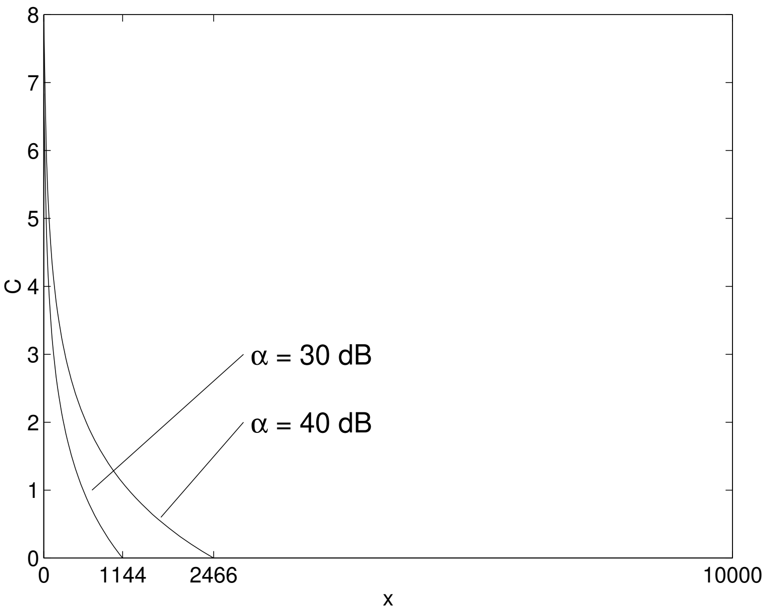

Figure 2.4: Capacity $C(x)$ as a function of distance, for the Infostation model with parameters $h = 10$, $r = 10000$ and $\alpha = 30, 40$ dB. Note that $C(x = 0)$ is a finite value

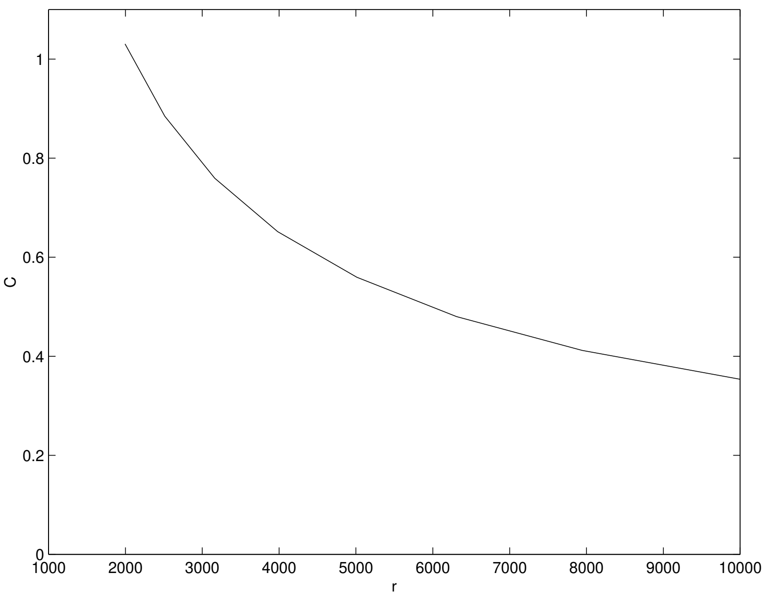

Figure 2.5: Average capacity for the Infostation model as a function of the Infostation radius r

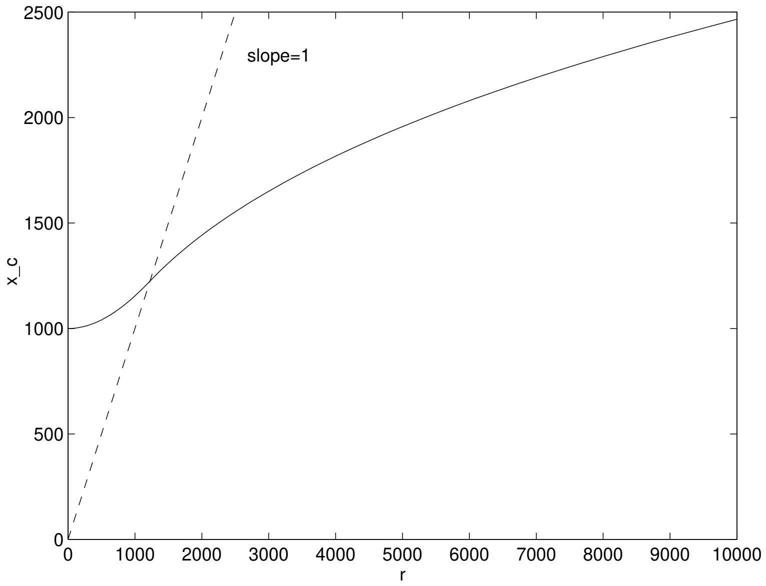

Figure 2.6: Relation between the threshold distance x_c and the Infostation radius r for capacity, with $\alpha = 40$ dB

2.3 BPSK Cutoff Rate and Optimal Power Gain

We focus now on a similar problem, in which we restrict ourselves to BPSK modulation, and instead of maximizing capacity, we maximize the cutoff rate R_0. Again, at a given distance x, we have an AWGN channel. The BPSK cutoff rate therefore is given by [18]

$$R_0(x) = 1 - \log_2\left(1 + \exp(-\mathrm{SNR}(x))\right), \tag{2.15}$$

and the average cutoff rate is

$$R_0 = \int_0^r R_0(x)\,\pi(x)\,dx. \tag{2.16}$$

Using the expression for the SNR in equation (2.7), the optimization in this case becomes

$$R_0 = \max_{g(x)} \int_0^r R_0(x)\,\pi(x)\,dx, \tag{2.17}$$

such that

$$\int_0^r g(x)\,\pi(x)\,dx = 1 \tag{2.18}$$

and

$$g(x) \geq 0. \tag{2.19}$$

Following the same procedure as for capacity, the optimal power profile $g(x)$ that results is

$$g(x) = \begin{cases} \dfrac{x^2+h^2}{\alpha h^2} \ln\left(\dfrac{2x_c^2 - x^2 + h^2}{x^2+h^2}\right) & \text{for } x \leq x_c, \\ 0 & \text{for } x_c \leq x \leq r, \end{cases} \tag{2.20}$$

where x_c again can be seen as a threshold distance beyond which no power is allocated and the transmitter just shuts off. Of course, this x_c needs not to be equal to the one in the capacity case. To determine x_c we can apply the constraint in equation (2.18) for $g(x)$ and solve numerically.

Figure 2.7 shows the optimal power control policy for the example $r = 1000$ m, $h = 10$ m and $\alpha = 20, 30$ dB. As we can see, the optimal policy reduces the power spent when approaching the Infostation, because with little power it is able to approach the maximum efficiency the BPSK modulation can render: 1 bit/symbol. For instance, for $\alpha = 30$ dB the value for the average cutoff rate R_0 in this case is 0.478 bits/symbol, which compares with a capacity of 0.743 bits/symbol.

Qualitatively similar results are obtained for $r = 10000$ m, $h = 10$ m and $\alpha = 30, 40$ dB, as shown in Figure 2.8.

Figure 2.9 shows the dependence of the average BPSK cutoff rate R_0 with the Infostations' radius r for parameters $h = 10$ m and $\alpha = 40$ dB. For $r = 10000$ m, we have plotted in Figure 2.10 the cutoff rate versus the distance.

As we can see, the maximum value for the BPSK cutoff rate is 1 bit/symbol, and is almost attained at $x = 0$ with little power gain because the conditions are

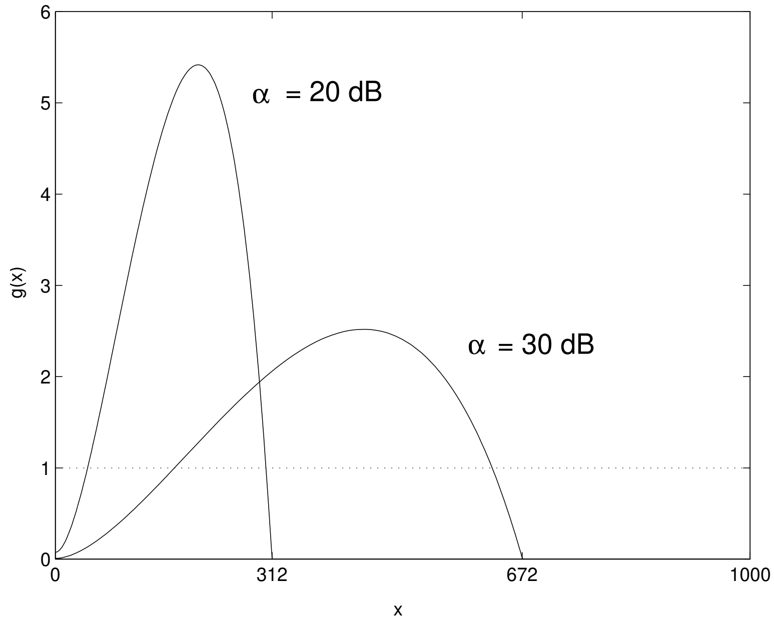

Figure 2.7: BPSK optimal power allocation as a function of distance, for the Infostation model with parameters $h = 10$, $r = 1000$ and $\alpha = 20, 30$ dB

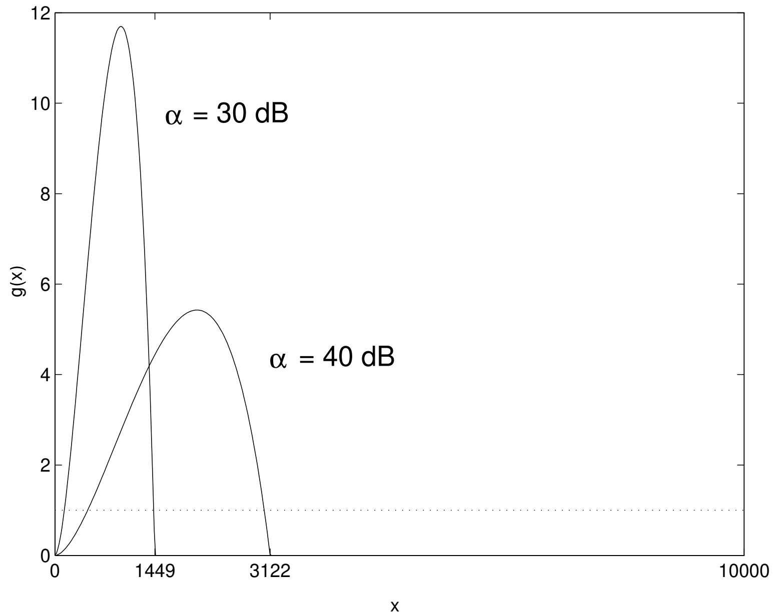

Figure 2.8: BPSK optimal power allocation as a function of distance, for the Infostation model with parameters $h = 10$, $r = 10000$ and $\alpha = 30, 40$ dB

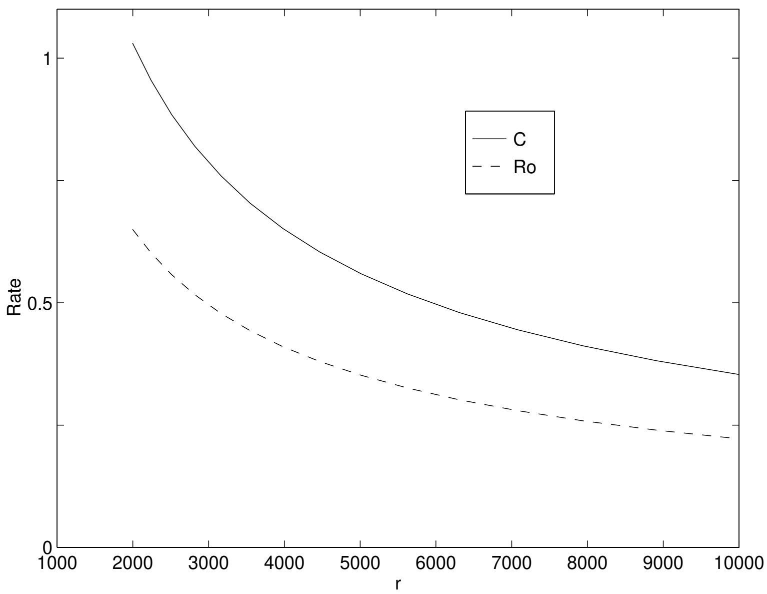

Figure 2.9: Average capacity and average BPSK cutoff rate for the Infostation model as a function of the Infostation radius r

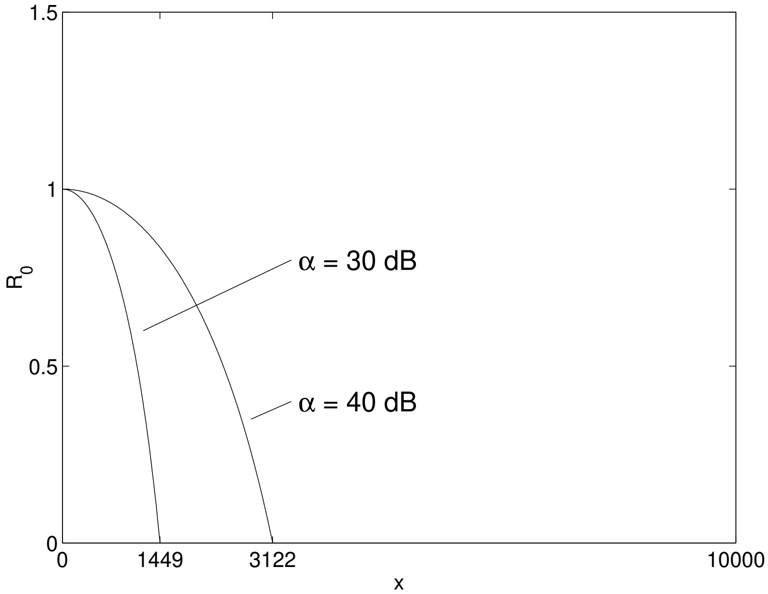

Figure 2.10: Cutoff rate as a function of distance, $R_0(x)$ for $h = 10$, $r = 10000$ and $\alpha = 30, 40$ dB

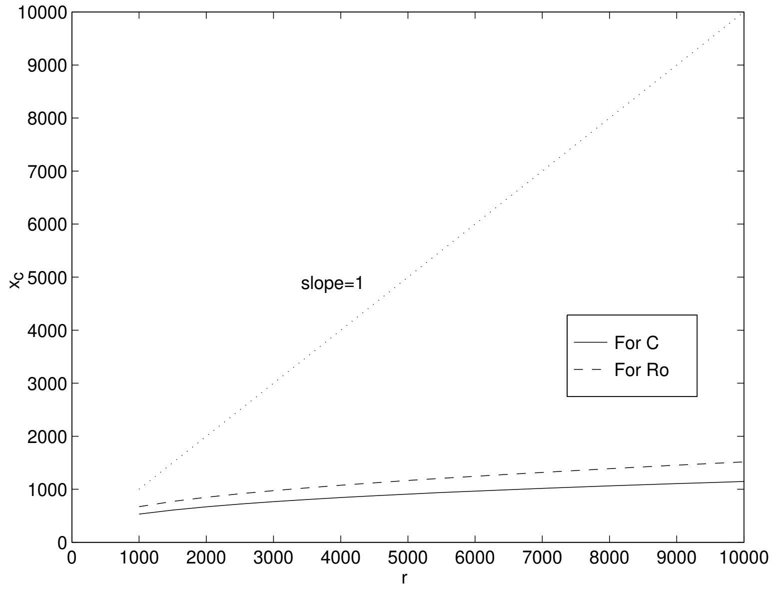

Figure 2.11: Relation between the threshold distance x_c and the Infostation radius r for capacity and for BPSK cutoff rate, with $\alpha = 30$ dB

already very favorable. As we move away from $x = 0$, the spectral efficiency keeps decreasing although more power gain is allocated. Finally, beyond x_c there is no communication.

For $\alpha = 30$ dB, Figure 2.11 shows the relation between the threshold distance x_c and the radius r. In comparison with Shannon capacity optimization, the threshold distance for BPSK modulation is always larger.

2.4 Suboptimal Power Gain

We examine now a suboptimal power gain which is more convenient to use but keeps the idea of using the channel only when conditions are good. It consists of a constant gain up to a certain threshold distance, and zero from there on. Thus, we just need to keep track of the distance between mobile terminal and Infostation. Then, we will either turn the transmitter on or off depending on whether this distance is smaller or greater than the threshold distance. Of course, for a fair comparison, the average power constraint will still hold. Hence, the power gain is given as

$$g(x) = \begin{cases} g_0 & \text{for } x \le x_c, \\ 0 & \text{for } x_c \le x \le r, \end{cases} \tag{2.21}$$

with

$$\int_0^r g(x)\,\pi(x)\,dx = 1 \quad \Rightarrow \quad \frac{g_0 x_c}{r} = 1 \quad \Rightarrow \quad g_0 = \frac{r}{x_c}. \tag{2.22}$$

Restricting to a policy of this kind, the expression for the average capacity becomes

$$C = \max_{x_c} \int_0^{x_c} \frac{1}{2}\log_2\left[1 + \frac{r}{x_c}\frac{\alpha h^2}{x^2+h^2}\right]\pi(x)\,dx. \tag{2.23}$$

Solving numerically for x_c, we have found that the threshold distance is smaller than the optimal case, but the resulting average capacity is almost the same. See Figure 2.12 for a plot of the average capacity as a function of r for $h = 10$ and $\alpha = 40$ dB. Although Figure 2.12 resembles a single plot at first glance, it contains both the optimal and the suboptimal cases. Figure 2.13 shows the capacity as a function of distance for $r = 10000$, $h = 10$ and $\alpha = 40$ dB. We can appreciate that the shapes are quite similar.

Similarly, we can look at what happens if we use this policy with BPSK modulation. We have to optimize the following expression for the cutoff rate

$$R_0 = \max_{x_c} \int_0^{x_c} \left(1 - \log_2\left[1 + \exp\left(-\frac{r}{x_c}\cdot\frac{\alpha h^2}{x^2+h^2}\right)\right]\right)\pi(x)\,dx. \tag{2.24}$$

Again, we have to solve numerically for x_c. Figure 2.14 shows the average cutoff rate as a function of r for an example. We can see that the difference here is more noticeable, but still the result is quite good if we account for the simplicity of the power policy. Figure 2.15 shows the cutoff rate as a function of the distance for $r = 10000$. In this case the shapes are less similar, but with comparable areas.

To summarize, Figure 2.16 shows the average capacity and the average cutoff rate for the optimal and the suboptimal policies. We can say that by using the simple

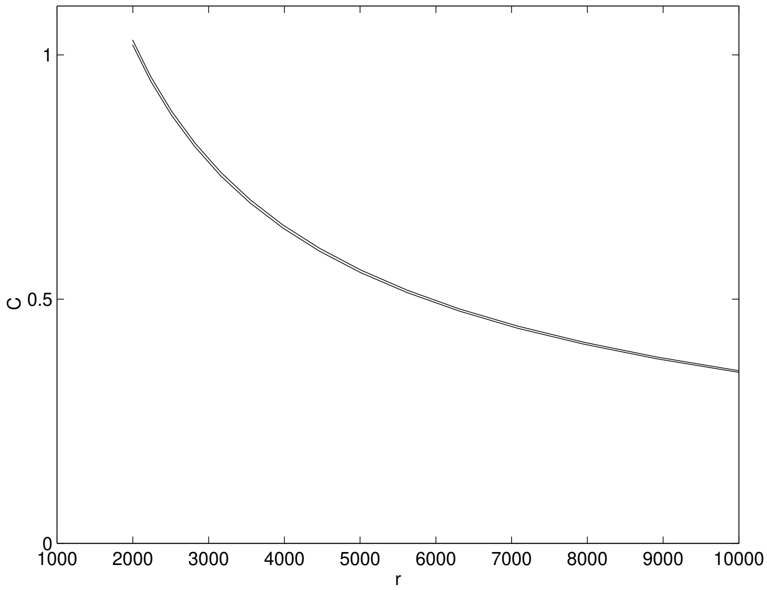

Figure 2.12: Capacity as a function of r for optimal $g(x)$ and for constant g_0

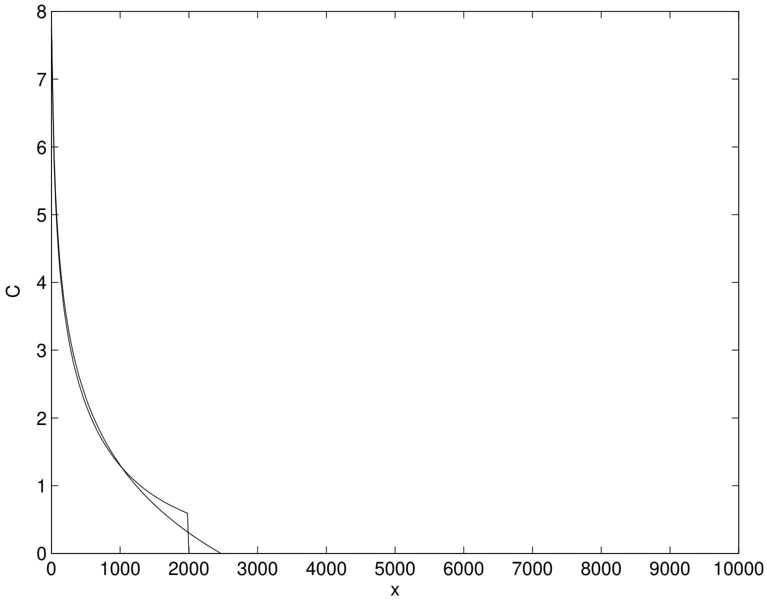

Figure 2.13: Capacity $C(x)$ for constant gain as a function of distance, for fixed $r = 10000$ and $\alpha = 40$ dB

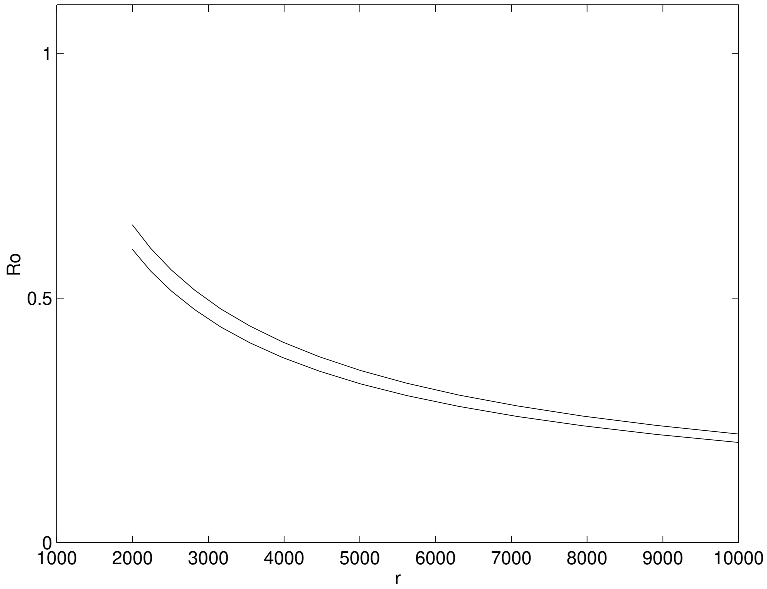

Figure 2.14: Cutoff rate as a function of r for optimal $g(x)$ and constant g_0

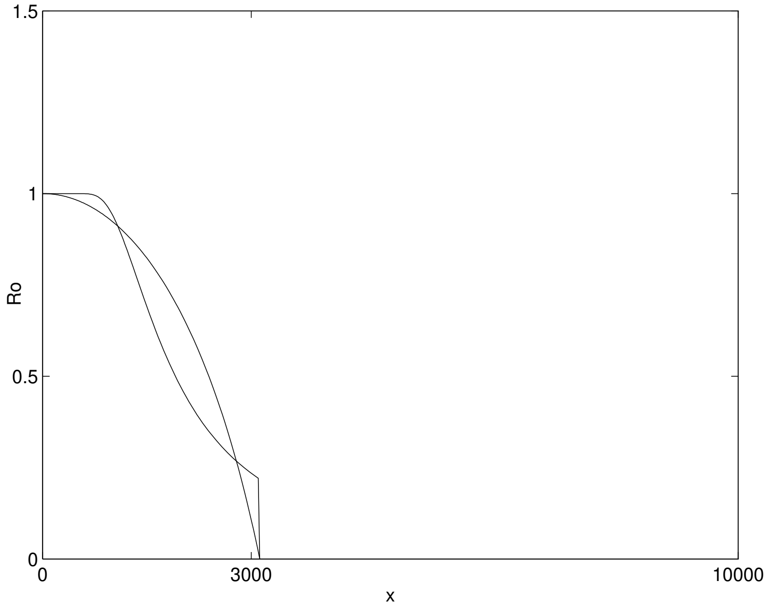

Figure 2.15: Cutoff rate $R_0(x)$ for constant gain for $h = 10$, $r = 10000$ and $\alpha = 40$ dB

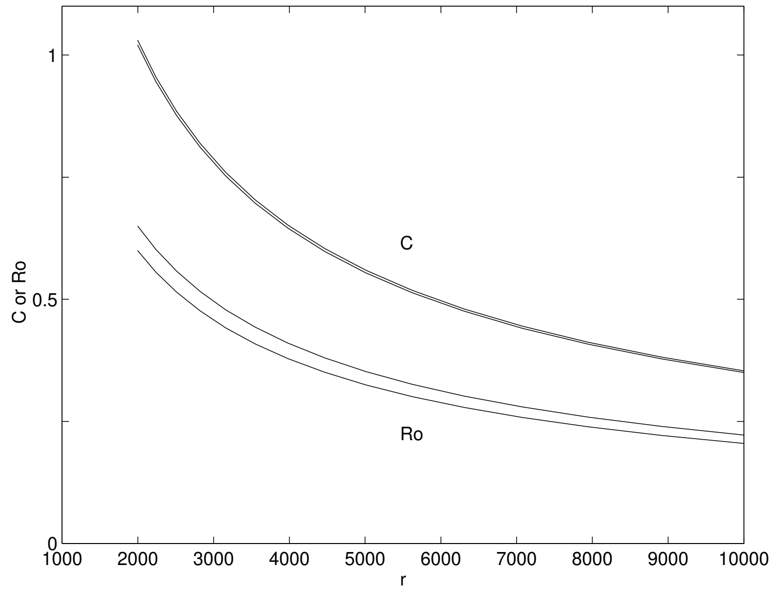

Figure 2.16: Capacity and cutoff rate as a function of r

suboptimal power policy the efficiency is not seriously compromised. Note that whether we use an optimal or suboptimal power profile, we must keep in mind that achieving such throughputs in practice requires complex rate-adaptive modulations.

2.5 Stochastic Model

So far we have assumed that Infostations are spaced at regular fixed intervals. Here we change this assumption, such that the distances between Infostations become a set of i.i.d. exponential random variables. That is, the distance from Infostation i to Infostation $i+1$ (see Figure 2.17) is a random variable X_i with probability density function (pdf)

$$f_{X_i}(x_i) = u \exp(-u x_i). \tag{2.25}$$

With this choice of distance distribution, mobiles moving at constant speed v pass by Infostations according to a Poisson process with rate vu.

As in the periodic model, to determine the power profile we need the pdf of X,

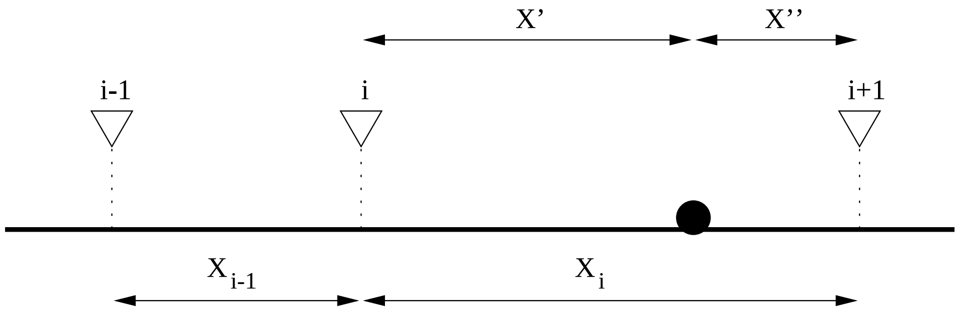

Figure 2.17: Distances in the stochastic model

the distance from the mobile to the base of the closest Infostation. It follows from the memorylessness of Poisson processes that, at an arbitrary point (where the mobile is located), the distance X' to the previous Infostation and the distance X'' to the next Infostation are i.i.d. random variables with

$$f_{X'}(x) = f_{X''}(x) = f_{X_i}(x). \tag{2.26}$$

If we note that the distance to the closest Infostation is

$$X = \min(X', X''), \tag{2.27}$$

the pdf of X becomes

$$f_X(x) = 2u \exp(-2ux). \tag{2.28}$$

Knowing $f_X(x)$, we can use the results of the periodic model. We will have the same power control strategies because, as shown in Appendix A, the structural form of the power profile $g(x)$ is independent of $f_X(x)$. Only the constants will have to be adjusted according to the new pdf.

For capacity, the power profile will be given by equation (2.11), adjusting the constraint in equation (2.10) by replacing $\pi(x)$ with $f_X(x)$ in equation (2.28). The constraint results in

$$\int_0^{x_c} \frac{x_c^2 - x^2}{\alpha h^2} 2ue^{-2ux}\, dx = 1, \tag{2.29}$$

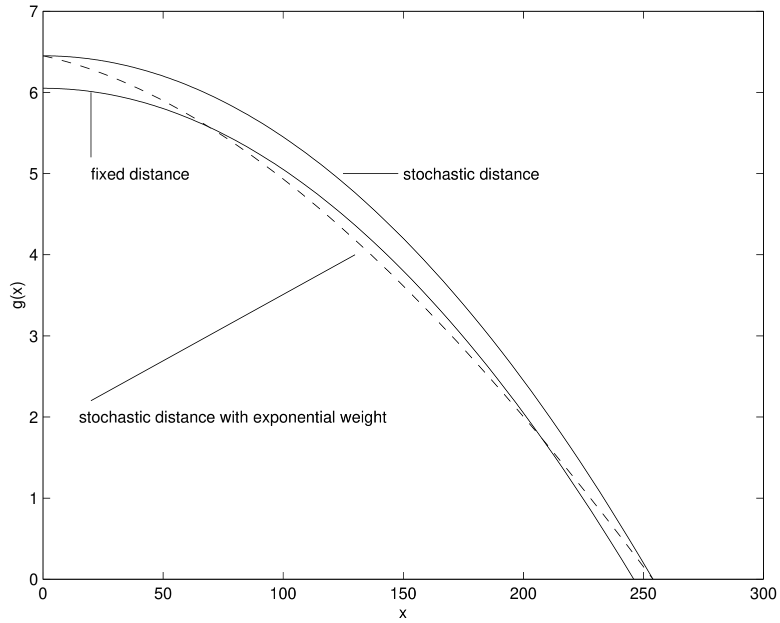

Figure 2.18: Power allocation as a function of distance, for stochastic and fixed distance between Infostations

which determines the new cutoff distance. This time, though, we cannot solve for an expression of x_c, but we rather have to find its value numerically (as we did for BPSK cutoff rate).

To compare with the case of regular intervals between Infostations, we can take u such that the mean distance between Infostations is equal to the distance in the fixed case, $2r$. This equates $2r$ with $1/u$.

For instance, with parameters $\alpha = 20$ dB, $h = 10$, and $r = 1000$, we get $x_c = 246$ in the fixed distance case versus $x_c = 254$ in the stochastic case. In Figures 2.18 and 2.19, we show the power and capacity profile, respectively, for these two cases, plus an exponentially weighted version of the stochastic case's profiles, to appreciate the effect of $f_X(x)$.

The average capacity is also affected by $f_X(x)$, but we don't have a closed-form solution for an exponential pdf. If we calculate it numerically for the example, we get an average capacity of $C = 0.323$, which has to be to compared with $C = 0.333$

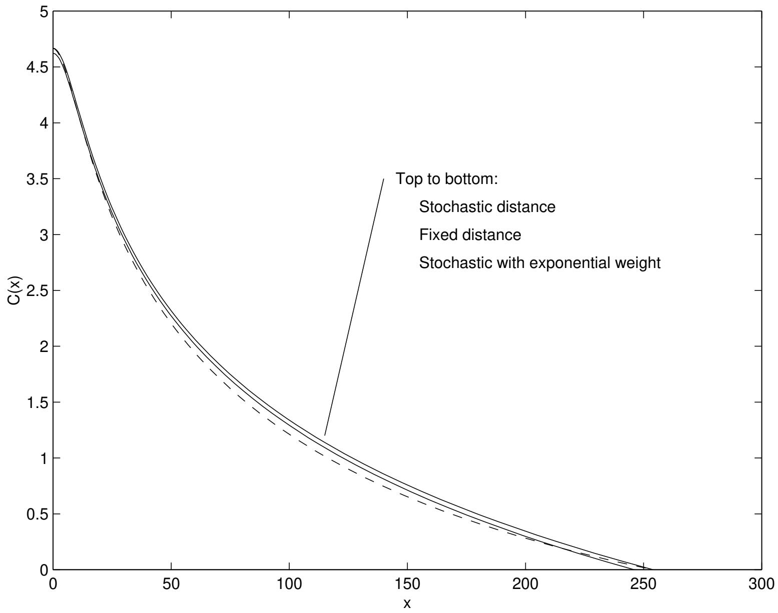

Figure 2.19: Capacity $C(x)$ as a function of distance, for stochastic and fixed distance between Infostations

for the fixed-distance case. As we could predict from Figure 2.19, the values are very similar.

What is peculiar in the stochastic case is that we have continuous coverage every time the actual x_i (the distance between Infostations) is smaller than $2x_c$. Thus, we just need to switch from one Infostation to the next at halfway. Figure 2.20 shows an example of one such power profile.

2.6 Conclusions

In this chapter we have considered a single user moving along a line which communicates with Infostations periodically distributed. Assuming a constraint on the average power used, we have found the optimum power control for capacity and for BPSK cutoff rate. Both results exhibit a reduced coverage, with a cutoff distance beyond which no communication takes place, giving an information-theoretic argument in favor of the Infostation idea.

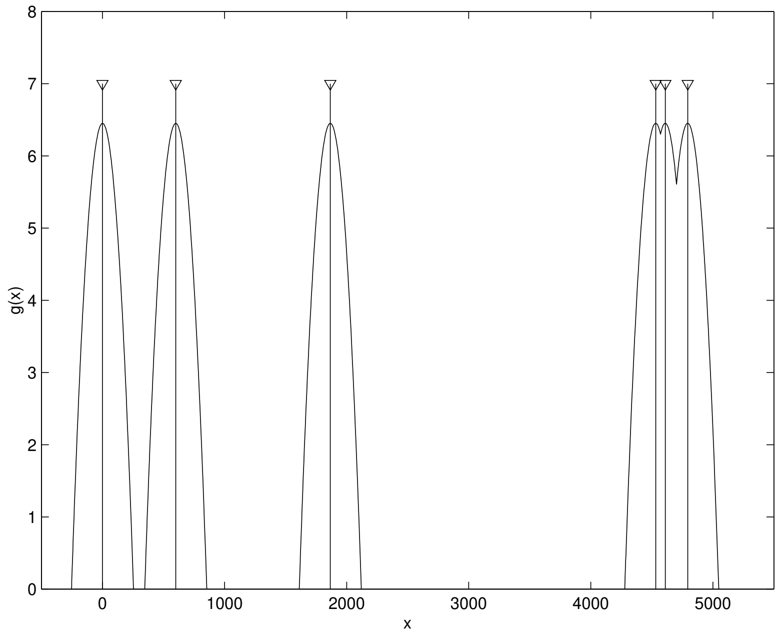

Figure 2.20: Example of power allocation for randomly located Infostations

The actual shape of power as a function of distance is different for capacity and BPSK cutoff rate. In the case of capacity, the closer the mobile gets to the Infostation, the more power is used. This is not true for BPSK cutoff rate, but nonetheless we have shown that the cutoff rate achieved is quite insensitive to the shape of power function, as long as it is concentrated between the Infostation and the cutoff distance.

An alternative model with Infostations at stochastic distances shows a slight decrease in capacity, although it does not capture the effect of interference that would hamper the operation of Infostations located too close to one another.

Chapter 3
Single Infostation

This model considers a single Infostation, the objective being to maximize the number of data bits transmitted in a single encounter of the mobile with the Infostation. Several cases are studied, according to the number of different rates allowed for transmission.

3.1 Model

This model consists of an isolated Infostation and a terminal moving in a straight line at a constant speed, v m/s. The terminal approaches the Infostation reaching a minimum distance $d_{\min}$ meters from the Infostation antenna before moving away from the Infostation (see Figure 3.1). Depending on the speed of the terminal relative to the distance to the next Infostation on the terminal's route, it may take long before there is another opportunity for communication. Hence, we want to maximize the amount of information transferred while the terminal is in contact with the present Infostation.

We assume that the services we want to offer need a certain quality of service in terms of required bit error rate (BER). At a given distance from the Infostation, we can find a modulation, bandwidth and coding scheme such that the mobile is able to transmit at the desired data bit rate while keeping the BER lower than the operational threshold. If the mobile moves away from the Infostation, the SNR drops due to increasing path loss. Eventually, the SNR is such that the BER meets the threshold and moving further away without any change in the transmission scheme

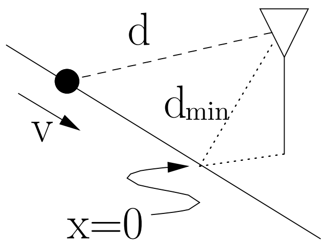

Figure 3.1: Single Infostation model.

will cut the communication link. To keep the same BER, we can change parts of the communication system, which may or may not result in a change of data bit rate. This brings the possibility of using not only a single, small coverage area, but a series of concentric rings, where coverage is provided with possibly diminishing data rates, through a variable rate mechanism in the transmitter/receiver pair. We will need to find the corresponding coverage radii and the total amount of data that can be downloaded.

There are several mechanisms used in communications engineering to provide for adaptation. All of them can be seen as starting from a given time-frequency slot and a certain amount of average power, and changing the way they use these resources. For instance, we can change the transmission bandwidth and we will have a variable symbol rate. If we change the modulation, we are changing the signal space in that time-frequency block. Coding is also a way of restricting the signal space, and finally we can vary the transmit power over the time-frequency tile. Some of these variable schemes are suitable for adaptation over a continuum, such as choosing the data rate under a BPSK modulation by choosing a corresponding amount of bandwidth. However, implementation constraints and the overhead introduced by adaptation, reduce the possibilities to a finite number, and more often than not, a rather small number.

We can change the modulation type, the bandwidth used, the coding scheme, and/or the power control scheme. Let us consider each of them, one at a time.

- Bandwidth (Symbol rate adaptation): If we reduce the symbol rate (effectively the bandwidth used) and filter appropriately, the noise power will be reduced. This will boost the SNR, lowering the BER. Therefore, the coverage will be expanded at a reduced bit rate since the ratio of bit rate to symbol rate has not changed. In this way, we can assign different rates at different distances (continuously or discretely), if we are able to adjust the filter accordingly. This requires dynamically adjustable filters.

- Coding: If we are willing to change the coding scheme, we have two cases. If we can keep the same coding rate but lower the BER by using a better (i.e. more complex) code, then we can extend the coverage without changing the bit rate. Otherwise, we can lower the coding rate, lowering the BER. The coverage is extended at a reduced data bit rate.

- Modulation: Again, there are several possibilities. We can find a more efficient modulation (without changing the bit-rate to symbol rate ratio); or we can reduce the number of levels of the modulation scheme, effectively increasing the energy per bit, which yields a better BER. The result is extended coverage with reduced bit rate, although the symbol rate and transmission bandwidth are the same.

  A third possibility is the use of multicarrier modulation (OFDM) to distribute power to more or less subcarriers, depending on signal quality. Assuming white noise, if we are far away from the Infostation and the power is spread equally among the subcarriers, the SNR may be too low to achieve a desired BER. But we may still use a subset of subcarriers, implying a reduction in data rate, if we concentrate in them all the power, thus boosting their SNR. As we get closer and the received power increases, we can distribute the transmitted power among more subcarriers, resulting in a higher data rate. This approach has the bonus of being implementable using digital signal processing techniques.

- Power control: We can change the transmitted power to compensate for the path loss. Usually we will have an average power constraint that will limit the extent to which this measure can be applied. As was made apparent in Chapter 2, the appropriate power control algorithm will depend on whether it is used in combination with other changes in the transmission scheme.

Generally, a combination of these methods turns out to be the best solution in terms of maximum information transfer. One example is trellis-coded modulation, which combines modulation and coding to outperform other coding methods which do not account for the modulation used. However, a primary concern in Infostations design is simplicity of the communications system. A related problem is how fast we can make the changes and within which limits. For instance, in modem transmission, there is the possibility of changing the modulation. This is quite slow a process that nonetheless is adequate because it is relatively fast compared to call duration. In Infostations, call duration can be extremely short, and with rapid changes in the channel conditions. This fact will demand the use of variable schemes that are able to adapt quickly enough.

In this chapter we will study the effect on throughput of varying the symbol rate and varying the modulation scheme.

3.2 Symbol Rate Adaptation

This method is the theoretically simplest. We just vary the data rate by varying the symbol rate, which is nothing but changing the amount of bandwidth used. We also need to account for the amount of power needed to keep a certain SNR. If we increase bandwidth, we will have to increase the total power to counteract the additional receiver noise. Or we can keep the transmitted power fixed if the received power has increased thanks to a smaller distance between mobile and Infostation.

If we are to increase the symbol rate, what we are actually doing is to increase the bandwidth used. And if we want to keep the same signal to noise ratio, we will have to increase the power used (unless we decide to change because the SNR conditions have improved due to proximity). Apparently, this is one of the simplest methods to vary the rate, if we have a fast enough clock and frequency dividers. The problems that arise are due to wideband effects that were not present in a narrowband signal, like frequency selective fading. Of course, with the appropriate receiver technology, this might also be an asset. The other main problem is government regulations restricting the amount of bandwidth/power usable, and the type of modulation. For example, to employ the 902-928 MHz ISM band, one must use spread spectrum with a minimum spreading ratio.

Symbol rate adaptation is uncommon in radio systems because bandwidth is scarce and has to be shared. This situation results in the division of the frequency band in chunks alloted to systems, and these systems further divide their allotments into channels for each user. One user can be given several channels but these need not be contiguous, as it would be necessary for a variable symbol rate scheme. Still, we can view the channel as the maximum bandwidth (thus, symbol rate), and use smaller bandwidths, decreasing the rate from this maximum.

3.3 Symbol Rate Adaptation for BPSK

We assume that the base station is able to operate at a transmit power P_T and that the minimum signal-to-noise ratio required at the mobile receiver is γ. We also assume that the mobile terminal is moving in a straight line. Thus, without loss of generality, we can assume that the terminal is moving along the x axis with the origin, $x = 0$, at the point in which the distance between the terminal and the Infostation is a minimum at $d_{\min}$ meters. We further assume an additive white Gaussian noise channel with noise power density N_0 and propagation exponent n. The design problem is to find the Infostation data bit rate and coverage distance that maximize the amount of information transferred. If P_R is the received power and $R(x)$ bps is the bit rate of a terminal at position x, the SNR constraint can be written as $\frac{P_R}{R(x)N_0} \geq \gamma$. Hence, the bit rate is constrained by

$$R(x) \leq \frac{P_R}{\gamma N_0} = \frac{KP_T}{\gamma N_0 (x^2 + d_{\min}^2)^{n/2}} = R_{\max}(x) \tag{3.1}$$

where K is a constant characterizing antenna gains, carrier frequency and system losses not related to propagation [20].

For simple Infostations, we may use a single rate within the coverage area. In this case, at a maximum distance x_c meters, this rate will be $R_{\max}(x_c)$ bps. Therefore, we can choose the maximum coverage distance x_c meters such that we maximize the number of bits transmitted to the terminal,

$$I = \max_{x_c} \frac{x_c}{v} R_{\max}(x_c) \text{ bits,} \tag{3.2}$$

where the ratio $\frac{x_c}{v}$ seconds is the time spent within coverage, i.e., the duration of the transmission. By substituting equation (3.1) into equation (3.2), differentiating with respect to x_c, and setting the derivative to zero, we find the optimal x_c:

$$x_c = \frac{d_{\min}}{\sqrt{n-1}} \tag{3.3}$$

As we observe from equation (3.3), the optimal distance x_c meters is independent of the terminal speed v. However, it is a decreasing function of the propagation exponent n. The amount of information transferred is a decreasing function of both v and n,

$$I = \left[\frac{(n-1)^{n-1}}{n^n} \right]^{1/2} \frac{KP_T}{v\gamma N_0 d_{\min}^{n-1}} \tag{3.4}$$

For the special case of free space propagation ($n = 2$), I becomes

$$I = \frac{KP_T}{2v\gamma N_0 d_{\min}}. \tag{3.5}$$

In order to compare the information transferred using a single rate against a continuously changing rate, we plot in Figure 3.2 the maximum rate possible as a

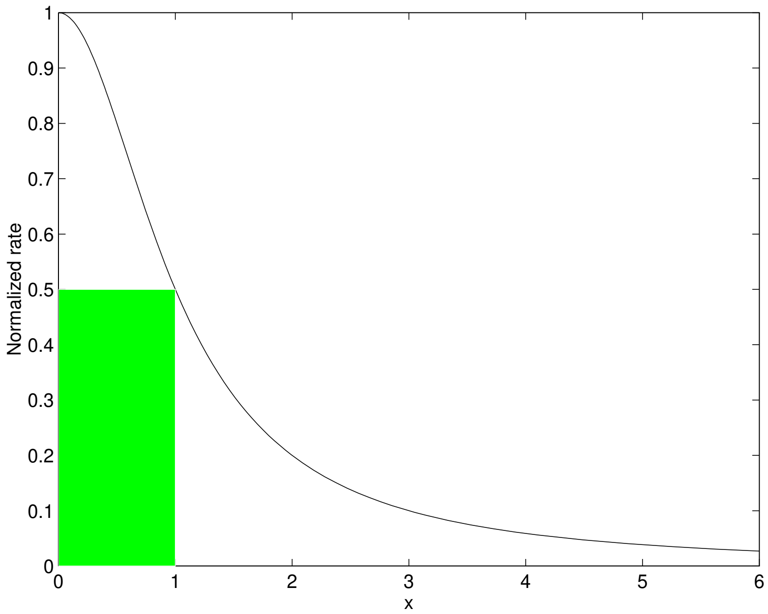

Figure 3.2: Single rate

function of x and the single rate used. In the Figure, $n = 2$ and the distances plotted are normalized by $d_{\min}$. Thus, the value of x corresponds to $d_{\min} = 1$ meter. The vertical axis is the transmission rate relative to the maximum rate possible when the terminal is at $x = 0$, a distance of $d_{\min}$ meters from the Infostation antenna. The actual rate is the rate on the vertical axis times $R_{\max}(0)$. The area of the rectangle is the number of bits transferred at the rate corresponding to the height of the rectangle. Equation (3.3) indicates that the rectangle shown, with the boundary $x = 1$, is the largest rectangle that can fit under the curve. The area under the curve is the number of bits that would be received from an Infostation transmitting exactly $R_{\max}(x)$ bps at each point x using a variable rate scheme. From Figure 3.2, we see that the constraint of a single rate can be significant. Since Infostations could have zones of different allowable rates, we next consider the situation of using more than one rate. This problem is equivalent to approximating the area under the curve in Figure 3.2 with a series of rectangles. Figure 3.3 shows the case of 3 rates.

As an illustration, we calculated numerically the best rates when we allow the

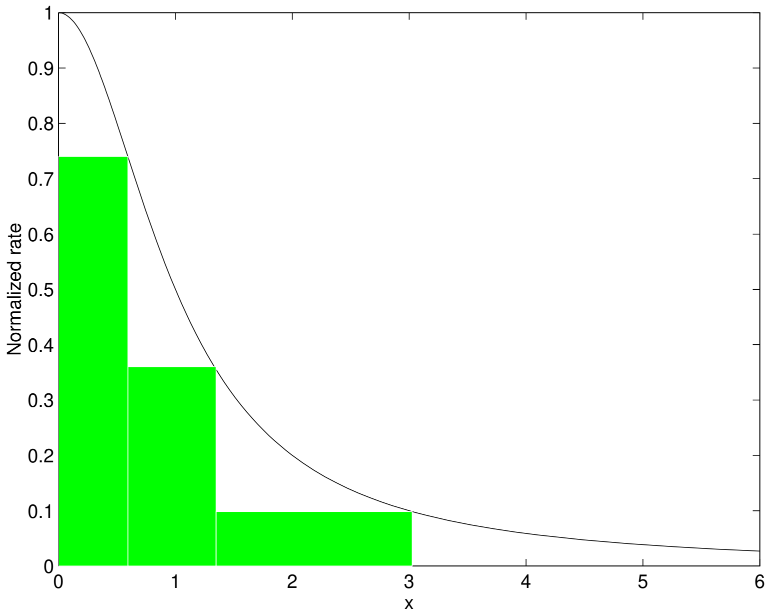

Figure 3.3: Three rates

use of two, three and four different rates. The results are summarized in Figure 3.4, again for $n = 2$, in terms of total information transfer normalized to the case of using a continuously changing rate for every position. Thus the vertical axis in this Figure is the number of bits transferred divided by the area under the curve in Figure 3.2. For one, two, three and four different rates, the outer coverage distances x_c are $d_{\min}$, $1.95d_{\min}$, $3.02d_{\min}$ and $4.24d_{\min}$ respectively. The number of bits transferred using four rates (60% of the maximum) is approximately double the single-rate quantity. Improvements due to adding additional rates are small as the values plotted in Figure 3.4 approach 1 very slowly.

3.4 Symbol Rate Adaptation for Other Modulations

We consider now modulations other than BPSK, by using the spectral efficiency

$$\eta = \frac{R}{W} \tag{3.6}$$

which, for a given modulation, is a constant. Examples are:

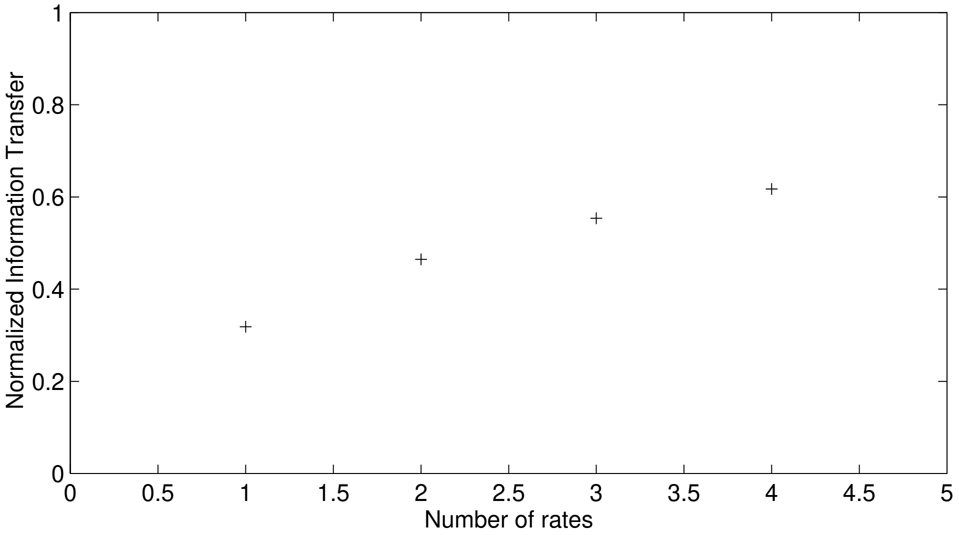

Figure 3.4: Normalized information transfer for several rates

- M-ASK, with $R/W \approx \log_2 M$,
- M^2-QAM, with $R/W \approx 2\log_2 M = \log_2 M^2$,
- M-PSK, with $R/W \approx \log_2 M$,
- MSK, with $R/W \approx 2$.

With these modulations, we will have again a certain threshold SNR, γ, which will depend on the application and the modulation. From equation (3.6), we observe that if at position x we wish to transmit at rate $R(x)$, then we will have a bandwidth requirement $W(x)$. Thus, we have a constraint

$$SNR = \frac{P_R}{W(x)N_0} = \frac{P_R}{(R(x)/\eta)N_0} \geq \gamma, \tag{3.7}$$

which means that the bit rate is constrained by

$$R(x) \leq \frac{\eta P_R}{\gamma N_0} = \frac{\eta K P_T}{\gamma N_0 (x^2 + d_{\min}^2)^{(n/2)}} = \frac{K' P_T}{\gamma N_0 (x^2 + d_{\min}^2)^{(n/2)}} = R_{\max}(x). \tag{3.8}$$

We can see that the resulting constraint is the same as equation (3.1) for BPSK except that constant K is now some other constant K'.

Since the optimal coverage distance x_c when using a single rate in BPSK was independent of K, this result will be the same here,

$$x_c = \frac{d_{\min}}{\sqrt{n-1}}. \tag{3.9}$$

That is, *if we restrict ourselves to a single rate, the coverage distance is independent of the modulation we use.* The actual amount of information transferred will depend on the modulation. Note that the coverage distance is fixed by $d_{\min}$, so that mobiles that get closer have a smaller coverage distance. From equation (3.2), the total amount of information transferred is

$$I = \frac{x_c}{v} R_{\max}(x_c) = \frac{x_c}{v} \frac{\eta K P_T}{\gamma N_0 (x_c^2 + d_{\min}^2)^{n/2}} = \left[\frac{(n-1)^{n-1}}{n^n}\right]^{1/2} \frac{\eta K P_T}{v \gamma N_0 d_{\min}^{n-1}} \tag{3.10}$$

We observe from equation (3.10) that I is proportional to the spectral efficiency and inversely proportional to $d_{\min}^{n-1}$. If instead of a single rate we use several rates, the optimum coverage distances are also independent of the modulation, but we don't have closed-form expressions.

If we consider now an ideal modulation that provides capacity, we have

$$R = W \log\left(1 + \frac{P_R}{W N_0}\right), \tag{3.11}$$

which does not give a constant spectral efficiency. Suppose that, for synchronization purposes, we have a threshold SNR, γ. This means that

$$W \leq \frac{P_R}{\gamma N_0}. \tag{3.12}$$

As R is monotone increasing in W, we maximize R by choosing equality in the previous equation. This gives

$$R(x) = \frac{K P_T}{\gamma N_0 (x^2 + d_{\min}^2)^{n/2}} \log(1+\gamma). \tag{3.13}$$

We can recognize again that this expression will result in the same coverage distance as the BPSK case.

If we lift the constraint on the SNR and allow W to approach infinity, we have that

$$R_\infty = \frac{KP_T}{N_0 \ln 2 (x^2 + d_{\min}^2)^{n/2}}, \tag{3.14}$$

and, again, the same coverage distance.

Note finally that we have used the symbol γ throughout as the threshold SNR, but that for every modulation this γ will be a different value, depending on the bit error rate constraints. Thus, we cannot just take the formulas for $R_{\max}$ for every modulation and compare them in terms of the same γ. To be fair, we have to compare them in terms of the same bit error rate, which will effectively reduce the amount of bandwidth used by higher level modulations. This is so because higher level modulations usually require a higher threshold SNR to keep the same bit error rate.

For instance, for a bit error rate of 10^{-3} and modulations BPSK, QPSK and 16-QAM, we need (approximately) 8.8 dB, 9.8 dB and 18 dB, respectively [18]. These different thresholds (that is, different γ) result in (normalized) data rates of 1, 1.58, and 0.48 (instead of 1, 2, 4, as would correspond if we had equal bandwidth). That is, even though we still have a net gain in data rate by switching from BPSK to QPSK, we loose when switching to 16-QAM. The latter modulation is more bandwidth efficient but we have to restrict the amount of bandwidth used, in order to comply with the bit error rate constraint.

3.5 Random Minimum Distance

We have shown in the previous section that the cutoff distance when using a single rate is the same for all modulations. Still, this cutoff distance (and associated data rate) is dependent on the mobile's minimum distance to the Infostation, $d_{\min}$.

It might be, though, that distance $d_{\min}$ is not a fixed value, but rather a random value in a certain range. In this case, even restricting to a single rate for every possible $d_{\min}$, we still have a whole range of possible rates. Thus, we would like to find the cutoff distance and best single rate when restricting to just one rate for all possible $d_{\min}$ values.

For example, suppose that $d_{\min}$ may take values from h (the height of the Infostation) to D (such that $D > h$) with uniform probability. We will solve only the case for propagation exponent $n = 2$, which will serve to illustrate the effect of restricting to a single rate.

Now that $d_{\min}$ may vary, we cannot fix the data rate just by choosing a single cutoff distance. Rather, if we want a single rate, we will have a different cutoff distance for every possible $d_{\min}$ (see equation (3.1)). Thus, we fix the quantity $z = \sqrt{x_c^2 + d_{\min}^2}$ that determines the rate, and then maximize the average information transfer with respect to z,

$$\bar{I} = \max_z \int_h^D \frac{\sqrt{z^2 - s^2}}{v} R_{\max}\left(\sqrt{z^2 - s^2}\right) \frac{1}{D - h}\, ds. \tag{3.15}$$

For $n = 2$, this maximum happens at $z = \sqrt{D^2 + h^2}$, which gives a cutoff distance $x_c = \sqrt{D^2 + h^2 - d_{\min}^2}$ and average information transfer of

$$\bar{I} = \frac{1}{2v} \frac{D^2 + h^2}{D - h} \left[\arctan\left(\frac{D}{h}\right) - \arctan\left(\frac{h}{D}\right)\right] R_{\max}\left(\sqrt{D^2 + h^2 - d_{\min}^2}\right). \tag{3.16}$$

Figure 3.5 shows the information transfer for every $d_{\min}$ in two cases: when using a single rate which changes for every $d_{\min}$ (that is, with $R_{\max}$ as in equation (3.8)); and when using a single rate which is the best overall and is the same for all $d_{\min}$ (that is, $R_{\max}\left(\sqrt{D^2 + h^2}\right)$, which is independent of $d_{\min}$). Of course, the first case gives always better information transfer because it adapts the rate to $d_{\min}$, but it is not a real single rate system. The two cases coincide only at

$$d_{\min}^* = \sqrt{\frac{D^2 + h^2}{2}}, \tag{3.17}$$

where the rate is the same for them both.

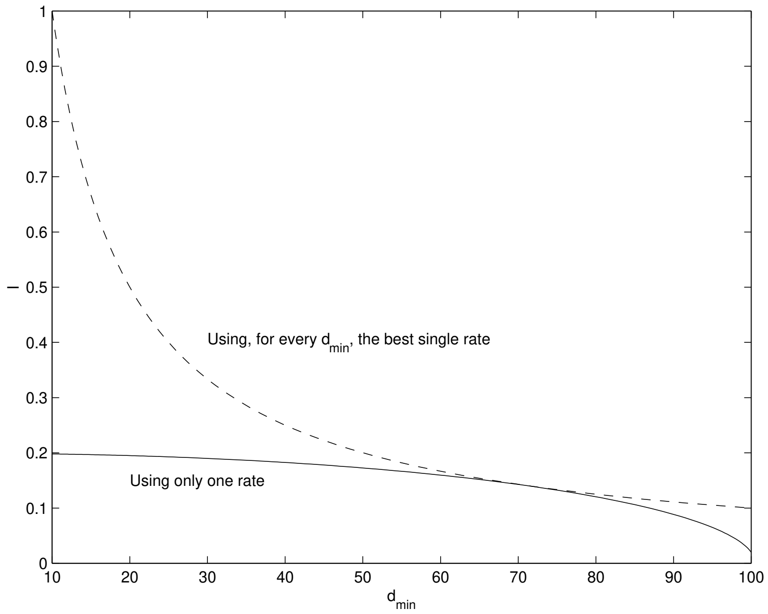

Figure 3.5: Normalized information transfer for single rate, depending on $d_{\min}$

3.6 Variable Modulation

The example of using a variable modulation scheme can be found in wireline modems, which during call establishment decide the highest level modulation usable with the quality of the given line. Also, if errors occur during the connection, they switch to a lower level modulation. Earlier modems employed QAM modulations, but nowadays they use fairly complex lattice modulations in higher dimensions, usually combined with coding [21].

Still, the channel that we find in wireline transmission for a given call is fairly time invariant. In radio systems, though, the presence of fading brings the need for special provisions, with more robust modulations that are easier to synchronize and able to work at relatively low SNRs. This has almost prescribed the use of higher-than-four level modulations in mobile applications. In Infostations, though, the situation will be one of relatively high SNR, albeit for a short time. This opens the possibility of using higher level modulations.

Whatever the modulations we are given, once we know the type of channel we are dealing with and the required bit error rate, we can translate every modulation to a different SNR threshold value. And these SNR values will determine the coverage threshold up to which we can use every modulation. Of course, at every location, we want to use the most efficient modulation available, as this will maximize throughput.

We call α the SNR at location $x = 0$ (see Figure 3.1). If we assume that α and the minimum distance $d_{\min}$ are given, we can express the SNR at location x as

$$\mathrm{SNR}(x) = \alpha \left(\frac{d_{\min}^2}{x^2 + d_{\min}^2} \right)^{n/2} = \alpha \left(\frac{1}{1 + \left(\frac{x}{d_{\min}} \right)^2} \right)^{n/2} . \tag{3.18}$$

For all x locations where $\mathrm{SNR}(x)$ is above a required threshold, we will be able to use the corresponding modulation.

For instance, if we consider three DPSK modulations in a Rayleigh fading channel, namely DBPSK, DQPSK and 8-DPSK, with a required BER of 10^{-3}, the corresponding required SNR values are 27, 32, and 37 dB, respectively [18]. Figure 3.6 shows the contour of these required levels for the SNR in equation (3.18), as a function of α and normalized location $x/d_{\min}$ (and we used propagation exponent $n = 4$). The parameter α gives a measure of the overall quality of the communication channel. If we increase this quality, we are able to use higher level modulations. We can see also that for high quality, it is possible to have rather small transition regions.

To see the impact of varying the modulation, we calculate the amount of data that can be delivered when using a single modulation against using the best at any moment. The amount of information transferred will be equal to the time within coverage times the data rate used,

$$I = \frac{2x}{v} R, \tag{3.19}$$

where R is the data rate used. For comparison purposes between several data rates,

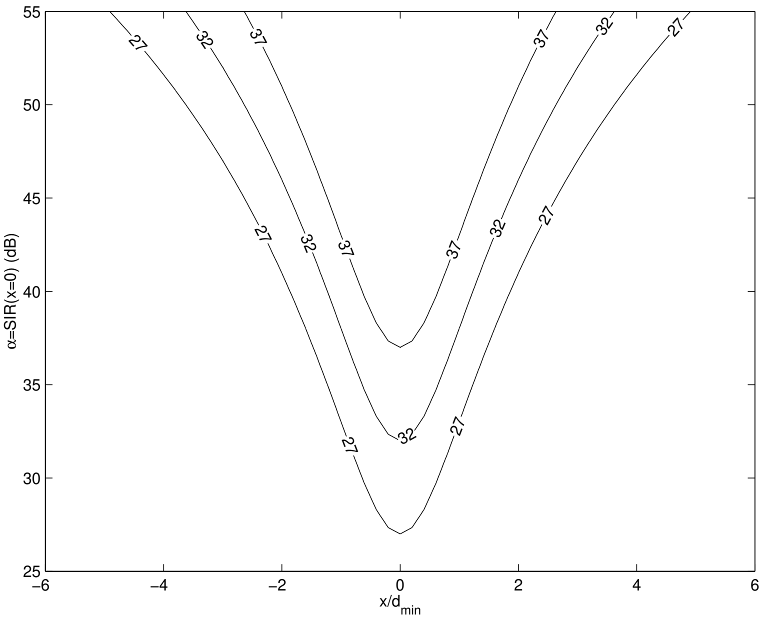

Figure 3.6: SNR contour as a function of the SNR α at the minimum distance and location x

we can use a normalized information transfer,

$$\bar{I} = \frac{I\,v}{2d_{\min}R_{\text{low}}} = k\frac{x}{d_{\min}}, \tag{3.20}$$

where R_{low} is the lowest data rate used in the comparison (in the example, the rate of the DBPSK modulation), and k is the ratio between the actual data rate and R_{low}. Then $x/d_{\min}$ can be related to the desired SNR through equation (3.18), such that for every required SNR we can find the corresponding $\bar{I}$. We plot $\bar{I}$ in Figure 3.7 as a function of α, for the three modulations in the example. Also, in Figure 3.7 we show $\bar{I}$ when using the best modulation at every location. In this case, $\bar{I}$ is a summation of contributions from each of the modulations and their corresponding coverage areas. Depending on channel quality, reflected by α, there will be a best choice of single modulation. When α is small, higher level modulations will either not be usable or the location range will be too small. As quality improves, higher level modulations become the best choice. If we consider variable modulation, we will always have the best throughput. In addition, the improvement from using a

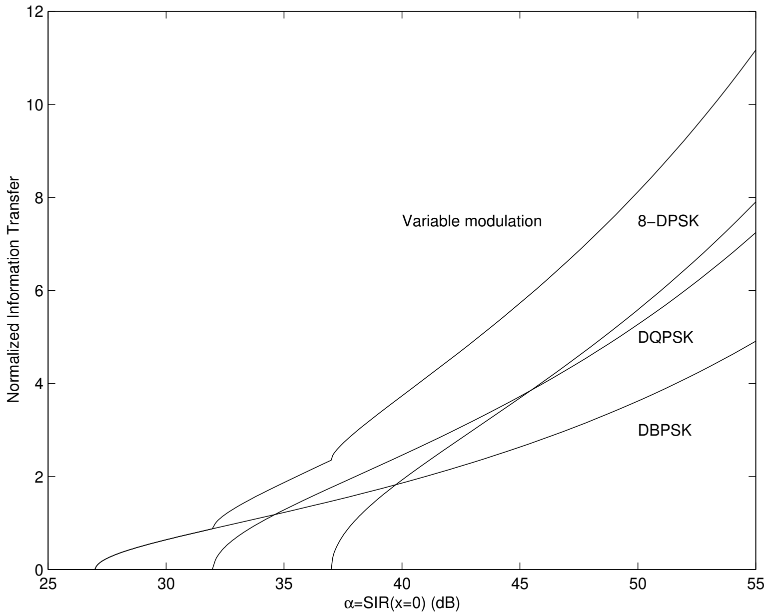

Figure 3.7: Normalized information transfer as a function of the SNR α at the minimum distance

single modulation can be substantial, even given the rather small zones where we would use lower level modulations. Still, the change between modulations requires some resynchronization that could reduce the gains.

3.7 Conclusions

In this chapter, we have considered a single user that tries to download the maximum amount of data from an Infostation. We have considered two possibilities of rate adaptation: variable symbol rate and variable modulation.

For variable symbol rate, we have found the maximum information transfer that can be achieved when continuously varying the symbol rate of a BPSK modulation with the distance to the Infostation. We then compared this result with the cases of being constrained to a single rate and to a finite number of rates. For a single rate, we have provided the optimum threshold distance and optimum symbol rate. We have also extended the single rate results to an arbitrary modulation characterized by its spectral efficiency, and to an ideal modulation that provides capacity.

For variable modulation, we have determined how we can relate each modulation to a certain coverage area. From this relation, we find the gains in information transfer of a variable modulation scheme with respect to a fixed modulation scheme.

Chapter 4
Infostation Overlays in Cellular Systems

4.1 Introduction

Consider the problem of downloading messages to mobiles from a base station in a cellular system. For cellular systems, it is usually assumed that ubiquitous coverage must be provided. From the cell geometry we can find the worst-case SIR, which in turn will dictate the data rate we can use. However, for wireless data, we might consider instead using reduced-coverage Infostations, co-located with cellular base stations.

What are the consequences of using a reduced coverage? On the one hand, we will have areas where communication is not possible. This makes the system unsuitable for real-time services, but it is not a problem for services that tolerate delay, like most messaging services do. Messages are stored in the user's mailbox, ready to be downloaded as soon as the mobile gets within coverage. On the other hand, we have observed that by reducing the coverage, the worst-case SIR increases, such that higher data rates are possible. Further, we might have more bandwidth available if, thanks to the additional spatial separation, we can use a smaller cluster size. At this point, it is not clear whether the improvement in data rate will allow a higher system throughput. In this chapter, we characterize this tradeoff between increased rate and time within coverage, in order to optimize the coverage area of an Infostations' system.

We model each Infostation as a queueing system with a single server, an arrival process and reneging. The arrival process is given by mobiles that get within coverage and have messages to download in their mailboxes. We have reneging when a mobile leaves coverage during or before downloading. The assumption of a single server amounts to using the whole available bandwidth as a single channel. An infinite queue size is also assumed. We will not deal with the problems of how the mobile registers or how the initial random access works. We assume here that every mobile knows its place in the queue, or rather, the Infostation knows whom to serve first.

This queueing system is described by the distributions of the arrival process, the service time, the reneging time, and the queueing policy. These distributions may or may not be influenced by the choice of coverage, depending on cell geometry and user mobility. The resulting combination, though, is what will ultimately decide the performance of the system. First, we need to relate these distributions to the coverage radius.

In general, we can say that if coverage increases,

- The worst-case SIR will decrease resulting in a lower data rate, which decreases the queue service rate for a given message bit length. We can improve the SIR by using frequency reuse, but then we have less bandwidth available.

- The mobiles' dwell time (time within coverage) will increase, and thus the reneging rate will decrease.

- The flow of mobiles entering the coverage area will not decrease (it may increase).

The first effect will reduce throughput whereas the other two effects will increase it. Thus, it seems that there might be a certain value of coverage that will optimize throughput. In order to find this value, we need to make more assumptions, to be able to relate coverage to system parameters in a more definite way.

The parameters that will be given to us for a specific situation are the cell geometry, the user density u, the message arrival rate, λ_u, per user per second,

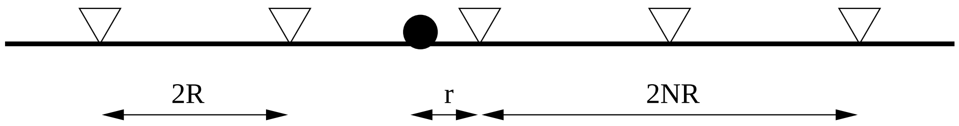

Figure 4.1: One-dimensional Infostation system

the average message length m in bits, and the mobility model. As cell geometry, we want to consider two idealized cases: a one-dimensional model with equidistant Infostations, which can be related to a highway, and a two-dimensional model with hexagonal cells, typical of cellular systems. The user density, the number of message arrivals per user per second and the message length in bits are parameters that we can set to usual values. The mobility model is related to the cell geometry. Although we could consider endless possibilities, few allow a practical analysis. For a linear model we will consider that mobiles move in a certain direction with a certain speed (that may be random). For two dimensions, we will use a model similar to the one in [22], in which mobiles move in straight lines, and we will also consider a random walk model.

4.2 Worst-case SIR and Coverage Radius

Unlike cellular systems, where the coverage radius, r, is equal to the cell radius, R, here we have a coverage radius that may be smaller than the cell radius. We just need to account for this difference in calculating the worst-case SIR.

4.2.1 One-dimensional Model

In this case, we have Infostations along a line, at regular intervals of length $2R$ (Figure 4.1). The worst-case SIR will happen when the mobile is at the edge of the coverage zone. We will only consider the interference of the two closest cochannel Infostations, making the assumption that all Infostations operate at the same power levels. The SIR is given by the expression

$$\mathrm{SIR} = \frac{P\left(\frac{d}{r}\right)^n}{P\left(\frac{d}{D_1}\right)^n + P\left(\frac{d}{D_2}\right)^n}, \tag{4.1}$$

where P is the power measured at a certain distance d in the far field of the Infostation, n is the propagation exponent (we will use $n = 4$ in the examples and figures), and D_1, D_2 are the distances to the interfering Infostations. For a certain frequency-reuse cluster size, N, we have $D_1 = 2NR - r$ and $D_2 = 2NR + r$. Thus, from equation (4.1), we see that

$$\mathrm{SIR} = \frac{1}{(2N\frac{R}{r} - 1)^{-n} + (2N\frac{R}{r} + 1)^{-n}}. \tag{4.2}$$

Equation (4.2) shows that we can keep the same SIR if we keep a constant relation between N and r/R. Figure 4.2 shows the SIR in dB as a function of r/R, for several values of N. We can appreciate for instance that we get the same SIR of 27 dB for $r/R = 1$, $N = 3$, as for $r/R = 1/3$, $N = 1$. In the first case we have full coverage but only one third of the bandwidth is available in each cell, whereas in the second case we have coverage only in one third of the cell but using the whole bandwidth.

To relate the SIR to the data rate c, we can either look at the Shannon capacity formula, $c = B\log(1+\mathrm{SIR})$, to find the maximum theoretically attainable data rate, or we can consider a more practical approach by choosing from a finite number of modulation schemes. Here, we will follow the second approach.

The dotted lines in Figure 4.2 mark the SIR level necessary for DPSK modulations with 2, 4, and 8 phases in a fading environment, for a bit error rate of 10^{-3} [18]. We will consider, as an example, that we are restricted to these modulations, and we want to obtain the best combination of $(N, r/R)$ and modulation, in terms of throughput. The solution will lie between the extremes of $(3, 1)$ with DBPSK and $(1, 0.195)$ with 8-DPSK, with respective data rates of $B/3$ and $3B$. We will solve this problem in section 4.3.

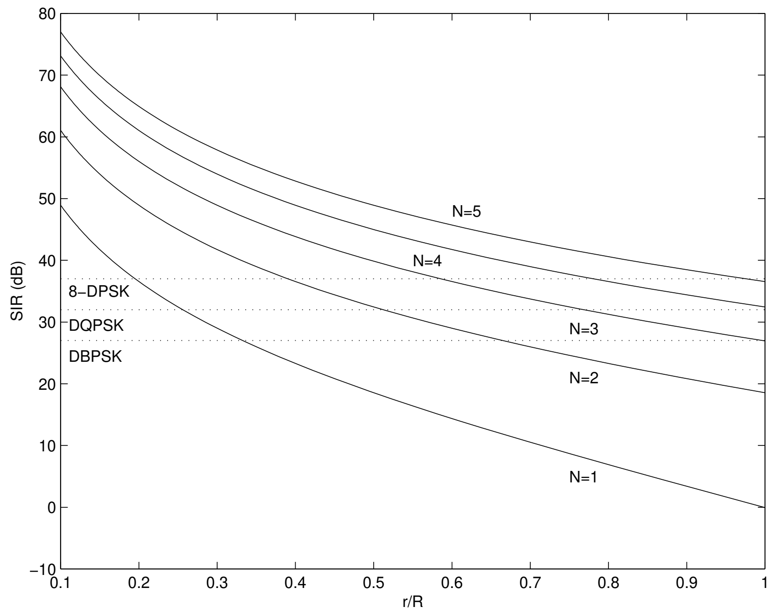

Figure 4.2: SIR as a function of r/R for a one-dimensional system

4.2.2 Two-dimensional Model

We will assume that we have cells with hexagonal geometry and radius $R > r$, with Infostations in their centers, all of them operating at the same power level. In the worst-case, the mobile will be at a distance r from the intended Infostation and distances D_i, $i = 1, \ldots, 6$, from the closest cochannel Infostations (Figure 4.3). With all Infostations transmitting at the same power level, the resulting SIR is

$$\mathrm{SIR} = \frac{P\left(\frac{d}{r}\right)^n}{\sum_{i=1}^{6} P\left(\frac{d}{D_i}\right)^n}, \tag{4.3}$$

with the same definitions as the one-dimensional case. The expressions of D_i are given in Appendix B for cluster sizes $N = 1, 3, 4, 7, 9, 12$. Using these expressions, we can get the worst-case SIR as a function of N and r/R, which we plot in Figure 4.4 as solid lines.

If $D_i \gg r$, then D_i can be approximated as $\sqrt{3N}R$, resulting in an approximate

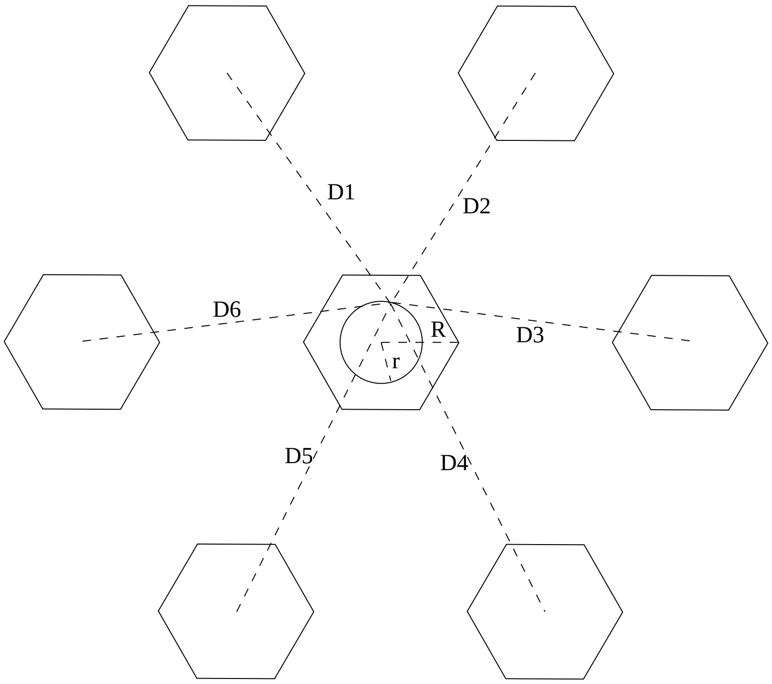

Figure 4.3: Two-dimensional Infostation system

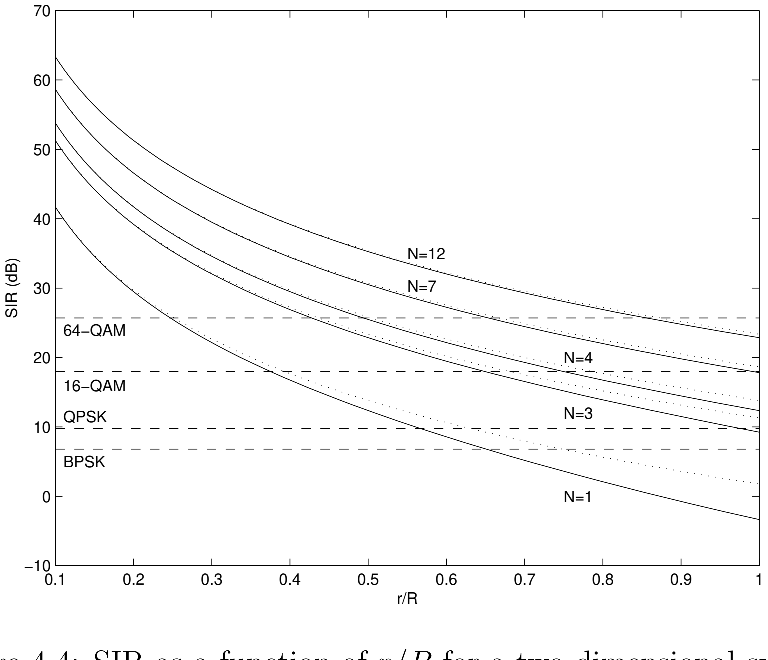

Figure 4.4: SIR as a function of r/R for a two-dimensional system

expression for the SIR given by

$$\mathrm{SIR} \approx \frac{1}{6}\left(\frac{\sqrt{3N}R}{r}\right)^n, \tag{4.4}$$

which is plotted in Figure 4.4 as dotted lines. In Figure 4.4, we observe that the approximation (4.4) generally works well and improves as N increases and r/R decreases. Moreover, in this two-dimensional case, the approximation (4.4) indicates that we can keep a constant worst-case SIR if we keep a constant relation between the cluster size N and the coverage-to-cell area ratio $(r/R)^2$. For instance, for an SIR of 12.35 dB we can either use full coverage and a cluster size of $N = 4$, or just cover a quarter of the cell area, $(r/R)^2 = 0.25$, with cluster size $N = 1$.

As an example, for the two-dimensional case, we will consider modulations BPSK, QPSK, 16-QAM and 64-QAM, assuming that the effects of fading are negligible (that is, we will assume an AWGN channel). The dashed lines in Figure 4.4 show the SIR levels necessary for these modulations, for a bit error rate of 10^{-3} [18].

And before continuing, just a reminder of the effect of the propagation exponent on the SIR values. As we mentioned, we will be using a propagation exponent $n = 4$ in the examples. But it is necessary to keep in mind that depending on this value, the SIR calculations will vary greatly. Figure 4.5 shows the SIR for a cluster size $N = 3$ and propagation exponents $n = 2.5$, 3, 4, and 5. A dashed line indicates the required SIR for 16-QAM.

4.3 The All-exponential Model

We will assume that all the distributions characterizing the queueing system are exponential. We will choose the corresponding average values according to a certain relation to the coverage radius. Although these distributions may not be very realistic, they allow an analytical solution of the system. This solution can be later compared to simulations using more realistic distributions to see if it can be used as an approximation.

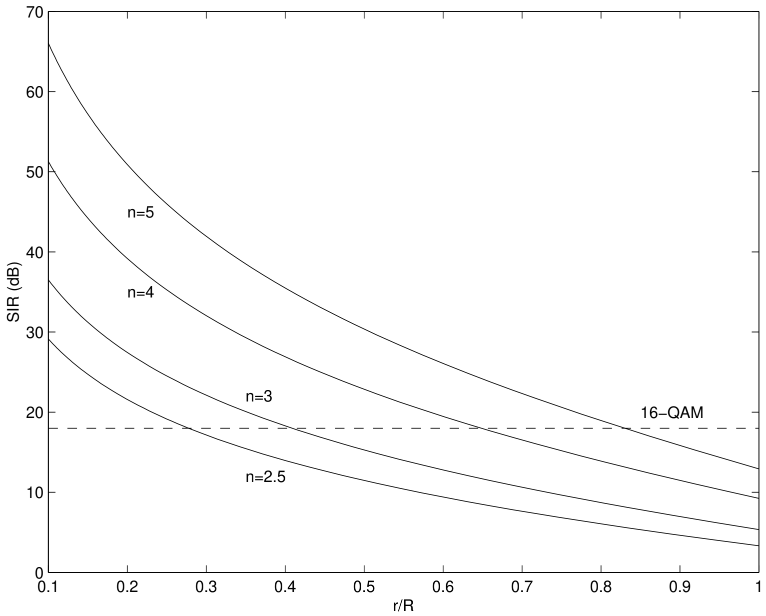

Figure 4.5: SIR as a function of r/R for a two-dimensional system, cluster size $N = 3$, and varying propagation exponent n

The queueing system can be represented by a birth-death process with birth rate λ and death rate at state k equal to $\mu + k\nu$ (where μ is the service rate and ν is the reneging rate). The steady-state probabilities of this process are given by (see Appendix C)

$$p_k = \frac{\lambda^k}{\prod_{j=1}^{k}(\mu + j\nu)} p_0 = \frac{(\eta\rho)^k}{k!} \frac{(\eta\rho)^\eta \beta(\eta, k+1)}{e^{\eta\rho}\gamma(\eta, \eta\rho)}, \tag{4.5}$$

where $\eta = \mu/\nu$, $\rho = \lambda/\mu$, $\beta(x, y)$ is the beta function, and $\gamma(x, y) = \int_0^y u^{x-1}e^{-u}du$ is the incomplete gamma function. Then, $(1-p_0)$ will give us the Infostation utilization, that is, the long-term proportion of time the server is busy. As our payload are bits and not seconds, we will also be interested in normalizing this utilization with the data rate, to get the average throughput

$$\zeta = c\,(1 - p_0). \tag{4.6}$$

We now need to relate the arrival, service, and reneging rates to the coverage radius.

4.3.1 One-dimensional Model

We have a one-dimensional model with Infostations separated by a distance $2R$ and with coverage radius r. All mobiles move in the same direction, with speed V chosen randomly from distribution $f_V(v)$. Every mobile receives λ_u messages per second, with an average length of m bits.

When mobiles cross the coverage boundary, they join the queue of mobiles waiting for service, staying in the system until they either get full service or leave the coverage area (in which case we have reneging). As shown in [23], the speed distribution of the boundary crossing mobiles is biased

$$f_V^*(v) = \frac{v\, f_V(v)}{E[V]}. \tag{4.7}$$

The flow α of mobiles through the coverage boundary can be related to the user density u and mobile speed as $\alpha = uE[V]$. This flow gives us directly the system arrival rate λ of the assumed exponential interarrival distribution. Thus, we have

$$\lambda = uE[V]. \tag{4.8}$$

The average time between visits to Infostations is given by

$$\tau_c = \int_0^\infty \frac{2R}{v} f_V^*(v) = \frac{2R}{E[V]}, \tag{4.9}$$

where we have used the speed distribution in equation (4.7).

To find the service rate, we assume that every mobile has an associated mailbox in the Infostation system. In this mailbox, messages are stored until the mobile gets within coverage of an Infostation. The size of this mailbox (in seconds) gives us the service time for every arrival. Note here that we relate the value in seconds to the value in bits through the transmission data rate c, which provides the influence of the coverage radius.

Between Infostation visits, the mailbox will keep accumulating the messages intended for the mobile in question. We will assume that the accumulated mailbox size between Infostation visits is given by an exponential random variable X. The mean $E[X]$ is found as the product of the message arrival rate λ_u, the expected time τ_c between Infostation visits, and the average message length m/c in seconds,

$$E[X] = \lambda_u \tau_c (m/c) \tag{4.10}$$

We say that an Infostation visit is successful if the mailbox is downloaded before the mobile leaves the coverage area. An unsuccessful visit, corresponding to reneging in the queue, can greatly complicate the queueing analysis. Thus we need to employ a simplifying assumption to ensure the service time will be statistically the same for every Infostation visit. Two such assumptions are

- *After an unsuccessful visit, the residual contents of a mailbox are discarded.*
- *After an unsuccessful visit, the mailbox will not accept new messages until it is emptied.* When the mobile downloads only part of the mailbox, say t, the residual mailbox size is given by random variable Y with density

  $$f_Y(y) = f_X(t + y | X > t) = f_X(y). \tag{4.11}$$

  Thus, random variable Y is identical to X, and as the mailbox will be backlogged, its size will not increase as the mobile travels to the next Infostation.

Under either assumption, the service time at an Infostation will be exponential with rate $\mu = 1/E[X]$. With respect to the average throughput ζ given by (4.6), these assumptions are conservative in that ζ would be higher if messages were never discarded (this is shown in Section 4.5, where alternative assumptions are considered).

Finally, the average reneging time is given by the average time the mobile spends within coverage,

$$\frac{1}{\nu} = \frac{2r}{E[V]}. \tag{4.12}$$

At every Infostation visit, a mobile will leave coverage without being able to finish downloading the mailbox with a certain probability P_{out}. This outage probability is given by (see Appendix C)

$$P_{out} = \sum_{k=1}^{\infty} \frac{k\nu p_k}{\lambda} = 1 - \frac{\mu}{\lambda}(1 - p_0), \tag{4.13}$$

and will indicate the percentage of backlogged mailboxes.

4.3.2 Two-dimensional Model

In the two-dimensional model, we assume we have a mobility model similar to that in [22], which is used very often in cellular literature. In this model, the hexagonal cell shape of radius R_{hex} is approximated by a circle of the same area (and radius $R \approx 0.91R_{hex}$). Mobiles are spread evenly over the area of the cell and travel in a straight line with direction uniformly distributed between $[0, 2\pi)$. The mobile speed V is chosen randomly from distribution $f_V(v)$.

From Figure 4.6, we observe that a cell-boundary crossing mobile will only cross the coverage area if its direction of travel θ lies between $-\phi$ and ϕ, where $\phi = \arcsin(r/R)$. Otherwise, communication won't take place in this particular cell (this is a specific characteristic of Infostations, different from cellular systems, where coverage is ubiquitous). It may seem that boundary crossing mobiles have angle θ uniformly distributed between $-\pi/2$ and $\pi/2$ with respect to the boundary normal. However, it was shown in [23] that boundary crossing mobiles have a direction bias toward the normal which is given by

$$f^*_\Theta(\theta) = \begin{cases} \frac{1}{2}\cos\theta & -\frac{\pi}{2} < \theta < \frac{\pi}{2} \\ 0 & \text{otherwise.} \end{cases} \tag{4.14}$$

From (4.14), we observe that this direction bias implies

$$P(-\phi < \theta < \phi) = r/R. \tag{4.15}$$

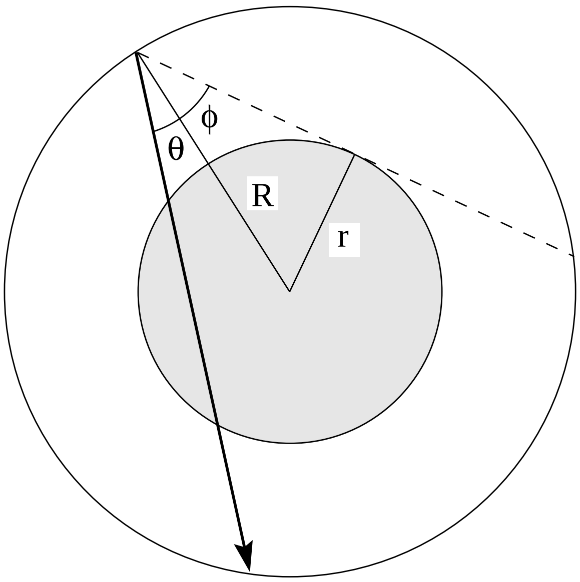

Figure 4.6: Geometry for the mobility model

The bias in speed distribution from equation (4.7) also applies.

The flow, α, of mobiles entering the cell is proportional to the cell perimeter and is given by

$$\alpha = 2\pi R \frac{u}{2} E[V], \tag{4.16}$$

where u is the mobile user density. Note that we use $u/2$ because only half of the mobiles in the boundary will be directed towards the cell.

For the Infostation queueing system, the mobile arrival rate equals the average flow into the coverage area, which is given by

$$\lambda = \alpha P(-\phi < \theta < \phi) = \pi r u\, E[V]. \tag{4.17}$$

The average time between visits to Infostations, or cycle time, is given by (see derivation in Appendix D)

$$\tau_c = \frac{\pi R^2}{2rE[V]}. \tag{4.18}$$

The cycle time differs from the one-dimensional case in that for one dimension when a mobile enters a cell, eventually that mobile will enter the coverage zone, yielding a cycle time that is independent of the coverage radius. In two dimensions, we might enter the cell and leave without ever crossing the coverage area of that cell. Thus, when completing a cycle time of Infostation visits we might have visited several cells. The smaller the coverage radius, the more cells are visited on average before we hit a coverage area.

Analogously to the one dimensional case, the mean mailbox size is

$$E\left[X\right] = \lambda_u \tau_c(m/c), \tag{4.19}$$

and its inverse will give us the service rate μ.

The average dwell time is given by (see derivation in Appendix D)

$$\tau_d = \frac{\pi r}{2E[V]}. \tag{4.20}$$

The reneging rate will just be $\nu = 1/\tau_d$.

4.4 Numerical Examples

4.4.1 One-dimensional Model

We show an example with Infostations in a highway spaced 2 km apart ($R = 1$ km). Cars move at an average speed of $E[V] = 45$ mph (20 m/s). The number of message arrivals per car per second is $\lambda_u = 0.01$, with an average of $m = 4$ Mbits per message. We want to find the most suitable choice of radius r and cluster size N, with DBPSK, DQPSK and 8-DPSK as possible modulation choices, with a total bandwidth of 1 MHz. User density will range from 0 to 0.05 cars per meter (which gives a flow between 0 and 3600 cars per second, and we will have between 0 and 100 cars per cell).

With these parameters, we get the system values shown in Table 4.1. We now consider just 8-DPSK modulation and look at the effect of varying the cluster size.

Mod.	N	$c(Mbps)$	r/R	λ	$E[X](sec)$
DBPSK	1	1	0.33	up to 1 car per second	4
	2	0.5	0.66		8
	3	0.33	1		12
DQPSK	1	2	0.25		2
	2	1	0.51		4
	3	0.67	0.76		6
	4	0.5	1		8
8-DPSK	1	3	0.19		1.33
	2	1.5	0.39		2.66
	3	1	0.58		4
	4	0.75	0.78		5.33
	5	0.6	0.97		6.66

Table 4.1: Parameters for one-dimensional example. Note that $cE[X]$ is the mailbox size in bits; as in 1D the cycle time τ_c is independent of coverage radius r, all cases get the same amount of bits accumulated from Infostation to Infostation.

Figures 4.7, 4.8, and 4.9 show the average throughput ζ, the outage probability, and average delay, respectively, in the range of user density.

The dotted line in Figure 4.7 shows the offered traffic per Infostation $\lambda E[X]$, as an upper bound to ζ. For small loads, all cases are able to handle the offered traffic, but as load increases, throughput starts to saturate to the maximum the system can handle in each case. We can appreciate that the throughput improves with smaller cluster sizes, thanks to the wider bandwidth available per Infostation. The smaller coverage radius associated with a smaller cluster size barely affects the throughput. The reason is that we only consider a few users at a time but very efficiently, such that we rarely get backlogged mailboxes.

Figure 4.8 reflects the smaller throughput of increasing cluster sizes on the outage probability P_{out}. We note here that as the user density tends to zero, the outage probability tends to a nonzero value given by

$$\lim_{u \to 0} P_{out} = \frac{\nu}{\mu + \nu}, \tag{4.21}$$

which for a given modulation is independent of cluster size N. Note that the limiting P_{out} is just the probability that a message entering service departs the coverage area

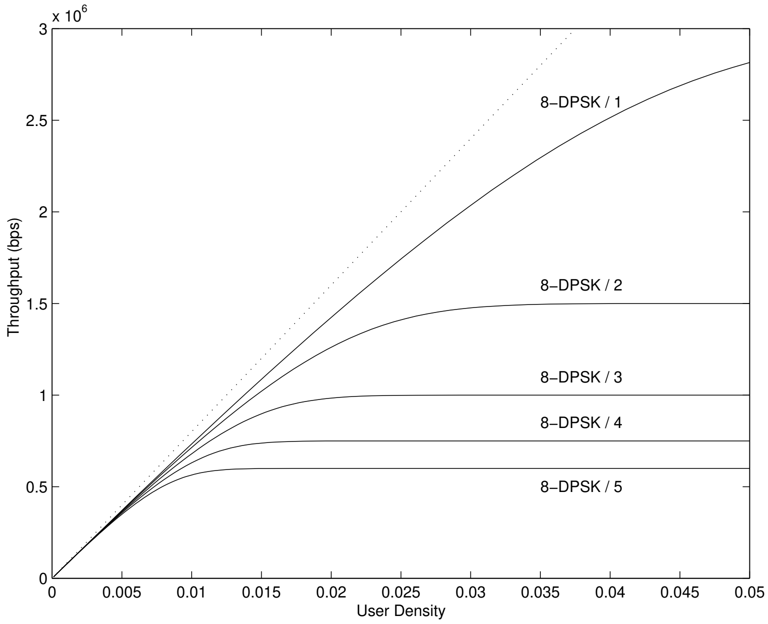

Figure 4.7: Throughput as a function of user density for one-dimensional case, 8-DPSK modulation

before completing service.

The average delay in Figure 4.9 is found as the sum of cycle time weighted by the average number of Infostation visits, plus the queueing time. As the average number of Infostation visits is just $1/(1-P_{out})$, we have that the average delay is given by

$$\text{delay} = \frac{\tau_c}{1-P_{out}} + \tau_q. \tag{4.22}$$

The queueing time τ_q is calculated for an M/M/1 system with reneging and FCFS queueing policy (see Appendix C). The average delay results favor again smaller cluster sizes. This is due to the fact that a higher throughput allows downloading the mailbox in fewer Infostation visits, and thus with a smaller delay. That is, τ_c is the same for all cases, and what is really changing is the reneging probability P_{out}. The queueing delay τ_q has a less relevant impact and is responsible for the bumps in the graphs.

If we now consider fixing the cluster size to $N = 1$ and vary the modulation

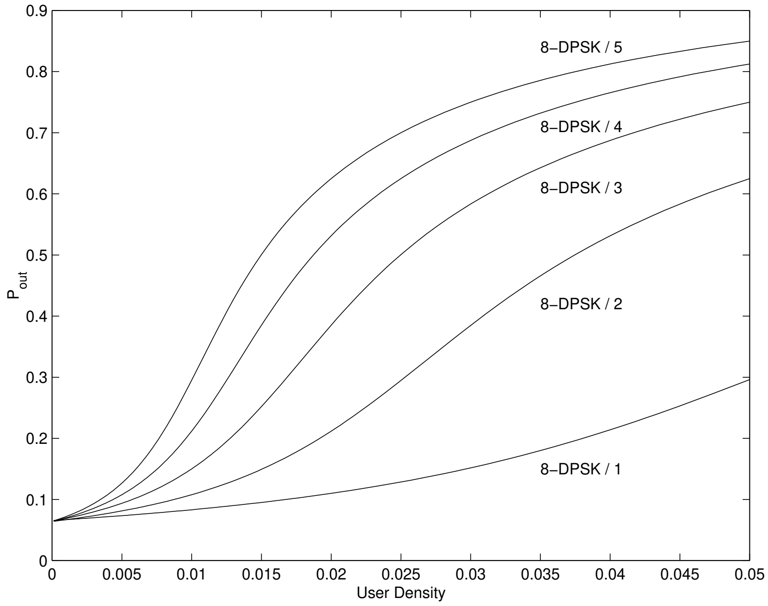

Figure 4.8: Outage probability as a function of user density for one-dimensional case, 8-DPSK modulation

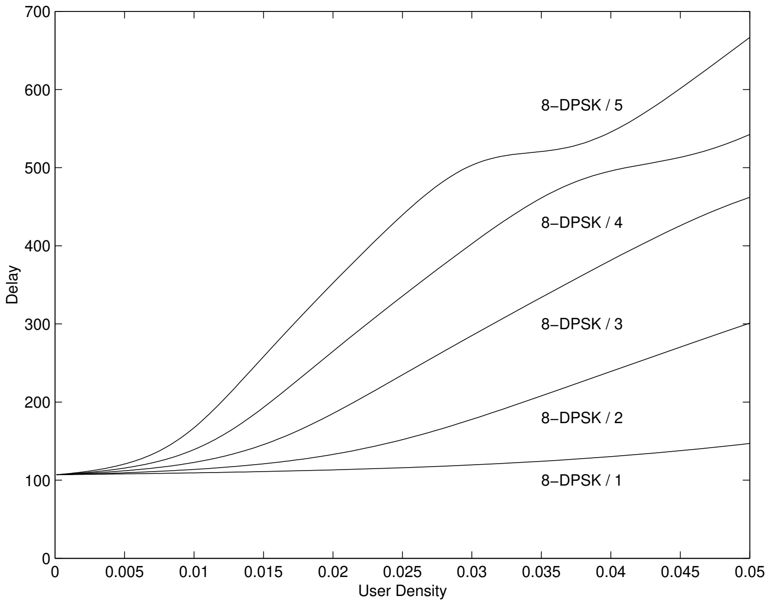

Figure 4.9: Average delay as a function of user density for one-dimensional case, 8-DPSK modulation

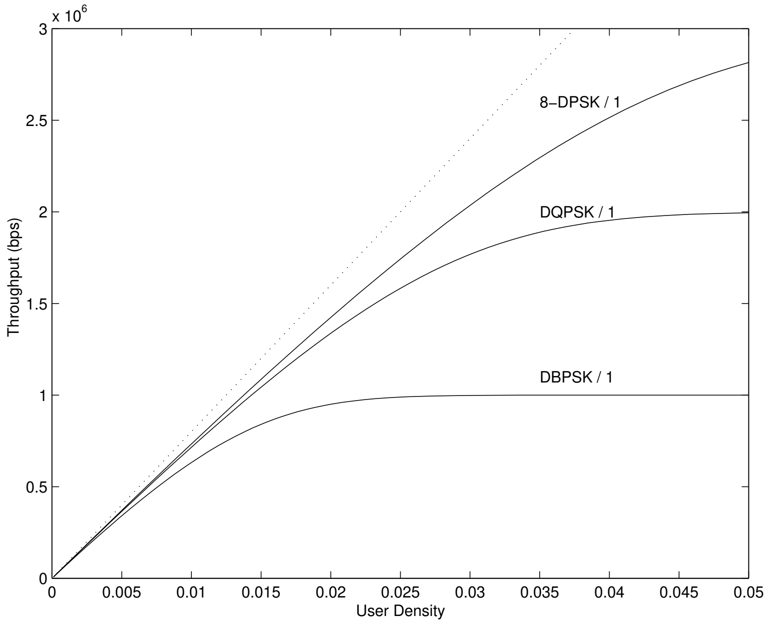

Figure 4.10: Throughput as a function of user density for one-dimensional case, cluster size $N = 1$

scheme, we get the throughput, outage probability, and average delay in Figures 4.10, 4.11, and 4.12. The results favor higher level modulations (and thus, smaller coverage radius again), although depending on user density the use of more complex modulations might not be justified enough when the gains are not very large.

Note in Figure 4.11 that now every case tends to a different limiting value of P_{out} when the user density goes to zero, although the expression is still given by equation (4.21).

We also want to remark that the results for throughput and outage probability are independent of mobile speed. Although faster mobiles stay less time within coverage, they visit Infostations more often and their mailboxes are smaller. The average delay results do depend on mobile speed, but the relative merits between modulations and between cluster sizes remain unaltered.

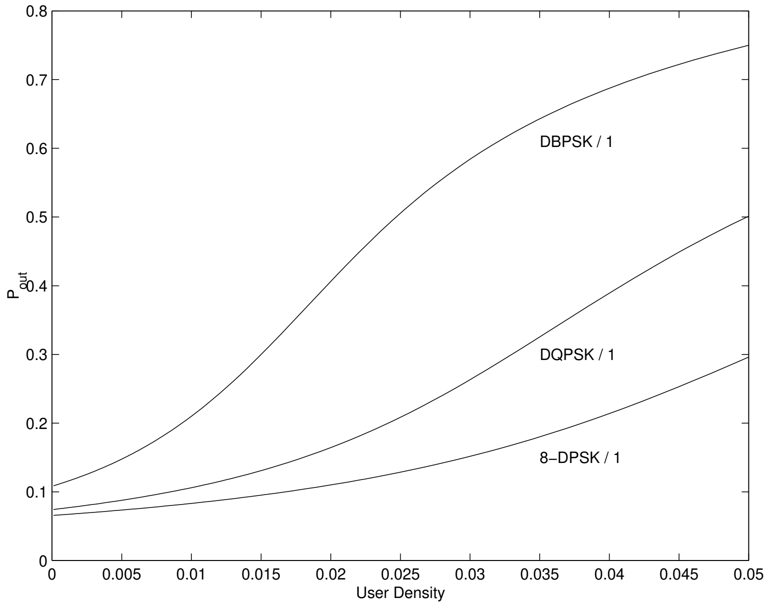

Figure 4.11: Outage probability as a function of user density for one-dimensional case, cluster size $N = 1$

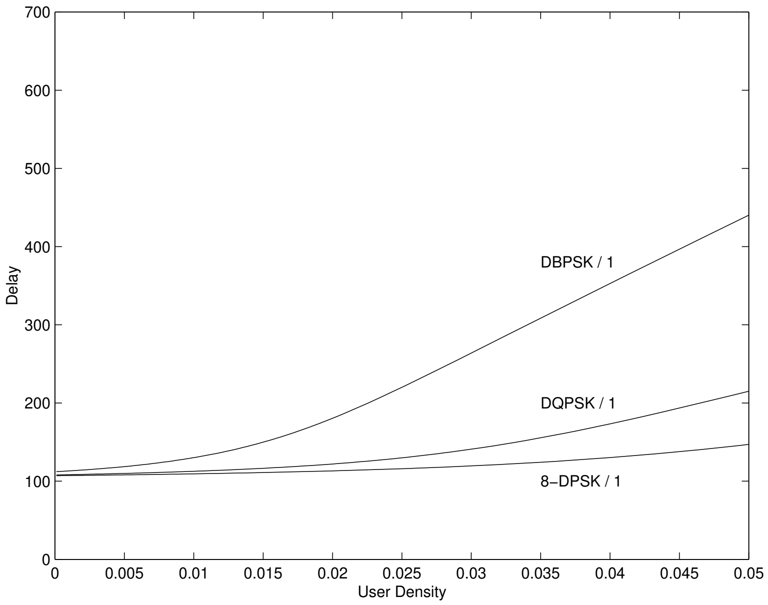

Figure 4.12: Average delay as a function of user density for one-dimensional case, cluster size $N = 1$

Mod.	N	$c(Mbps)$	r/R	$(r/R)^2$	λ	$E[X](sec)$
BPSK	1	1	0.66	0.44	0.26	9.52
QPSK	1	2	0.56	0.31	0.22	5.61
	3	0.67	0.97	0.94	0.38	9.72
16-QAM	1	4	0.37	0.14	0.15	4.25
	3	1.33	0.64	0.41	0.25	7.36
	4	1	0.74	0.55	0.29	8.49
	7	0.57	0.99	0.98	0.39	11.11
64-QAM	1	6	0.25	0.06	0.10	4.19
	3	2	0.42	0.18	0.16	7.48
	4	1.5	0.49	0.24	0.19	8.55
	7	0.86	0.65	0.42	0.26	11.28
	12	0.5	0.85	0.72	0.33	14.78

Table 4.2: Parameters for two-dimensional example

4.4.2 Two-dimensional Model

In this example we will consider hexagonal cells with equivalent radius of R = 500 m, a user density varying from 0 to 0.0004 users per m^2 (that is, from 0 to 314 users per cell), $\lambda_u = 0.01$ messages per user per second, average message length of $m = 2$ Mbits, and mobile speed $E[V] = 2.5$ m/s. Here we want to compare the possibilities with BPSK, QPSK, 16-QAM and 64-QAM modulation choices, also for a 1 MHz bandwidth. The resulting parameters are in Table 4.2.

Like in the one-dimensional case, we first consider fixing the modulation. Figures 4.13, 4.14, and 4.15 show the throughput ζ, the outage probability, and average delay, respectively, in the range of user density, for 64-QAM.

The results for throughput and reneging probability are very similar to the one-dimensional case, with the exception that now the cluster sizes do not follow the sequence of positive integers, providing a most pronounced jump in throughput from $N = 3$ to $N = 1$. Regarding delay (which is given again by equation (4.22)), this time the choice is not as clear-cut. The reason is that here the cycle time is not fixed, but depends on the ratio r/R. We can appreciate that a smaller r/R value will imply a higher cycle time τ_c, which will translate in an increased delay. This is why

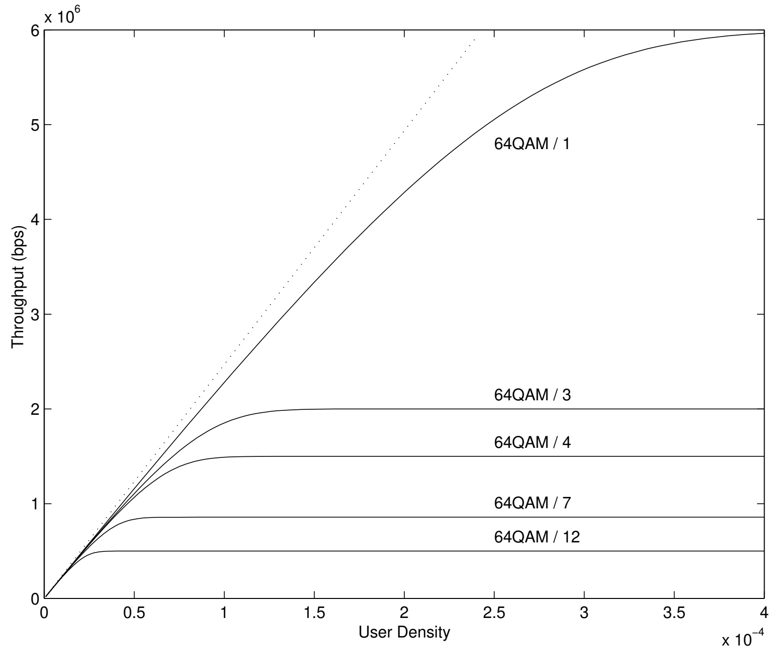

Figure 4.13: Throughput as a function of user density for two-dimensional case, 64-QAM

larger cluster sizes have a better delay response at low user densities, that is, because they cover most of the cell (and thus cycle time is smaller) and user density is small enough not to produce high queueing delays and outage probability. For higher user densities (and higher offered load), the throughput advantage of smaller cluster sizes shows up and delay becomes best as the previous cycle time disadvantage is offset by smaller queueing delay and outage probability.

Thus, for small loads, we are better off using a large cluster size, providing a fuller coverage, with enough throughput and smaller delay. As load increases, we will be shifting to ever smaller cluster sizes. And if we can handle a medium delay and are interested in having a large load range, we will use the smallest cluster size.

If we now fix the cluster size to $N = 1$ and try different modulations, we get the results in Figures 4.16, 4.17, and 4.18. What these results show is that the effect produced by higher level modulations when cluster size is fixed is very similar to the

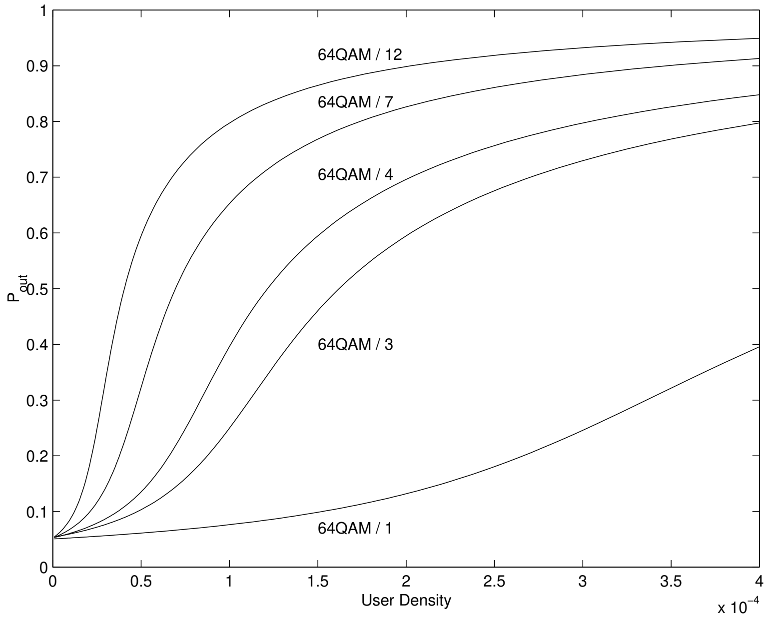

Figure 4.14: Outage probability as a function of user density for two-dimensional case, 64-QAM

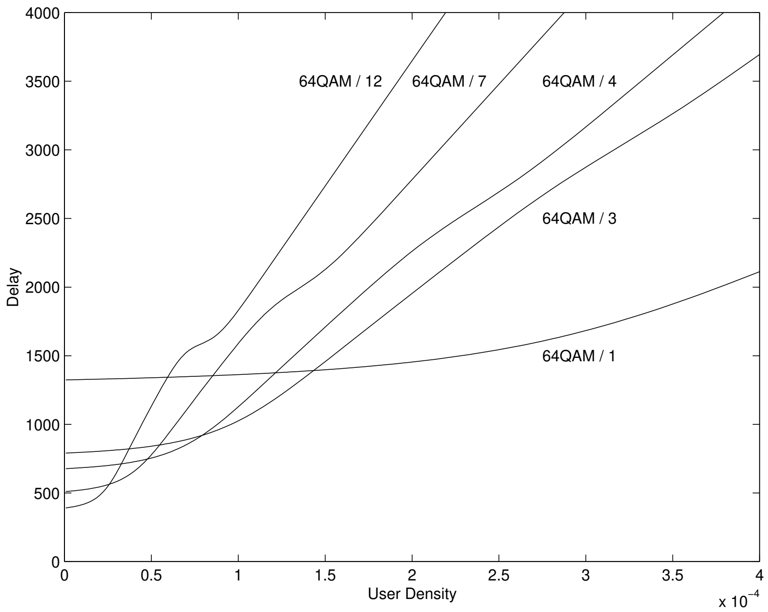

Figure 4.15: Average delay as a function of user density for two-dimensional case, 64-QAM

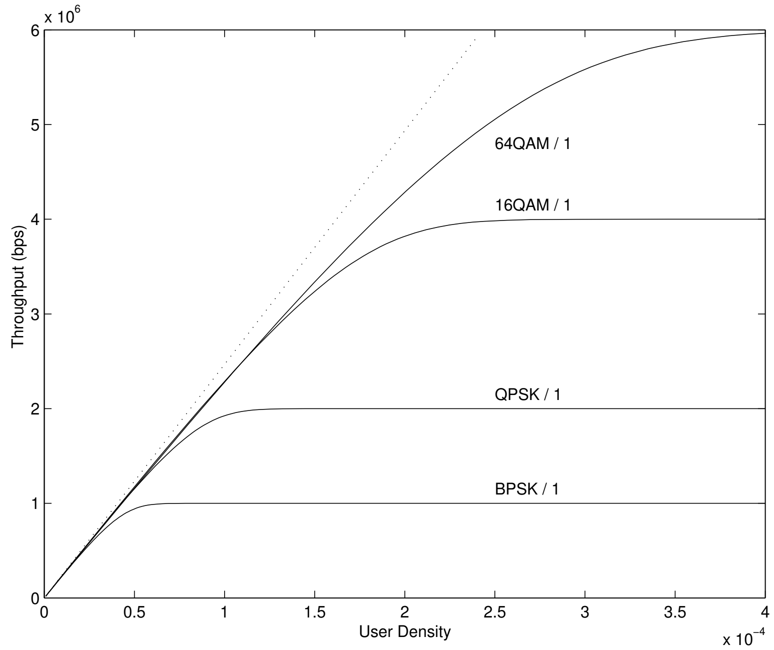

Figure 4.16: Throughput as a function of user density for two-dimensional case, cluster size $N = 1$

effect of using smaller cluster sizes with a fixed modulation, which we just studied.

We can see in Figure 4.16 that higher level modulations (corresponding to smaller coverage areas) can achieve a better throughput as user load increases. But unlike the case of fixed cluster size, smaller coverage does not imply a better throughput for the whole range of user load. As load decreases, lower level modulations become slightly better. This fact is barely distinguishable in Figure 4.16, as the effect is not very significant. The reason why this happens can be recognized in Figure 4.17, where we can see that as load decreases the outage probability of 64-QAM eventually gets worse than that of lower level modulations. Thus, even though the modulation is more efficient, the smaller coverage makes the limiting value of outage probability (see equation (4.21)) slightly larger, resulting in a slightly worse throughput. This didn't happen for fixed modulation, because the limiting value of the outage probability can be shown to be independent of cluster size N.

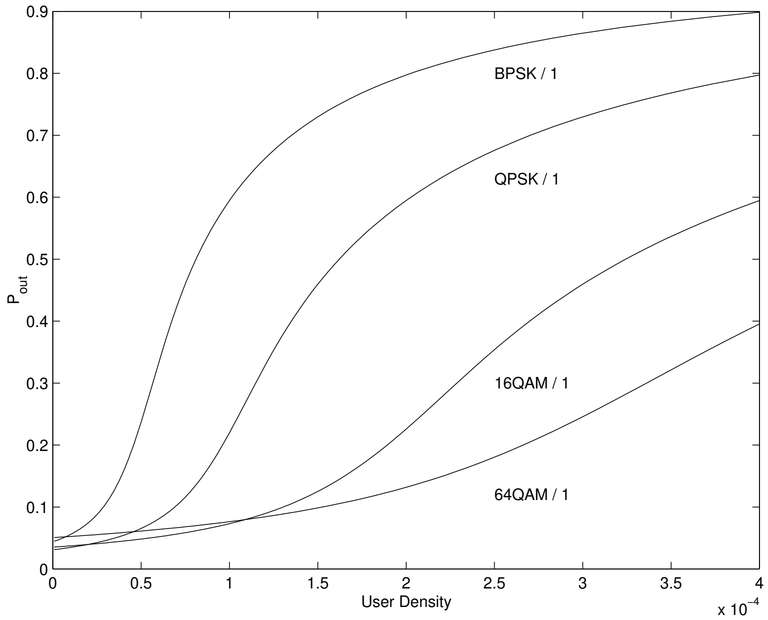

Figure 4.17: Outage probability as a function of user density for two-dimensional case, cluster size $N = 1$

The average delay performance in relation to other modulations depends again on the user density (see Figure 4.18). Higher level modulations only become best as load increases. Otherwise, we are better off with a simpler modulation providing an extended coverage, which reduces the cycle time. The Infostation might want to change the modulation scheme (and thus coverage) depending on the perceived load, thereby adjusting the system for the smallest possible delay.

4.5 Alternative to Backlogged Mailboxes

4.5.1 Analysis

In the context of multiple access algorithms evaluation, two complementary assumptions are usually considered: either *No buffering* or *Infinite set of nodes* [24]. *No buffering* assumes that new packets are discarded when a node is backlogged whereas for *Infinite set of nodes* each newly arriving packet arrives at a new node. In the

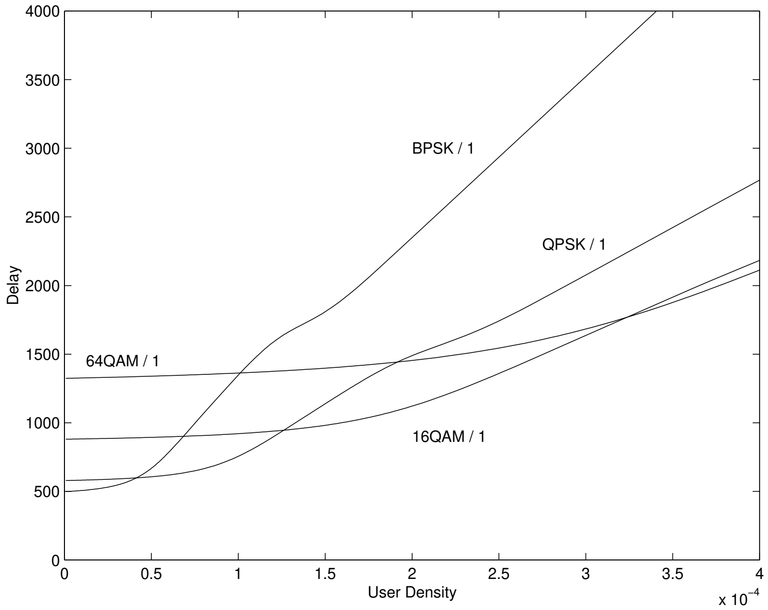

Figure 4.18: Average delay as a function of user density for two-dimensional case, cluster size $N = 1$

analysis of access delay, these assumptions provide respectively a lower and an upper bound to the delay of a wide variety of systems with buffering and flow control.

In our context, we can identify the *No buffering* assumption with our assumption in the past section of backlogged mailboxes, which do not accept new messages until they are completely emptied. We are going to consider now an alternative inspired by the *Infinite set of nodes* assumption. The idea is that this way we will provide an upper bound to delay which will complement the lower bound given by the previous model.

In this alternative model, a message will be created in the network, destined to a certain user. The user location, though, is unknown until the user gets within Infostation coverage, when it will register. Then, the message is put on the Infostation queue, and it will either get served (because the user stays within coverage for enough time) or not (the user leaves coverage before finishing service). If the message is not served, the mobile will eventually visit the coverage of another Infostation, the message will join the corresponding queue, and the process will start again.

The Infostation is modeled once more as an M/M/1 queue with reneging. But now we need to capture the effect that reneging in one queue has in all other queues. That is, in this case we won't have blocking and messages will stay in the system (understood as a network of Infostations) until they eventually get served (or forever, if the system is unstable). An exact calculation would need a multi-dimensional birth-death process approach, using a system-wide state, which is usually unmanageably large. Previous analytical models studying handoff in cellular systems get around this difficulty by isolating a cell of interest and invoking a Poisson process assumption for handoff arrivals to the cell. Interactions among cells are then characterized by relating the mean handoff and departure rates from cells [22, 25]. The validity of this approximation was shown in [26, 27]. We can use the same approximation here, assuming that arrivals that previously reneged in other Infostations form a Poisson process with rate λ_r. We then characterize the interactions among Infostations by equating the mean arrival rate of reneged messages λ_r to the mean reneging rate from an Infostation. To find delay, we will again be interested in the average number of Infostation visits before we are able to download. This is given as $1/(1-P_{out})$, which prompts us to calculate the outage probability P_{out}.

The queueing system is a birth-death process, but now the arrival rate is given by $\lambda' = \lambda + \lambda_r$, that is, the sum of rates of new arrivals and arrivals due to reneging at other queues. Given the service rate μ and the individual reneging rate ν, the death rate is $\mu + k\nu$, where k is the number of users in the system (state). In Appendix C we derive the state probabilities of this queueing system for arrival rate λ. In particular, if we adapt equations (C.7) and (C.8) to arrival rate λ', we have the null state probability

$$p_0 = \frac{(\eta\rho')^\eta}{\eta\, e^{\eta\rho'}\gamma(\eta, \eta\rho')}\,, \tag{4.23}$$

and the general expression for the state probabilities

$$p_k = \frac{(\eta\rho')^k}{k!}\frac{(\eta\rho')^\eta \beta(\eta, k+1)}{e^{\eta\rho'}\gamma(\eta, \eta\rho')}, \tag{4.24}$$

where $\eta = \mu/\nu$, $\rho' = \lambda'/\mu$, $\beta(x, y)$ is the beta function, and $\gamma(x, y) = \int_0^y u^{x-1}e^{-u}du$ is the incomplete gamma function. The mean reneging rate can be calculated as

$$\delta_r = \sum_{k=1}^{\infty} k\nu p_k = \bar{N}\nu, \tag{4.25}$$

where $\bar{N}$ is the average number of users in the system. Using equation (4.24), we can calculate $\bar{N}$ as [28]

$$\bar{N} = \sum_{k=1}^{\infty} kp_k = \eta\rho' - \frac{\gamma(\eta+1, \eta\rho')}{\gamma(\eta, \eta\rho')}. \tag{4.26}$$

If we take the relation $\gamma(x+1, y) = x\gamma(x, y) - e^{-y}y^x$, we can rewrite the expression for $\bar{N}$ as

$$\bar{N} = \eta\rho' - \eta + \frac{(\eta\rho')^\eta e^{-\eta\rho'}}{\gamma(\eta, \eta\rho')}, \tag{4.27}$$

where the structure of p_0 can be recognized (see equation (4.23)). Thus we get

$$\bar{N} = \eta\rho' - \eta(1 - p_0). \tag{4.28}$$

Following the previous discussion, we now relate the mean arrival rate from reneging to the mean reneging rate, that is,

$$\lambda_r = \delta_r. \tag{4.29}$$

Using the definition of ρ' and equations (4.28) and (4.29), we get

$$\rho' = \frac{\lambda + \bar{N}\nu}{\mu} = \frac{\lambda}{\mu} + \rho' - (1 - p_0), \tag{4.30}$$

which results in

$$p_0 = 1 - \frac{\lambda}{\mu}. \tag{4.31}$$

Thus, for a stable system, we have the condition

$$\frac{\lambda}{\mu} \leq 1. \tag{4.32}$$

Adapting equation (C.12) to the new arrival rate, the reneging probability is

$$P_{out} = 1 - \frac{1 - p_0}{\rho'}. \tag{4.33}$$

We don't have a closed-form expression for ρ', but from equations (4.26) and (4.30) we can get the following equation

$$\frac{\lambda}{\nu} = \frac{\gamma(\eta + 1, \eta\rho')}{\gamma(\eta, \eta\rho')}, \tag{4.34}$$

which can be solved numerically for ρ'.

Now that we have P_{out}, we find delay using the expression in equation (4.22), that we used in previous sections, that is,

$$\text{delay} = \frac{\tau_c}{1 - P_{out}} + \tau_q. \tag{4.35}$$

We will not consider throughput because, as we don't have blocking, we either serve all traffic or the system is unstable.

We look now at a numerical example that will compare the results using mailboxes with the results for infinite number of users. We choose just one of the examples, as the results are comparable in other instances. We take the case of a two-dimensional system with 64-QAM modulation and cluster sizes $N = 1$, 3, 4, 7 and 12. In Figure 4.19 are plotted the delay results for the two cases (dashed lines for mailboxes, solid lines for individual messages), using the same parameters as in section 4.4.2. We use only the first component of delay, that is, $\tau_c/(1 - Pout)$, because the influence of τ_Q is marginal and not relevant for comparison purposes. We can appreciate in Figure 4.19 how the two cases act as upper and lower bounds, and how delay for the infinite users case goes to infinity as the system reaches saturation. In fact, what is happening as $\lambda E[X]$ goes to 1 is that the reneging probability approaches 1, such that mobiles keep visiting Infostations forever without ever getting

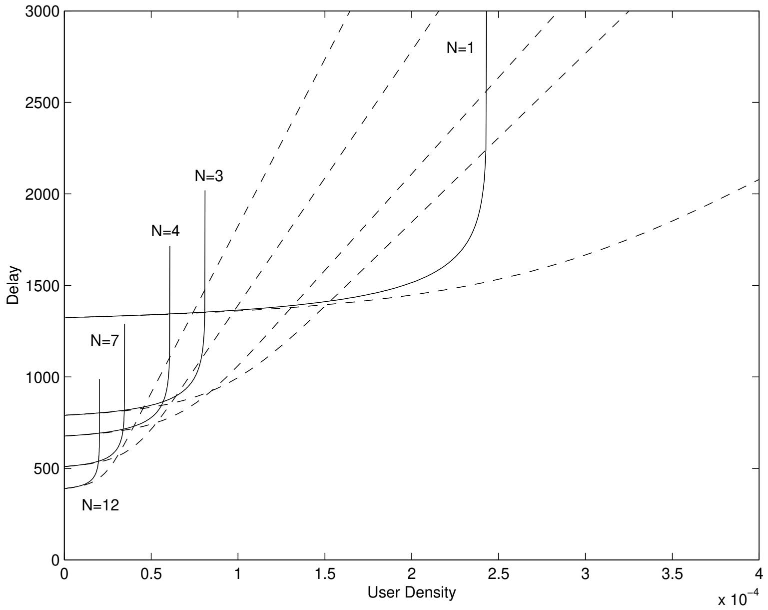

Figure 4.19: Average delay as a function of user density for two-dimensional case, fixed modulation, varying cluster size

service. See Figure 4.20 for the steep increase in reneging probability as we approach saturation.

4.5.2 Simulation Results

We have carried out a simulation experiment for the alternative to backlogged mailboxes (infinite node assumption), to compare with the analysis. We simulate a single circular cell where mobiles with a mailbox to download arrive according to a Poisson process. Then they start moving in a certain direction with constant speed until they either enter the coverage boundary or hit the cell boundary.

If they enter coverage, mobiles join a queue and wait for Infostation availability. While waiting (or even while in service), they might leave coverage, in which case they are removed from the queue (or the server) and the remaining mailbox will be served at some subsequent visit. Otherwise they get the full download and depart from the system.

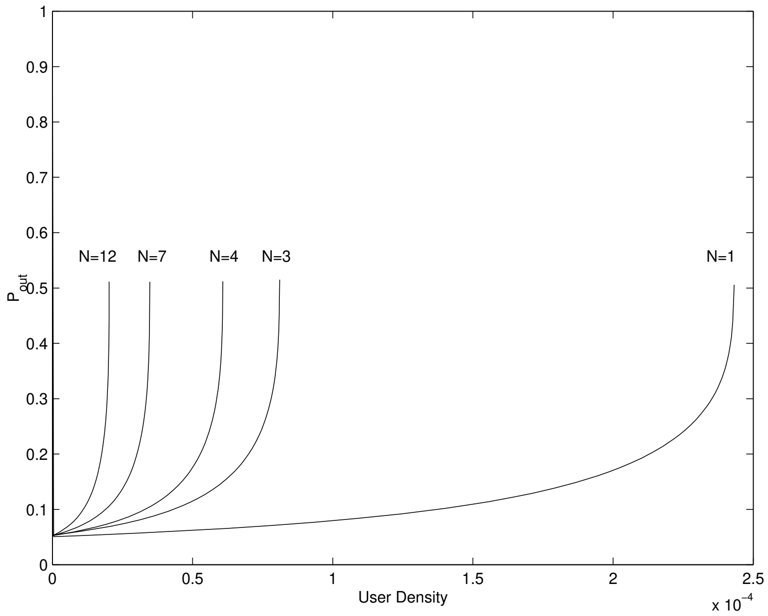

Figure 4.20: Outage probability as a function of user density for two-dimensional case, 64-QAM, varying cluster size $N = 1, 3, 4, 7, 12$

If they hit the cell boundary, mobiles choose a new direction towards the cell. The effect is as if the cell boundary were a reflecting barrier. The new direction is chosen according to the angle distribution given in equation (4.14).

We have considered two cases according to the initial location and direction distributions:

1. Location uniformly distributed at the coverage boundary and direction towards the cell center plus an angle deviation given by the distribution in equation (4.14). Although initially within coverage, mobiles will not get service until they enter coverage again. Thus, they will have to travel for a full cycle before getting a chance to download. This option matches the analysis assumptions in that a mailbox starts message accumulation in one Infostation visit and attempts download in the next visit.

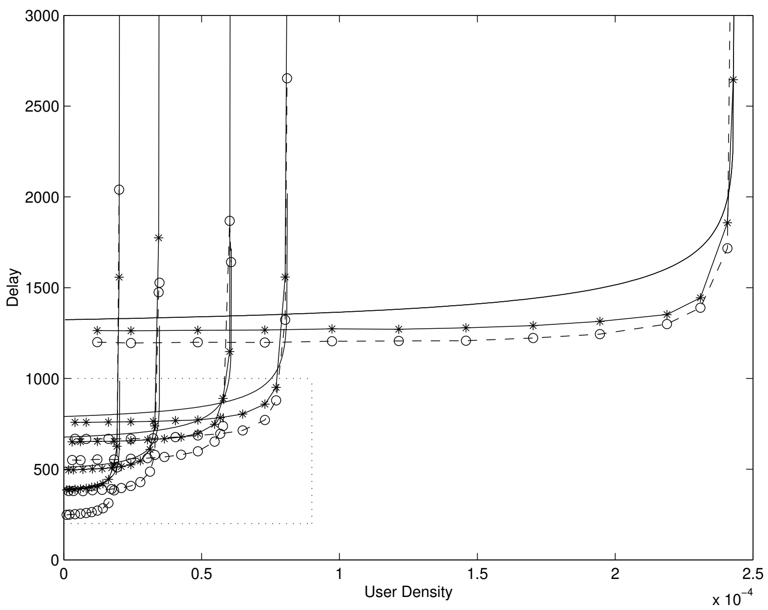

Figure 4.21: Simulation results for the alternative to backlogged mailboxes. Solid continuous lines correspond to analysis, solid lines and stars to simulation case 1, and dashed lines and circles to simulation case 2

2. Location uniformly distributed in the cell area, and direction uniformly distributed in $(0, 2\pi]$.

Simulations have been performed for coverage radii given by modulation 64-QAM and frequency reuse cluster sizes $N = 1, 3, 4, 7, 12$, as in the example in Figure 4.19. The parameter of interest is the average delay experienced by each mailbox, from arrival to departure (full service), which will be compared to $t_c/(1 - P_{out})$ from analysis. The results are shown in Figures 4.21 and 4.22 (the latter zooms in the dotted region in Figure 4.21).

We have plotted with solid continuous lines the results of analysis, with solid lines and stars the simulation results of case 1, and with dashed lines and circles the simulation results of case 2.

There are two sources of mismatch between analysis and simulation: one has to do with cycle time τ_c, the other one with reneging probability P_{out}. Simulation case

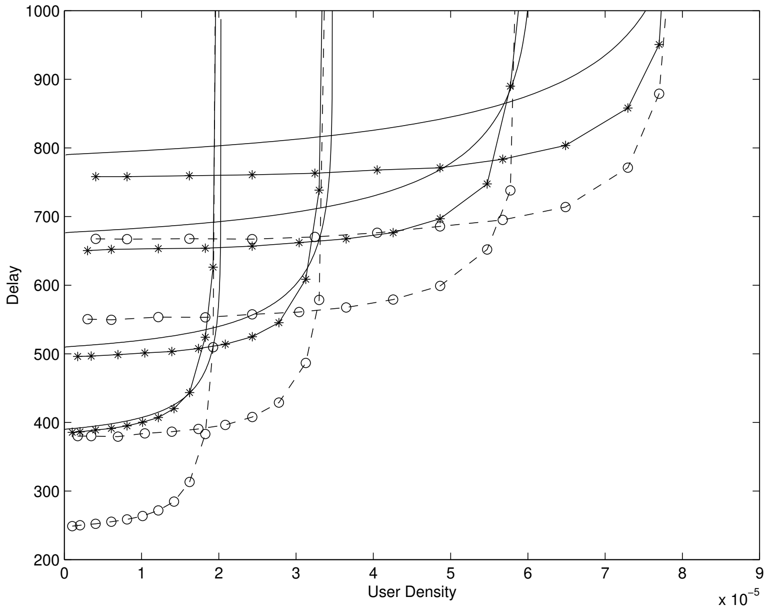

Figure 4.22: Simulation results for the alternative to backlogged mailboxes (zoom in). Solid continuous lines correspond to analysis, solid lines and stars to simulation case 1, and dashed lines and circles to simulation case 2

1 is only affected by the mismatch due to P_{out}, whereas case 2 is affected by both. In the theoretical study, we started counting delay from the previous Infostation visit, such that we always have a full cycle time before getting to the next Infostation. This is what happens also in case 1. In fact, if we make P_{out} very small (for instance, making the mailbox size very small), the theoretical results match case 1 perfectly. In case 2, on the contrary, mobiles may arrive everywhere. Thus, they may hit an Infostation much sooner than a cycle time, giving a smaller delay than in the theoretical analysis.

Regarding reneging probability P_{out}, simulation results give a much smaller value than that predicted by analysis. The reason is the difference in assumptions. In the theoretical study we have that all distributions related to the queueing system are considered exponential. In the simulation, the reneging time is not exponential. This makes P_{out} much larger in theory than in practice. The result is that average delay in the simulation is smaller than in the theory.

Hence, comparing case 1 and case 2, we can see the effect of not having full cycle times. Comparing case 2 with analysis, we have the two effects together.

4.6 Random Walk Mobility Model

We present here an alternative to the mobility model used in the two-dimensional case. This alternative is based on a random walk model in two dimensions that can be solved using finite Markov chains. This type of model is more appropriate for areas where the movements are constrained by a Manhattan-like street structure. It also captures the effect of rate of direction change, expressed as the probability of either going straight or turning at the next corner.

The methodology used is based on the random walk modeling proposed in [29] to calculate cell dwell times. We adapt this method to the case of Infostations to calculate the time it takes for a mobile to cross an Infostation coverage area. With this value, we are able to find the average delay experienced by a message from the instant it arrives to the system until it is finally delivered. We will illustrate this calculation with two cases, with different coverage areas. The analytical results will be compared to simulation results.

4.6.1 System Model

The scenario is an infinite 2-dimensional grid, where each mobile moves in a certain direction that can be changed at every crosspoint. Infostations are located regularly in a quasi-hexagonal tessellation (see Figure 4.23). There is an infinite mobile population, uniformly distributed, which receives messages according to a Poisson process.

From arrival to final delivery, a message will experience a certain delay that will depend on whether the mobile is within coverage or not, the Infostation availability,

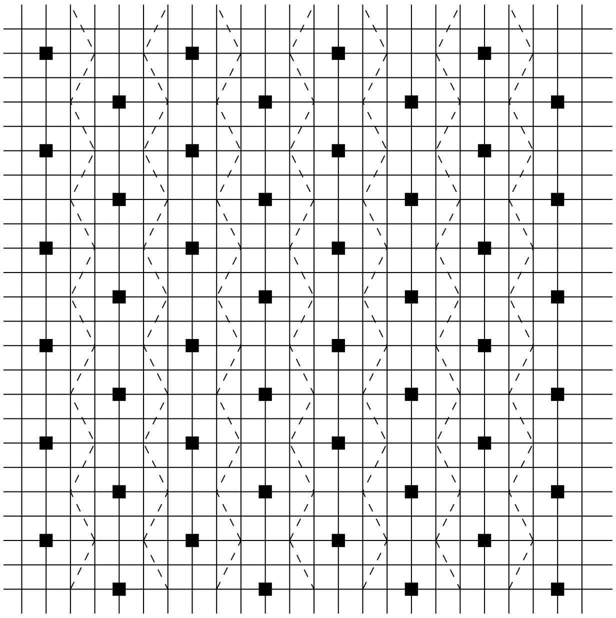

Figure 4.23: Cell layout for random walk mobility model

and the message length. If the mobile is not within coverage, we will have to add the time it takes until the coverage boundary is crossed. Once within Infostation coverage, if the Infostation is idle, message download is started; otherwise the mobile joins a queue and waits for its turn. In either case, the mobile might leave coverage before the message is totally downloaded. If this happens, the mobile will travel until it crosses another coverage boundary, and the process will start again.

We have seen in Section 4.3 how to model an Infostation as an M/M/1 queue with reneging. The result was that the Infostation was characterized by a certain reneging probability P_{out} and a certain wait plus service time, τ_q, in the finally successful Infostation visit. Now we also define τ_0 as the initial time until a coverage boundary is crossed, and τ_c as the cycle time from entering a coverage area until another one is entered. With these values, the average delay experienced by a message will be given by

$$\text{delay} = \tau_0 + \frac{P_{out}\tau_c}{1 - P_{out}} + \tau_q. \tag{4.36}$$

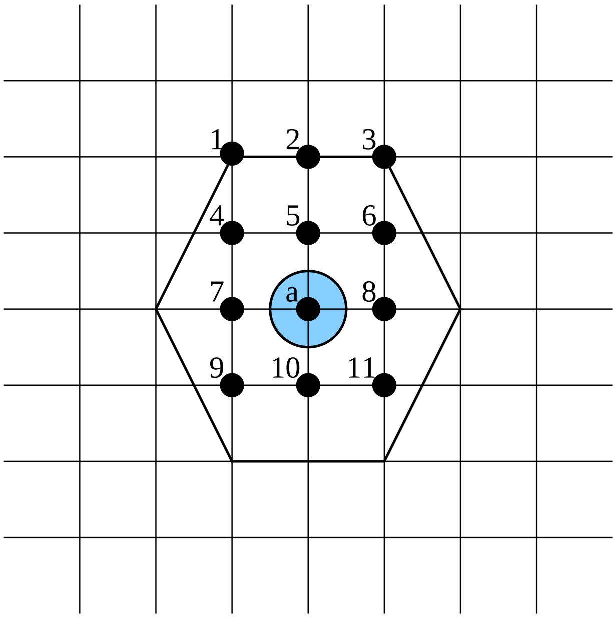

Figure 4.24: Example I

Our interest here will be to determine the values τ_0 and τ_c, as the effect of P_{out} and τ_q is independent of the mobility model, and has been studied already in Section 4.4.

To simplify the analysis, the possible mobile locations are reduced to the grid crosspoints of a single generic cell (hexagon). If the mobile crosses the cell boundary, it appears in the corresponding point of the same cell, as if the cell were folded onto itself. For instance, referring to Figure 4.24, if the mobile leaves point 1 in the upward direction, the next location will be point 9. Or if the mobile leaves point 11 moving to the right, it will appear in point 4. In the example of Figure 4.24, point "a" is the only one within coverage.

The movements between the possible locations will be governed by a random walk process in two dimensions. In this type of process, and in relation to the previous movement direction, the mobile will go straight with a certain probability p_1, will turn to the right (p_2), to the left (p_3), or will backtrack (p_4). Relevant parameters of a random walk process are calculated exploiting the underlying Markov chain that generates movement direction. Finite Markov chain theory gives results for the average number of steps it takes from a given state until another given state is visited for the first time [30]. We will see that we can use these results to calculate τ_0 and τ_c.

4.6.2 Random Walk

The state of the random walk process of a mobile will be given by the point location and the direction used in the preceding movement. Continuing with the example in Figure 4.24, we have 11 points out of coverage plus 1 point within coverage. As we can access every point from 4 different directions, we have 44 states out of coverage and 4 states within coverage.

To calculate τ_0 we need the average number of steps it takes from any state until one of the states within coverage is hit. This problem can be cast as an absorbing Markov chain, where we start at a certain state and the chain evolves until an absorbing state is reached. An absorbing state is one that, once entered, is never again left. In opposition to an absorbing state, a transient state belongs to a set T that, once left, is never again entered. Thus, in the calculation of τ_0, the out-of-coverage states are transient states and the states within coverage are absorbing states. Let us say that there are s transient states and $n-s$ absorbing states. The transition probability matrix of an absorbing chain can be expressed as [30]

$$P = \left(\begin{array}{c|c} I & O \\ \hline R & Q \end{array}\right) \tag{4.37}$$

where I is the $(n-s)\times(n-s)$ identity matrix, O consists entirely of zeros, the $s \times s$ submatrix Q concerns the process as long as it stays in transient states, and the $s\times(n-s)$ submatrix R concerns the transition from transient to absorbing states. The fundamental matrix of an absorbing Markov chain is defined as [30]

$$N = (I-Q)^{-1}, \tag{4.38}$$

with I the identity matrix of the appropriate dimensions. It can be shown that the elements n_{ij} of N give the mean of the total number of times the process is in state s_j given that the initial state was s_i, where $s_i, s_j \in T$. We also define the following vector

$$\tau = (t_1 t_2 \cdots t_s)^T = N\xi \tag{4.39}$$

where ξ is the column vector with all components equal to one. The ith component of τ can be shown to give the average number of steps needed to reach an absorbing state when starting in transient state s_i. If we start in an absorbing state, the time to absorption needs not be calculated as it is directly zero. Thus, with vector τ, the number of absorbing states, and the initial state probabilities, we have all the information we need to calculate the average over all states of the average time to absorption.

As a message may arrive at any location, to calculate τ_0, the initial state probabilities will be uniform. Thus,

$$\tau_0 = \frac{(\tau^T \xi)}{n} \qquad \text{(in steps)} \tag{4.40}$$

where n is the total number of states.

If we apply this solution to Example I in Figure 4.24, we first need to construct matrix Q with all the state transition probabilities of the transient states. The structure of Q will depend on the way the states are numbered and the geometric layout. The construction of Q is the most tedious part, as most of it has to be done manually. Once we have Q, the calculation of N, τ and τ_0 is straightforward. The resulting τ_0, though, is given in steps, and we would rather have it in time units. Thus, we need to multiply by the step size, L, and divide by the mobile speed, to get time units,

$$\tau_0 = \frac{(\tau^T \xi)}{n} \frac{L}{E[V]} \qquad \text{(in seconds).} \tag{4.41}$$

To calculate the cycle time τ_c, we can divide it in two components: the time it takes to leave coverage, τ_{c1}, and the time it takes to enter coverage again, τ_{c2}. To find τ_{c1}, we need to reverse roles: the states within coverage will now be the transient states and the out-of-coverage states become absorbing states. Once this change is made, τ_{c1} is readily calculated as we did for τ_0, with the only provision that not all states can be initial states equally likely. Only the states within coverage that can be reached from out-of-coverage states can be initial states. For Example I in Figure 4.24, these are the four absorbing states corresponding to point "a". In Figure 4.25, we show another example with a bigger coverage area; in this case, we also have four possible initial states, corresponding to the following pairs of location and previous direction: (b,down), (c,right), (d,up), and (e,left). If we call A the set of initial states, we have

$$\tau_{c1} = \frac{\sum_{s_i \in A} t'_i}{|A|} \frac{L}{E[V]} \qquad \text{(in seconds)}, \tag{4.42}$$

where t'_i is the ith component of the new vector τ' (same as τ in equation (4.39), but with new state structure), and $|A|$ is the number of elements in set A.

On the contrary, τ_{c2} can be calculated using the same matrices constructed for τ_0, as the only change is the set of initial states, which now only contains the out-of-coverage states that can be reached from states within coverage. If we call B this set of initial states,

$$\tau_{c2} = \frac{\sum_{s_i \in B} t_i}{|B|} \frac{L}{E[V]} \qquad \text{(in seconds)}, \tag{4.43}$$

where t_i is the ith component of vector τ.

4.6.3 Comparison between Analysis and Simulation Results

In this section, we find the values of τ_0 for Examples I and II in Figures 4.24 and 4.25. These examples correspon to a frequency-reuse cluster size of $N = 1$ and respective

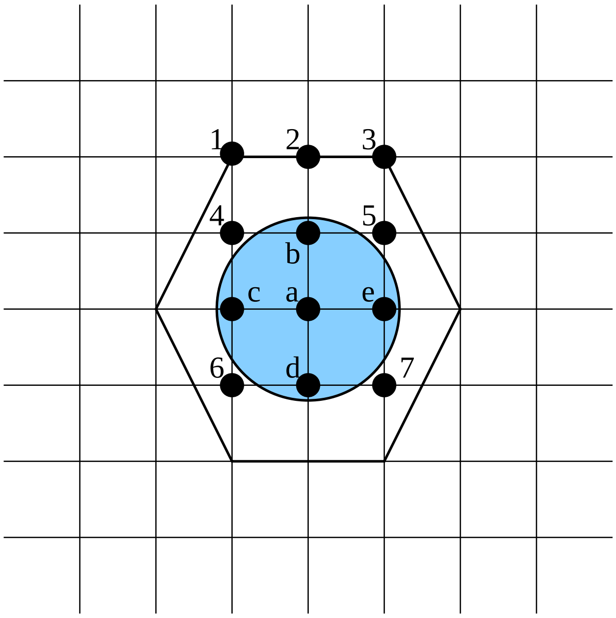

Figure 4.25: Example II

modulations of 64-QAM and BPSK. We then compare these results to a simulation experiment.

As is usual in vehicular mobility, we assume no backtracking ($p_4 = 0$), that we have a relatively high probability of going straight ($p_1 = p$, $p \geq 0.5$), and that we can turn to either side equally likely ($p_2 = p_3 = (1-p)/2$).

The simulation experiment is done using a modified version of MADRAS V3, a simulation environment developed to study radio resource management in wireless communication systems [31]. MADRAS V3 uses a Manhattan-like road grid structure like the one in Figure 4.23, but with a finite number of blocks arranged in a torus-like structure to avoid edge effects. The mobility model is also random walk in two dimensions, parameterized by p, the probability of going straight. Changes were made to MADRAS V3 to adapt the resource management algorithms to Infostations. Mainly, mobiles are allowed to stay in the system when there is no channel (in our case, Infostation) available, so that they can wait until they get into coverage of an idle Infostation.

	Example I		Example II	
p	τ_0 (Markov)	τ_0 (Simulated)	τ_0 (Markov)	τ_0 (Simulated)
0.5	861	852	115	75
0.6	900	885	113	73
0.7	986	969	111	69
0.8	1188	1158	107	68
0.9	1850	1888	106	65
0.95	3212	3174	105	62

Table 4.3: Results from Markovian analysis and from simulation

Although analysis and simulation are based on the same system model, there are the following main differences:

- In the analytical model, mobile locations are restricted to crossroads, whereas in the simulation they can be in any location in the grid lines (up to a certain resolution).
- In the analytical model, effective coverage is given by the outermost crossroad locations within coverage, not by the actual coverage.
- In the analytical model, τ_0 can be calculated directly, whereas in the simulation it is calculated as the message delay minus the average service time, assuming this is a good approximation if load is small (as both P_{out} and the queue waiting time are close to zero).
- In the analytical model, we only have one cell, folded onto itself. In the simulation, we have a structure of 12 by 12 blocks with block size of 500 m, with 12 Infostations in the center of quasi-hexagonal cells.

Table 4.3 shows the results from the Markovian analysis and from the simulation. We can observe that there is a good match for all p values in Example I, but it is not so good for Example II (which only shows an order-of-magnitude agreement). These results prompt us to adjust the analysis.

	Example I		Example II	
p	τ_0 (Markov)	τ_0 (Simulated)	τ_0 (Markov)	τ_0 (Simulated)
0.5	821	852	69	75
0.6	859	885	67	73
0.7	945	969	64	69
0.8	1148	1158	62	68
0.9	1809	1888	59	65
0.95	3172	3174	58	62

Table 4.4: Results from adjusted Markovian analysis and from simulation

4.6.4 Adjustment of Analysis

We adjust here the analytical results to approach the simulated model in two respects:

1. In the simulation, mobiles are born on average at a certain distance from the crossroad. We need to include this initial distance.

2. Coverage may begin in-between crossroads. Thus, the last step is usually smaller than one unit.

If we correct these two effects in the analysis, we get the results of Table 4.4, where we repeat the simulation results for convenience. We can appreciate that in this way the results for Example II show a better agreement with simulation and that the accuracy of Example I has not been affected.

4.7 A Note on Coding

In the past sections we have considered typical modulation schemes but without any coding. We were asking, however, for a high bit error probability of 10^{-3}, typical of voice systems. As our target are data services, we can add coding in order to lower the BER. The question then arises whether coding will reduce the data rate or the coverage. That is, the extra protection given by coding comes at the expense of a certain coding rate which reduces the effective data rate. An example will show that the gains of coding in terms of BER can outweigh what is lost due to coding rate. Of course, we will have to account for added complexity in the transmitter/receiver.

As an example we take uncoded 16-QAM modulation with a BER of 10^{-6}. The corresponding required SIR is 20.4 dB, and we get a bandwidth efficiency of 4. Applying equation (4.3) for a two-dimensional system, we get a corresponding coverage ratio $r/R = 0.33$.

Now we can consider a coded system which provides the same data rate (or the same combined bandwidth-coding efficiency). For instance, we can take 32-QAM as the modulation with a trellis coded modulation scheme providing a total coding rate of 4/5. As the bandwidth efficiency of 32-QAM is 5, the combined coding-modulation efficiency is 4, like uncoded 16-QAM. The coding gain of this scheme with respect to uncoded 16-QAM is 6 dB [18]. Thus, the required SIR for a BER of 10^{-6} is 12.4 dB, which for a two-dimensional system means a coverage ratio r/R=0.5.

Hence, we have two systems with the same efficiency, although the coded system has more coverage, which will result in a smaller delay. In this case, coding gain outweighs the loss in coding rate, making the coded system better. In general, coding is used only if, for a given efficiency, it provides a coding gain. Thus, we can say that a coded system will usually be better. But it will depend on every case whether the gains really justify the use of coding and its added complexity.

4.8 Conclusions

We have found the relation between worst-case SIR and coverage radius for a one-dimensional and a two-dimensional cellular system. We applied then this relation to find the effect of choice of coverage radius, frequency-reuse cluster size, and modulation in the throughput and delay of the Infostation system. Results for an example in the one-dimensional case show that the system works with better throughput and less delay when using a reduced coverage, smaller cluster size, and higher-level modulation. For the two-dimensional case, though, an example shows a trade-off between throughput and delay, so that the best solution will depend on the actual user density (offered load) and relative importance of throughput against delay.

We have also looked at an alternative formulation with an assumption of infinite number of users. The result shows an upper bound to delay that has the same behavior of dependence on load. We have given as well a delay analysis and simulation results for an alternative mobility model, using random walk in a Manhattan-like street structure. Finally, we note that coding can improve the results that we have considered for uncoded systems only.

Chapter 5
Cellular Excess Capacity for Infostations

5.1 Introduction

In Chapter 4, we examined Infostations that were co-located with cellular base stations. In this chapter, we consider Infostations that reuse cellular radio channels to carry data services. By using existing infrastructure, costs can be reduced dramatically. Furthermore, we propose using cellular frequencies by exploiting the excess capacity of some cellular systems. This excess capacity is due to the discrete number of possible solutions in the frequency-reuse pattern. For instance, we may not be able to use a cluster size of 4 by very few dBs, having to jump to cluster size of 7 and possibly having then a fairly good worst-case.

The reused cellular frequencies, though, will be used with a reduced coverage, such that the interference generated does not disturb the performance of the existing cellular system (otherwise the cellular system would already be using a smaller cluster size). The reduced coverage is not a problem for an Infostation, because the services it targets are non-interactive.

This solution should not be confused with the use of overlay/underlay cells in [32]. In that case, the cellular system uses cells that are actually divided in two areas, and there is handoff between them. Here, on the contrary, we reuse channels previously forbidden in a certain cell and utilize them in an Infostation system, while keeping the existing cellular system unchanged.

We will also explore how shadow fading actually increases the effective coverage area of an Infostation, such that fading might be an asset for Infostations.

5.2 Excess Capacity in Cellular Systems

In cellular systems, a threshold signal-to-interference ratio (SIR) is needed to guarantee a certain quality of service. Next, a cluster size, N, is chosen so that the SIR in the worst-case location is above the threshold. In this calculation, the propagation loss law and the use of sectorized antennas are taken into account. Finally, a frequency plan distributes frequencies among the N cells in the cluster.

From an already deployed cellular system like this, we propose to have Infostations that use frequencies forbidden in a particular cell, but restricting to a reduced coverage (that is, using a reduced power) such that the resulting interference to the cellular system is not harmful.

The idea is that we might have a worst-case SIR (say 17 dB) in the cellular system which is higher than the threshold SIR (say 15 dB) due to the fact that we only have discrete solutions to the reuse pattern ($N = 1, 3, 4, 7, \dots$). The excess SIR (in the example, 2 dB) can be used by the Infostation to function with the forbidden frequencies while generating extra interference to the cellular system, up to equating the worst-case SIR to the particular threshold SIR.

For a cellular system, the possibility of introducing such an Infostation system will be highly dependent on the cluster size, sectorization and propagation loss law, that will define the excess SIR available.

If we do have excess SIR, we can then calculate the fraction of power, α, that the Infostation can use relative to that used by cellular base stations. This power will finally give the coverage that the Infostation can provide for a certain Infostation SIR threshold, which is likely to be different from the cellular SIR threshold.

Then, Infostations can use the available cellular channels as a cellular base station would, or they can use higher level modulation if the SIR in the Infostation system

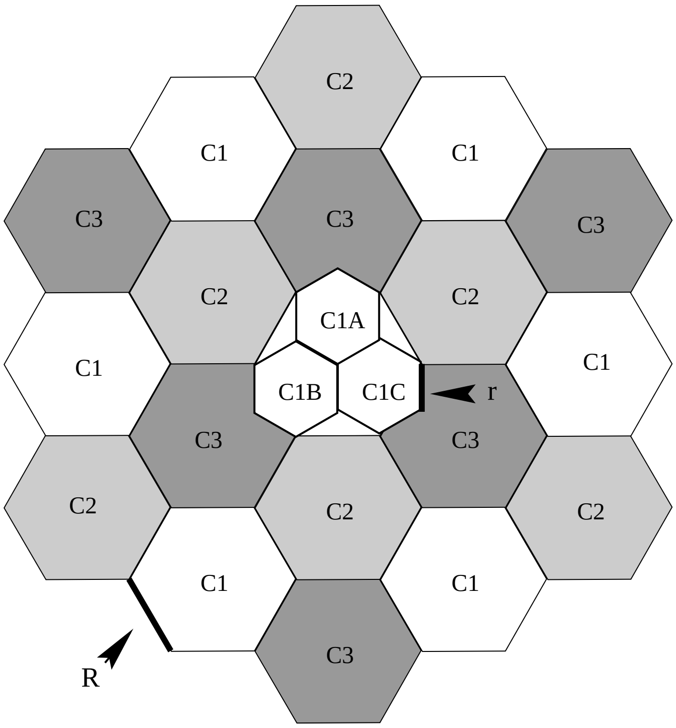

Figure 5.1: A 3/9 cellular layout

is improved, or finally they can pool several cellular frequencies to use as a single wideband channel. This last solution is hampered by the fact that frequency planning usually spaces assigned frequencies apart to avoid near-far effects, but the problem can be bypassed by the use of multicarrier modulation.

5.3 Example in a GSM System

To illustrate the calculation with numerical values, we consider a GSM system with threshold SIR of 15.6 dB and sectorized cells with clusters of type 3/9 (3 cells per cluster, 3 sectors per cell). The sectors are supposed to have hexagonal shape, with radius $r = R/\sqrt{3}$, where R is the cell radius. We have represented the layout in Figure 5.1, showing the sectors only for the central cell. Each type of cell (C1, C2, C3) will use a different set of channels, and each sector within a cell (for instance, C1A, C1B, and C1C for cells of type C1) will use a different subset.

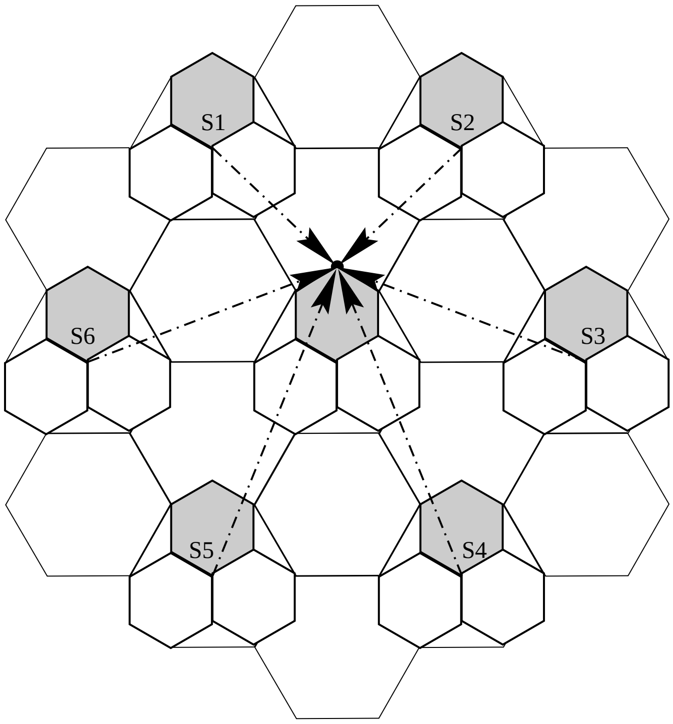

Figure 5.2: Cellular interferers for the worst-case cellular location

The propagation exponent used will be $n = 3.68$, for an urban environment [33]. The value of threshold SIR results from the minimum required SIR in a GSM system (9 dB) plus a 6.6 dB margin to provide for fading protection [33]. In any case, the calculation is illustrative and can be done for any other values.

The worst-case SIR in the cellular system is given by a mobile located at the tip of a sector, at a distance $2r$ from the base station (see Figure 5.2). This mobile will receive interference from six neighboring stations. However, the sectorized antennas result in that, in practice, only two base stations produce significant interference (see an example of antenna gains for corresponding angle directions in Table 5.1).

Assuming that all base stations transmit at the same power level, the worst-case SIR is

$$\mathrm{SIR} = \frac{(2r)^{-n}}{\sum_{i=1}^{6} g_i D_i^{-n}}, \tag{5.1}$$

Interfering station	r-normalized distance	Angle	Antenna gain g_i
S1 and S2	$\sqrt{13}$	134	10^{-4}
S3 and S6	$\sqrt{31}$	69	0.063
S4 and S5	7	21	0.75

Table 5.1: Parameters for 3/9 cluster type

where g_i is the antenna gain and D_i is the distance from a particular base station to the worst-case location. Using the antenna gains in Table 5.1 and the parameter values in the example, equation (5.1) evaluates to 17.5 dB. This means that we have a margin of 1.9 dB above the 15.6 dB required by the GSM voice system. We can use this excess capacity for Infostations.

Now we propose to put an Infostation at each base station location. The question we want to answer is which frequencies they will use and at which power level.

Due to the particular geometry of clusters of size 3 with sectorized antennas and the different antenna gains depending on angle direction, we have that cells C3 get more interference than cells C2 from frequencies used in cells C1 (refer to Figures 5.1 and 5.2). For this reason, we propose that only Infostations located in cells C2 reuse frequencies of cells C1. And analogously for frequencies of cells C2 and C3 (reused only by Infostations in cells C3 and C1, respectively).

Let's then focus on base stations in cells C1 and Infostations in cells C2 (they both use frequencies assigned to cells C1, and thus will mutually interfere). We will assume that the Infostations, unlike the base stations, are not sectorized, and thus use omnidirectional antennas. The worst-case mobile of sector C1A (in the central cell of Figure 5.3) will have an increased interference due to the introduction of Infostations nearby. If we account only for the four closest Infostations' interference (as shown in Figure 5.3), the worst-case SIR results in

$$\mathrm{SIR} = \frac{(2r)^{-n}}{\sum_{i=1}^{6} g_i D_i^{-n} + \sum_{j=1}^{4} \alpha d_j^{-n}}, \tag{5.2}$$

where α is the ratio of powers between an Infostation and a cellular base station,

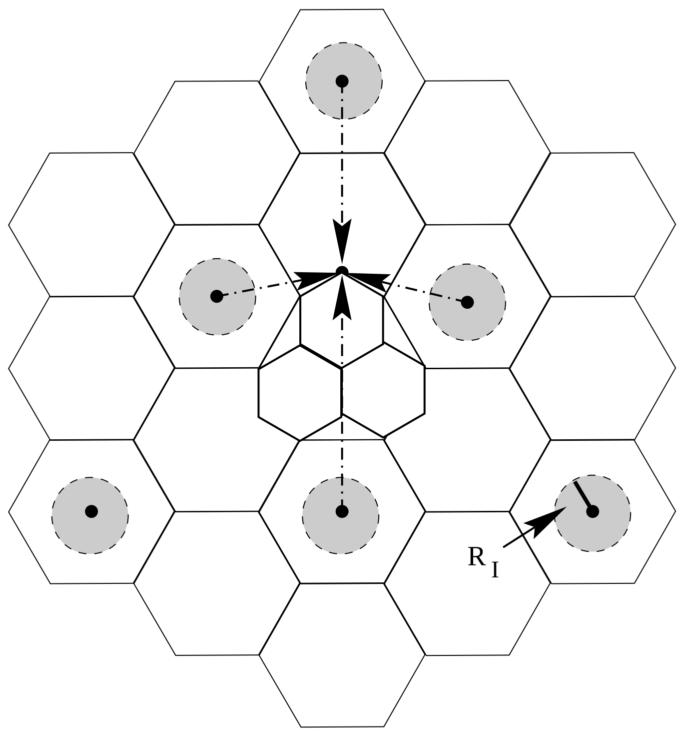

Figure 5.3: Interference generated by Infostations on worst-case cellular terminal location

and d_j is the distance from an Infostation to the worst-case location. Note that we don't use antenna gains for the Infostations, as we are assuming omnidirectional antennas. Now we can find for which value of α the worst-case SIR in the cellular system is equal to the threshold SIR of 15.6 dB. The resulting value is $\alpha = 2 \cdot 10^{-3}$. In other words, Infostations will have to transmit at a power 27 dB below the power transmitted by base stations in order not to interfere with their operation.

Once we have the power ratio α, we can calculate what the Infostation coverage radius R_I will be, assuming a certain value of Infostation threshold SIR. Let's say that in this example the required SIR is also 15.6 dB (we can easily consider any other value, but using this one we can also interpret the Infostation as an extension of the cellular system). We will measure the Infostation worst-case SIR on the location indicated in Figure 5.4.

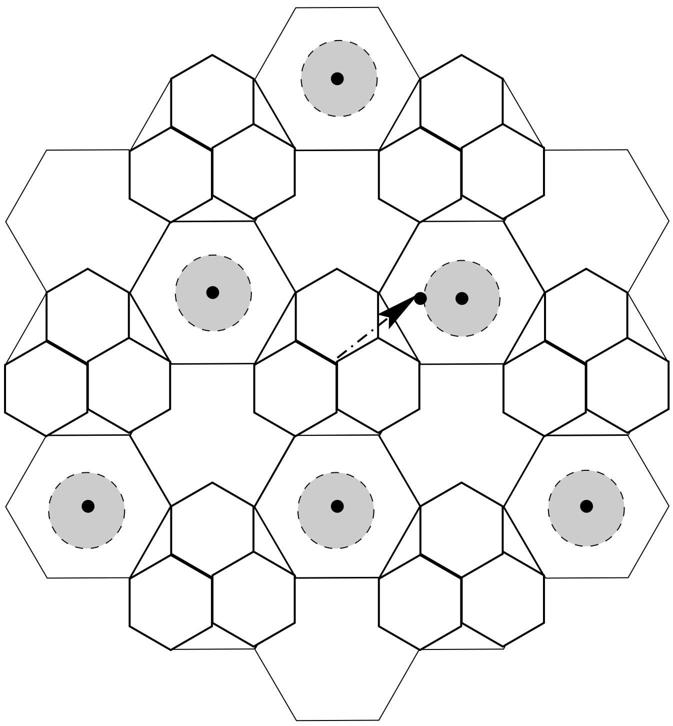

Figure 5.4: Main source of interference for a worst-case Infostation terminal

Due to cellular sectorization, we only need to account for the interference generated by one sector in one base station, in this case from a C1A sector, and we can neglect the influence of other base stations and Infostations. This is because either the antenna gain in the mobile direction is very small, or the antenna gain is high but belongs to a different sector, such that it does not affect the worst-case of the particular frequencies considered. The resulting worst-case SIR is then

$$\mathrm{SIR}_I \approx \frac{\alpha R_I^{-n}}{g\left(\left(\frac{\sqrt{3}R}{2}\right)^2 + \left(\frac{3R}{2} - 1\right)^2\right)^{-n/2}}, \tag{5.3}$$

where g is the base station antenna gain in the direction of the worst-case Infostation mobile location. Note that g is also dependent on the ratio R_I/R.

If we solve equation (5.3) for $\mathrm{SIR}_I = 15.6$ dB and the value of $\alpha = -27$ dB that we obtained, we get

$$\frac{R_I}{R} = 0.16. \tag{5.4}$$

If, for instance, this cellular system has 2 km radius cells, then we can use Infostations with coverage of 320 m radius, reusing cellular frequencies that were previously forbidden.

Although this value of coverage may seem too small, we have to recall that we will be able to reuse a whole set of frequencies, such that by pooling these frequencies the Infostation will be able to work at high data rates. These high data rates will allow message downloads even if we spend little time within Infostation coverage. Furthermore, if Infostation locations coincide with highways, roads or other locations with a high flow of mobiles, the system will be able to serve a high quantity of message downloads.

On the other hand, if mobiles around the base station location are quite stationary (for instance, business users during office hours), then the low rate of handoffs (in spite of small coverage) could make possible the use of the excess capacity by the cellular system itself, as a way to introduce a microcell without having to reorganize the existing frequency plan.

5.4 Effective Coverage in Shadow Fading

Cellular systems are designed from the assumption of ubiquitous coverage. Given that the receiver needs a certain threshold SIR to operate, we can calculate the necessary cluster size for a certain path loss model. However, with Infostations we don't have the requirement on ubiquitous coverage. Thus, as we showed in Chapter 4, we can find several solutions of (coverage, cluster size) pairs, with coverage areas smaller than the cell area. These solutions can then be compared in terms of throughput or delay.

When the propagation model also includes shadow fading, the result in cellular systems is that coverage is a probability cloud, with an increasing probability of outage as the mobile approaches the cell boundary. Ubiquitous coverage is not possible anymore, and there is a need to compromise between effective coverage (less than 100%) and required SIR (that is, cluster size).

In Infostations, the compromise does not exist, as there is no requirement on coverage. Thus, shadow fading could be seen as just reducing the effective coverage, probably affecting throughput and delay. Still, we will show that this is not the case, as the effective coverage is even increased "thanks" to shadow fading. The reason for this increase is that the coverage we gain in parts of the cell previously not covered outweighs what is lost in the previous coverage area.

5.4.1 Log-normal Shadowing

We will assume that the log-normal distribution describes the random shadowing effects. This is to say that the measured signal levels at a certain distance have a Gaussian distribution about the distance-dependent mean, when measured in dBs. The mean is calculated as we would calculate the signal level in a simple path loss propagation model [20].

We will also assume that the SIR is a log-normal random variable. This is an approximation, because when we have several interferers, even if they individually produce log-normal interfering signals, the resulting SIR does not follow a log-normal distribution (a simple interferer would still work). Still, the approximation is quite exact, especially when using the method proposed in [34] to determine the mean and standard deviation.

The SIR in dB will thus be a Gaussian random variable with mean $\overline{\mathrm{SIR}}$ and standard deviation σ. If the threshold SIR is γ, the probability of having coverage

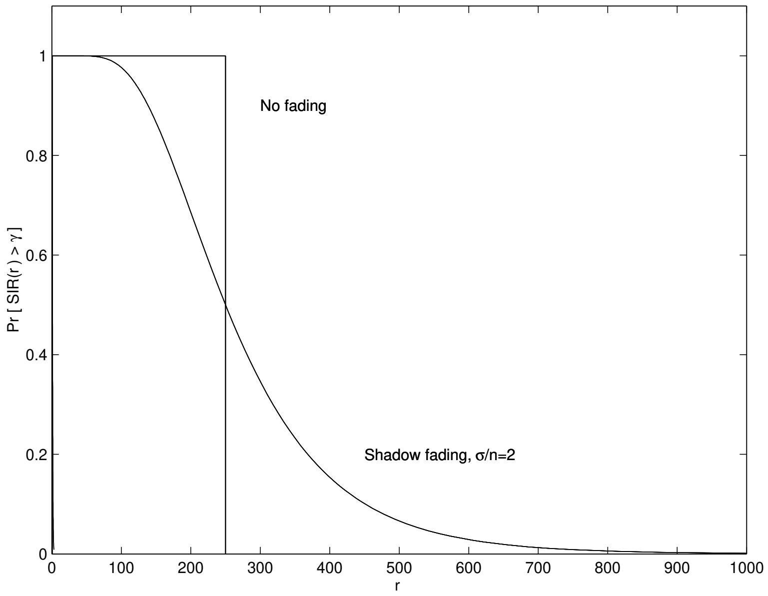

Figure 5.5: Probability of having coverage at distance r

at distance r is given by

$$\Pr[\mathrm{SIR}(r) > \gamma] = \frac{1}{2}\mathrm{erfc}\left[\frac{\gamma - \overline{\mathrm{SIR}}(r)}{\sqrt{2}\sigma}\right]. \tag{5.5}$$

Now suppose that r_0 is the coverage boundary when no fading is present. The introduction of shadow fading extends the coverage area, although with a less than one probability (see Figure 5.5). If we don't change the power levels, the mean SIR value at r_0 will coincide with the SIR value when we don't have fading (that is, $\overline{\mathrm{SIR}}(r_0) = \gamma$). Thus, the probability of having coverage at r_0 is 0.5.

Although the probability of coverage at every distance shows us that coverage is extended, it does not tell us whether the system is able to get to more users or not. That is, we know that we will be able to serve users further away from the Infostation, but we don't know if the total number of users that can be reached has increased. To solve this, we can find $U(r_0, R)$, the relative area covered within the cell boundary R with respect to the area covered when no fading is present (coverage radius r_0),

$$U\left(r_0, R\right)=\frac{1}{\pi r_0^2} \int_0^{2\pi} \int_0^R \Pr[\mathrm{SIR}(r)>\gamma]\, r\, dr\, d\theta. \tag{5.6}$$

Calling $b = 10n\log e/(\sigma\sqrt{2})$, $t = b\ln(r_0/r)$, and $T = b\ln(R/r_0)$, and using the fact that

$$\overline{\mathrm{SIR}}(r) = \overline{\mathrm{SIR}}(r_0) + 10n\log(r/r_0), \tag{5.7}$$

where n is the propagation exponent, we find

$$\begin{aligned} U\left(r_0, R\right) &= \frac{R^2}{2r_0^2} - \frac{1}{r_0^2}\int_0^R \operatorname{erf}\left(b\ln\frac{r}{r_0}\right) r\, dr \\ &= \frac{R^2}{2r_0^2} - \frac{1}{b}\int_{-\infty}^T \exp\left(\frac{2t}{b}\right)\operatorname{erf}(t)\, dt \\ &= \frac{1}{2}\left\{\frac{R^2}{r_0^2}\operatorname{erfc}\left(b\ln\frac{R}{r_0}\right) + e^{1/b^2}\left[1+\operatorname{erf}\left(b\ln\frac{R}{r_0}-\frac{1}{b}\right)\right]\right\}. \end{aligned} \tag{5.8}$$

From equation (5.8), we can see that $U(r_0, R)$ depends on r_0 and R only through the ratio r_0/R. Thus, it can be expressed as a single variable function, which we denote $U(r_0/R)$.

We show $U(r_0/R)$ in Figure 5.6 for several values of σ/n, where we can appreciate that shadow fading not only extends coverage, but it also might increase the fraction of total area with signal above threshold to more than 1. In cellular systems, this could not happen because coverage area (without fading) and cell area coincided. Here, there is room for expansion from the nominal coverage area up to the cell area. But this alone would just explain not losing coverage area. We are even increasing the coverage area because of the geometry: a differential ring has a greater area the greater the radius. Hence, we are able to get to more users if we have coverage at a longer distance from the Infostation. Of course, as can be observed in Figure 5.6, if r_0 is too close to R, the coverage gains from $r_0 < r < R$ do not compensate for the losses in $r < r_0$. The ratio σ/n determines how spread the coverage will be. If we assume a certain propagation exponent n, then the larger the shadow fading standard deviation σ, the higher the probability of having coverage at $r > r_0$, and the greater the gain in coverage area for small r_0/R ratios.

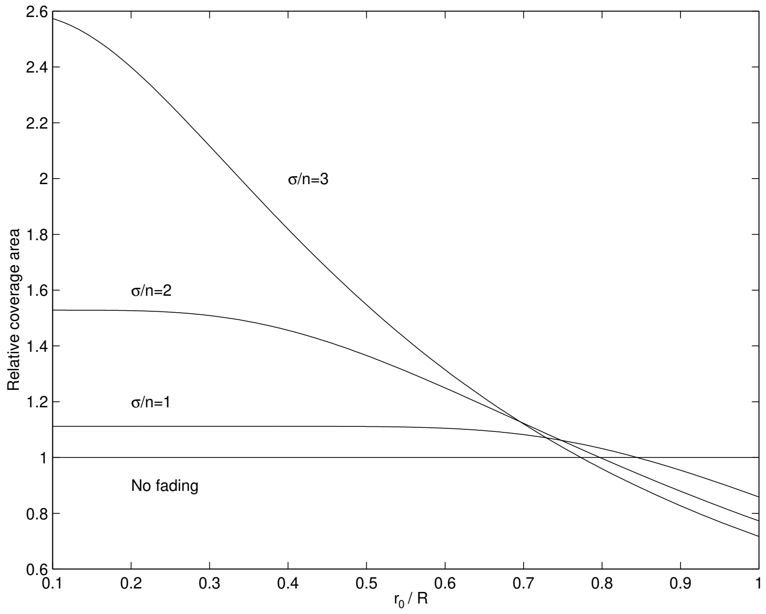

Figure 5.6: Fraction of nominal coverage area with signal above threshold

5.5 Conclusions

We have presented the idea of using excess capacity in cellular systems for Infostations. Through an example, we have shown how to calculate the interference budgets, the resulting power ratio between base stations and Infostations, and the resulting Infostation coverage, which will not affect the performance of the cellular system. The method can be easily applied to any cellular system and, depending on cluster size, it might be possible to achieve a universal frequency reuse with reduced coverage. We have also shown that shadow fading will actually increase the area covered, which may reduce the delay associated with reduced coverage.

Chapter 6
Uplink Access

We studied in Chapter 4 how to decide on a certain coverage radius depending on the combination of modulation, bit error rate and frequency-reuse cluster size desired. And we found that generally there is a best combination in terms of best throughput and delay.

In that model, though, it was assumed that there was no contention in accessing the Infostation, as the Infostation knew which mobile was the next to be served. The focus was on downlink transmission, downloading messages to mobiles that have already registered and contended through some other means. In a practical system, some kind of random multiple access will be used in the uplink in order to contend for the Infostation's attention. These random multiple access schemes usually have certain desirable operating points (or regions) where throughput is relatively high, while keeping the probability of saturation and instabilities relatively low.

We can also calculate for the uplink the coverage associated with a certain combination of modulation, BER and cluster size. But we need to find out how the desired operating point of the random access scheme affects the actual coverage we want to provide. We can have two situations: either the coverage area is so large that too many users try to contend and thus the access algorithm tends to instability; or the coverage area is too small and the Infostation is idle most of the time. In the first case, we would like to shrink the coverage in order to reduce the number of users in contention. In the second case, we can consider expanding coverage with a second ring, where mobiles use a lower data rate, such that we will have contention between

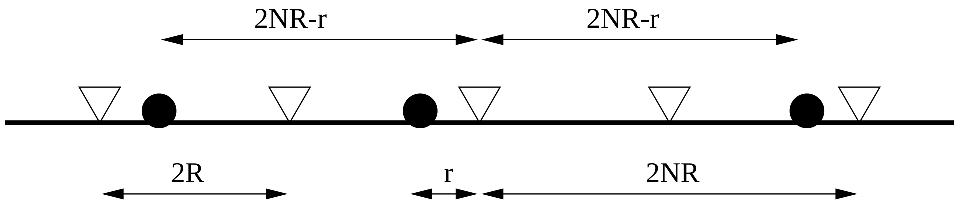

Figure 6.1: One dimensional Infostation system, with uplink interferers located at distance $2NR - r$

two types of users.

Implicit in the discussion is the new assumption that we are able to control the arrival rate by changing the area covered. This is not true in a system where message arrivals are kept in the system waiting for the time when the user gets within coverage. The reason is that all messages will need to be served eventually. If the system capacity cannot handle them, we will have saturation, with messages wandering forever. But we could think of a more static situation, where users barely move, such that only messages generated within coverage will be served. In this case, it makes sense to adjust coverage to control the arrival rate. We could relate this system to a sit-through scenario, like in an airport lounge, where only users in a certain area get service.

In the following, we find the uplink worst-case SIR for both one-dimensional and two-dimensional systems, and we analyze the relation between load and coverage, focusing on a two-dimensional system.

6.1 Worst-case SIR and Coverage Radius, Uplink

From the analysis done in Section 4.2 for the downlink, we can easily derive expressions for the uplink. Now, the receiver is an Infostation, which gets the desired signal from a mobile at the edge of its coverage area. It gets also interference from mobiles at the edge of the coverage area of cochannel Infostations (see Figure 6.1).

In a one-dimensional system, there are two cochannel interferers at a distance $2NR - r$ from the Infostation and the worst-case mobile is at distance r (we called N the frequency-reuse cluster size). With equal transmitted powers, the resulting SIR is

$$\mathrm{SIR} = \frac{1}{2}\left(\frac{2NR}{r} - 1\right)^n, \tag{6.1}$$

where n is the propagation exponent.

In two-dimensions, we will have six cochannel interferers. We approximate the distance from the interferers to the considered Infostation as

$$D_i \approx D - r = \sqrt{3N}R - r, \tag{6.2}$$

where D is the distance between cochannel Infostations. This approximation improves as N increases and r/R decreases, and is exact for some values of N and some ranges of r/R. The resulting SIR in two-dimensions is

$$\mathrm{SIR} = \frac{1}{6}\left(\frac{\sqrt{3N}R}{r} - 1\right)^n. \tag{6.3}$$

Equations (6.1) and (6.3) for uplink are very similar to equations (4.2) and (4.4) for downlink, respectively. If we compare them, we can see that the values of SIR for uplink will be somewhat below those for downlink. Thus, the uplink will require a smaller coverage radius for equal SIR threshold, although the difference is usually relatively small.

Uplink and downlink behave differently also when we have Infostations with heterogeneous coverage areas (different coverage depending on the Infostation considered), or when we have Infostations with several rings of coverage areas (with a different data rate in each). In downlink transmission, we can have Infostations with heterogeneous coverage without affecting the SIR calculations we made in Section 4.2. The reason is that, if all Infostations use the same power, the worst-case SIR is only a function of the mobile (receiver) location, as both intended transmitter and interferers are fixed in space. Thus, every Infostation can use a different modulation scheme (or different for every user, depending on the distance that separates them) without affecting the interference it is creating to its cochannel areas. The same reasoning applies when having several rings of coverage: the interference the mobile gets is the same, whatever ring is in use in the cochannel Infostations.

In uplink transmission, this flexibility is lost. If we have heterogeneous coverage areas, we will have to know the corresponding radii of each cochannel Infostation to calculate the worst-case SIR, as the worst-case interference will be given by the mobile at the edge of each cell. If we use several rings of coverage, the worst-case SIR will be different for every ring, but the worst-case interference is always given by the outermost ring of the cochannel Infostations. Thus, the worst-case SIR for a certain ring depends both on the outer radius of that ring and the radius of the outermost ring of cochannel Infostations. That is, the outermost radius dictates the worst-case interference, and we cannot change it without affecting neighboring cochannel areas. We will see this effect in Section 6.3, where we study the use of two coverage areas.

6.2 Random Multiple Access

Random multiple access algorithms are usually compared in terms of throughput, a dimensionless quantity that includes both the effects of arrival rate and service rate. This throughput is basically a utilization factor, that is, it gives us the probability the server is busy. If all compared options have equally fast servers, then the comparison is fair. But if we are to compare options with different data rates, we have to weight the utilization by the data rate. For instance, we can see in Figure 6.2 a fair comparison of throughput in bits per second of slotted Aloha for several data rates ($c = 1$, 2, 4, and 6 messages per unit time).

A higher data rate will provide an increased throughput for the same offered load and a wider range of offered load that can be served. Still, in the Infostation system

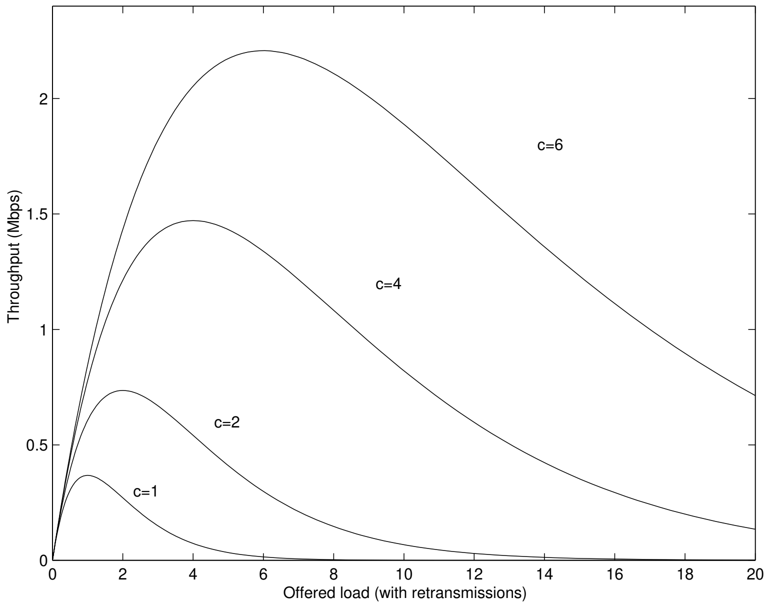

Figure 6.2: Throughput of slotted Aloha for different data rates, c

we don't get an improved data rate for free. We improve the data rate by a reduction in coverage, which in a static situation will affect the amount of new arrivals to the system. In turn, the rate of new arrivals will affect the offered load, such that we can't compare different rates in terms of the same offered traffic. If we take the case of two dimensions, we can consider comparing different rates when having the same rate of new arrivals *per unit area*, δ (assuming a uniform user distribution). In this way, the comparison will be fair, reflecting the fact that a higher data rate will have access to fewer arrivals. The rate of new arrivals will be (in messages per unit time)

$$\lambda(r) = \delta \pi r^2. \tag{6.4}$$

In equilibrium, if the system is stable, throughput will equal the rate of new arrivals (the offered load will be higher, due to collisions and retransmissions). Whatever random access algorithm we choose, it will impose a maximum achievable throughput, either the actual maximum or a smaller value, to provide a fair protection against instabilities. This maximum throughput will dictate the maximum rate of

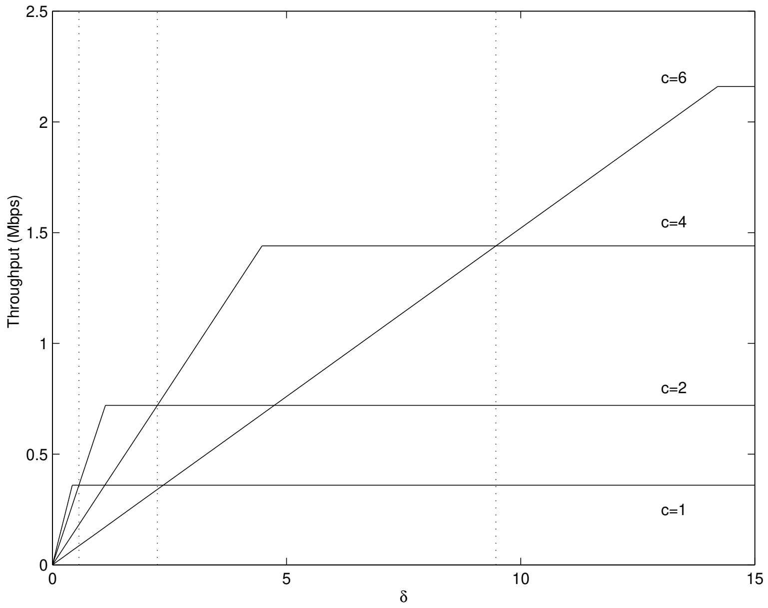

Figure 6.3: Throughput as a function of new arrival rate per unit area, δ, for several rates

new arrivals allowable, λ_{max}. Hence, we have the following constraint on the coverage radius,

$$r \leq \sqrt{\frac{\lambda_{max}}{\delta\pi}}, \tag{6.5}$$

if we don't want to hamper the access algorithm performance. The coverage radius is also affected by the constraint on SIR imposed by the modulation scheme in use and its required SIR, γ. Using equation (6.3), this constraint is

$$\frac{1}{6}\left(\frac{\sqrt{3N}R}{r} - 1\right)^n \geq \gamma. \tag{6.6}$$

From the previous discussion, it follows that if we want to maximize throughput, we will have to maximize the coverage radius subject to the constraints on SIR and maximum arrival rate. The optimum coverage radius is thus

$$r^* = \max\left(\sqrt{\frac{\lambda_{max}}{\delta\pi}}, \frac{\sqrt{3N}R}{(6\,\gamma)^{1/n} + 1}\right). \tag{6.7}$$

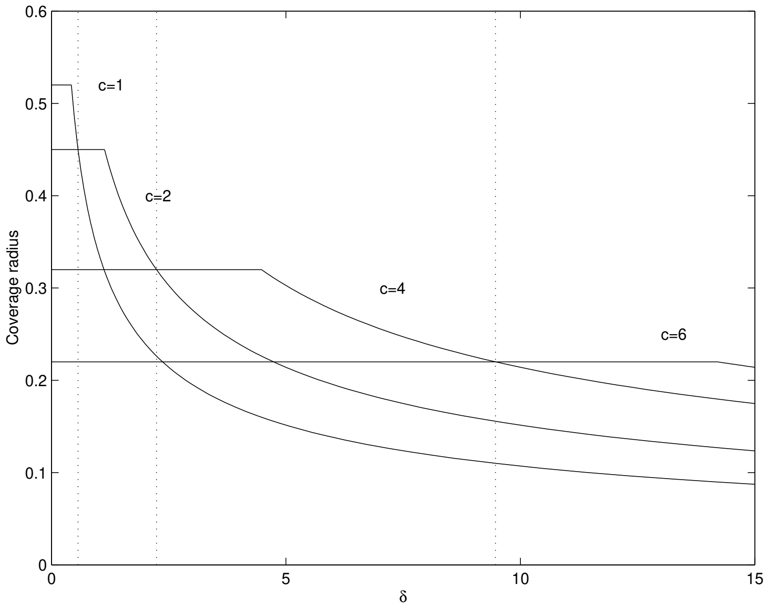

Figure 6.4: Coverage radius as a function of new arrival rate per unit area, δ, for several rates

For instance, if we use modulations BPSK, QPSK, 16-QAM and 64-QAM in AWGN and BER=10^{-3}, we get again relative data rates of $c = 1$, 2, 4, and 6. Let's assume we use slotted Aloha with maximum throughputs as shown in Figure 6.2. If we plot throughput as a function of δ, we get the result in Figure 6.3. We can appreciate that higher data rates will give higher maximum throughput, but it is not true that a higher data rate is always best, as the reduced coverage implies reaching less users. The horizontal portion of the curves corresponds to the access algorithm hitting its maximum throughput, and maintaining it there by reducing coverage as δ increases, according to equality in equation (6.5). Hence, depending on δ, we have a best option in terms of modulation (rate) and coverage. Figure 6.4 gives the corresponding radii as a function of δ, to get the throughput we have shown in Figure 6.3.

6.3 Using Two Coverage Areas

It became apparent in the previous section that, given several possibilities, there is a best coverage radius, with corresponding modulation and data rate, depending on the rate of new arrivals. We want to consider now if we get any improvement by using two coverage areas, instead of just one.

The effect of having two coverage areas (with corresponding data rates) is that a certain message length in bits corresponds to different message lengths in seconds, depending on which coverage area the mobile is located in. Thus, we have two types of users accessing the Infostation: high channel data rate and low channel data rate.

The literature on random access algorithms has considered the effect of two types of users with different data rates. However, the case usually considered is slightly different in that the users are distinguished by their *source* data rate. That is, the channel data rate is considered fixed. Still, some of the results can be extrapolated considering the duality of the two situations.

If we consider thus two channel data rates, we have two solutions for handling low channel rate users: they can either transmit short packets more frequently or they can send longer packets. Note that we refer to packet length in channel time units (say seconds or slots), not in bits.

We focus first in using two packet sizes (longer packets for low rate users). The effect of having variable-length packets on random access algorithms is usually a reduction in total throughput. It was shown in [35] that for Aloha (one channel rate), the mix of two packet sizes produces a reduction in total throughput, the more accused the greater the disparity between the packet lengths. We can apply the same analysis to two channel rates (with channel rates ratio k), trying different values of α, the ratio of long packet length in seconds to short packet length in seconds. The result we get is a throughput region (S_1, S_2) whose boundaries are

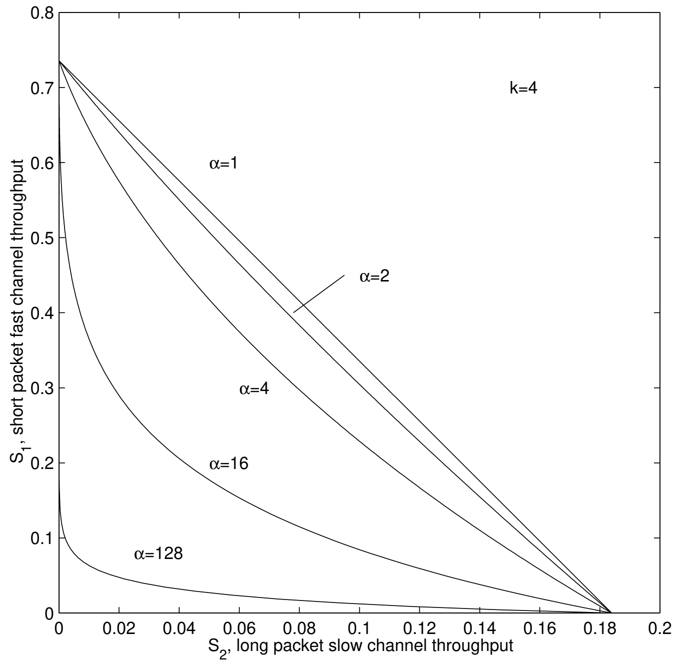

Figure 6.5: Achievable throughput regions in a unslotted Aloha channel with two channel rates and two packet lengths

given by the parametric equations

$$
\begin{aligned}
S_1 &= kG_1 \exp\left(-2G_1 - \left(1 + \frac{1}{\alpha}\right) G_2\right) &\quad (6.8)\\
S_2 &= G_2 \exp\left(-(1+\alpha)G_1 - 2G_2\right) &\quad (6.9)\\
G_2 &= \frac{1 - 2G_1}{\frac{(\alpha-1)^2}{\alpha}G_1 + 2}. &\quad (6.10)
\end{aligned}
$$

We plot in Figure 6.5 this boundary by varying G_1 from 0 (all long packets) to 1/2 (all short packets), with $k = 4$ and several values of α. We can appreciate how a mix of packet lengths degrades the performance, getting a total throughput always below what we could get with equal-length packets. In fact, [36] showed that channel throughput for Aloha is maximized over all possible packet length distributions with fixed length packets.

Similar results for CSMA in [37] show that a relatively small fraction of long packets in the traffic mix can result in a channel utilization close to that obtained with only long packets. However, as the fraction of long packets increases, the fraction of channel capacity due to long packets increases extremely rapidly to the detriment of that due to short packets, which decreases dramatically. This effect would be doubly pernicious when using two channel rates, as the most efficient packets (high data rate, short length) are the ones that get a smaller share.

These results prompt us to abandon the use of variable length packets in favor of the alternative solution of equal size packets, with more frequent packet arrivals for low channel data rate users. In this solution, throughput will be given by the weighted sum of traffic mixes, where the weight is the corresponding data rate. In terms of analysis, the usual assumption is that the source ensures that the arrival of short packets is still a Poisson process.

We apply now this case to the Infostation scenario, where we have a certain nominal value of new arrivals per unit area per second, δ. We consider two coverage areas of radius r_1 and r_2, with $r_1 < r_2$. The inner area uses a higher data rate, R_{c1}, thanks to the better SIR conditions, and the outer area uses a lower data rate, $R_{c2} = R_{c1}/k$. The users in the outer area will send new packets at a rate k times the nominal rate, to compensate for their lower data rate (and the fact of using a fixed packet length in seconds).

We assume that our random access algorithm may work up to a maximum rate of new arrivals, λ_{max}. Thus, the following relation must be kept,

$$\delta\pi r_1^2 + k\delta\pi(r_2^2 - r_1^2) < \lambda_{max}. \tag{6.11}$$

The total throughput will be given by

$$R_{c1}\delta\pi r_1^2 + R_{c2}k\delta\pi(r_2^2 - r_1^2) = R_{c1}\delta\pi r_2^2, \tag{6.12}$$

which, for a given δ, is maximized by taking the maximum radius r_2 possible. Of course, we have the constraints given by equation (6.11) and $r_2 < r_{2,max}$, where $r_{2,max}$ depends on the modulation scheme used and can be found from equation (6.6) and the required SIR on the outer ring, γ_2. Whatever r_2 value we choose, it will set a corresponding value for r_1. This is due to the fact that with two coverage areas the outer radius r_2 determines the location of the worst-case mobiles. Thus, to be able to use the higher level modulation in the inner area, the following relation must hold

$$\gamma_1 \leq \frac{1}{6}\left(\frac{\sqrt{3N}R - r_2}{r_1}\right)^n, \tag{6.13}$$

where γ_1 is the required SIR of the modulation scheme to be used in the inner area. Taking equation (6.13) with equality to just meet the requirement, we can express r_1 as a function of r_2, and substitute this expression into equation (6.11), to get a constraint on r_2 only. Then, we can find the optimum outer radius r_2 from whatever constraint is more restrictive, and finally this value will determine the inner radius r_1.

Figures 6.6 and 6.7 show the optimum radii and throughput as a function of δ for outer area using QPSK and inner area 64-QAM (a rate ratio of $k = 3$), as examples. The dotted lines in these figures show the corresponding values when using just one coverage area, revealing the gain in throughput when using two rings. When density δ is small, the more efficient inner area does not capture enough packets, and that is why it is worth having an outer area. As δ increases, eventually we hit the maximum rate of new arrivals λ_{max}. From this point onward, the increase in throughput is achieved by trading outer radius for inner radius, expanding the more efficient inner area, until we get the two radii to become one, having only one coverage area. From there on, the behavior is the same as for one coverage area.

6.4 Conclusions

We have presented the SIR expressions for uplink, which are complementary to those for downlink in Chapter 4. We then considered the problem of random multiple access, which is specific of uplink. We have assumed a static situation, where users

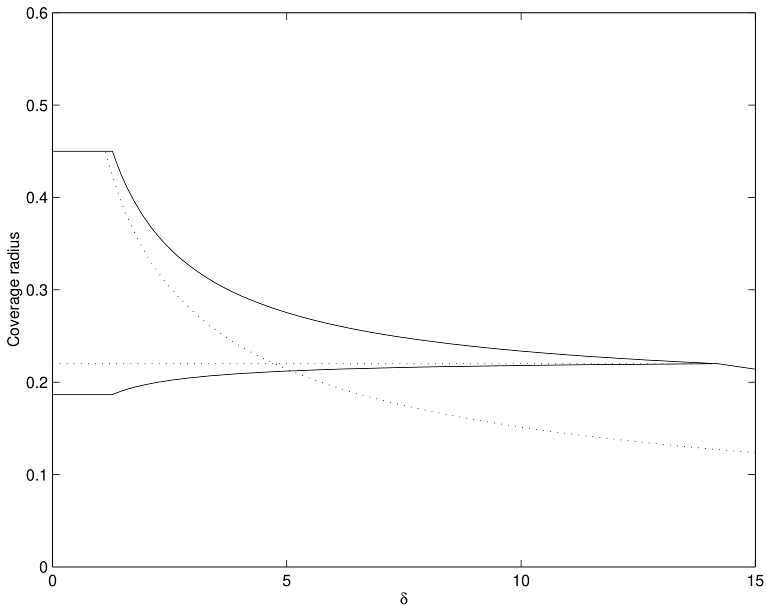

Figure 6.6: Coverage radius as a function of new arrival rate per unit area, δ, for two coverage areas

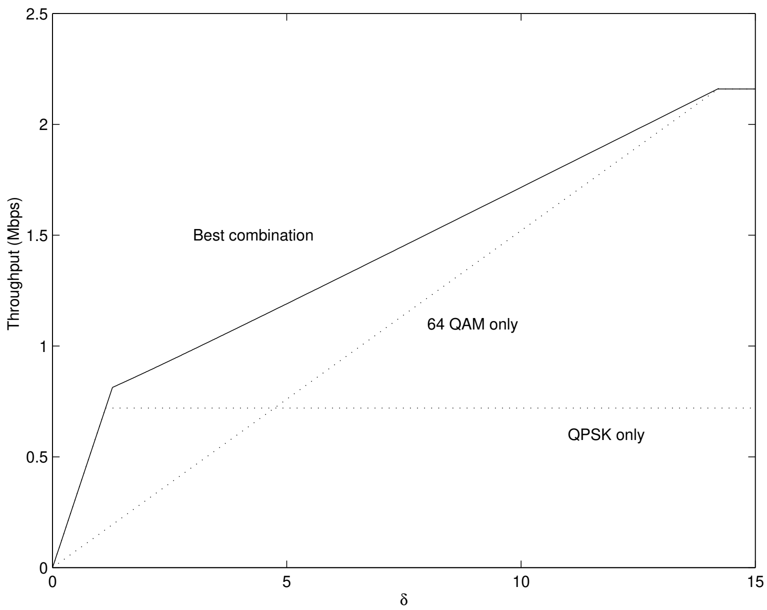

Figure 6.7: Throughput as a function of new arrival rate per unit area, δ, for two coverage areas

barely move, such that the Infostation may control the user load by adjusting the area covered. By characterizing random access algorithms with a maximum rate of new arrivals, we have found the optimal coverage radius that maximizes throughput. Finally, we have studied the case of two data rates, such that coverage is organized in two rings, and we have found the optimum radius for each coverage area.

Chapter 7
Conclusions

Infostations provide a new paradigm for wireless communication systems, particularly wireless messaging services. Its characteristic non-ubiquitous coverage breaks the usual constraint of cellular systems, opening new opportunities for research. Every design parameter of typical cellular systems needs to be challenged to find out how the constraints have changed, providing improved capacity.

This dissertation analyzes several possible Infostation scenarios, from single-user to multiple-user systems, from information-theoretic to more practical analysis with specific modulations. The aim is to show how coverage affects capacity and in some cases also how delay behaves.

7.1 Summary of Main Contributions

Chapter 1 gives an introduction to the idea of Infostations and to the main issues on Infostation design. It sets the stage on the possibilities that Infostations offer and where research should focus. A presentation of the different scenarios considered serves as a guide for the following chapters.

An information-theoretic analysis is presented in Chapter 2, where we consider a single user that travels indefinitely through a line, visiting Infostations periodically. The results show that a reduced coverage is the optimum for both capacity and BPSK cutoff rate.

Chapter 3 still considers a single user, but this time we look at specific modulations, with a certain constraint on the required SNR. We find how the use of several rates affects the performance for BPSK and show that the results are easily extended to any modulation. The effects of variable modulation have also been examined.

We study a multiple user system in Chapter 4, using a cellular layout as the Infostations locations. The reduced coverage of Infostations give an additional degree of freedom making the system design more flexible. The analysis is done for one dimension and for two dimensions, using several modulations and frequency-reuse cluster sizes. Several numerical examples show that for one dimension, the best choice in terms of throughput and delay is a combination of higher-level modulation and small cluster size, that is, the smallest coverage possible. In two dimensions, the best choice depends on the load, resulting in smaller coverage as the load increases.

Chapter 5 shows how Infostations can be introduced in an existing cellular system without using additional bandwidth. An example is provided for a GSM system. We have also explored the possibility of reduced delay thanks to shadow fading.

The special problem of uplink access is considered in Chapter 6, for a static scenario where load depends on coverage. Thus, by controlling coverage we can control load, assuring the stability of whatever random access algorithm is used.

In summary, the contributions of this dissertation are outlined below:

- The information-theoretic capacity for a periodic model is given by a reduced coverage, with power increasing as the mobile approaches the Infostation (Chapter 2).
- The BPSK cutoff rate for a periodic model is given by a reduced coverage, with power that eventually decreases as the mobile approaches the Infostation (Chapter 2).
- The BPSK cutoff rate is insensitive to the use of a suboptimal power control (Chapter 2).
- Best choice of rates (by varying the symbol rate) for a single user using any

modulation scheme (Chapter 3).

- Model for Infostations in a cellular layout, for one and two dimensions (Chapter 4).

- Analysis for one dimension, showing that higher level modulation and smaller cluster size (which result in the smallest coverage) is always the best solution, thus backing the Infostation idea of reduced coverage (Chapter 4).

- Analysis for two dimensions, showing a trade-off between throughput and delay. The best solution depends on the load, with smaller coverage best as load increases (Chapter 4).

- Introduction of an Infostation system in a cellular system without additional bandwidth required (Chapter 5).

- Analysis of the coverage radius that provides optimum throughput in the uplink, for one and two coverage areas (Chapter 6).

7.2 Directions for Future Research

7.2.1 Fading Models

In this dissertation we have been assuming we have AWGN channels, with path loss to account for radio propagation, or fading channels with a certain fading margin. But radio channels are best characterized using randomly time-varying channel models [18]. Even though the effect of shadow fading on coverage has been considered, we would like to look more thoroughly at the influence of random signal fluctuations in the rates and amount of information that can be sent to/from an Infostation. Both log-normal shadowing and small-scale fading (Rayleigh or Rician) need to be considered [20]. The influence of mobile speed will be reflected in the Doppler spread.

7.2.2 Fairness

While working on this dissertation, we have found that obtaining the best schedule and resource allocation policies is not an easy task. The sole definition of "best" policy is already a tricky problem, because of conflicting individual and collective needs. This is the problem of fairness: how to optimize the utilization of resources while providing a satisfactory level of performance for each user or class of users [38].

We can identify suitable performance objectives for the Infostation system and how fairness can be arbitrated. Once we have the performance measures in place, we can study how we can give the same statistical opportunities to all users. Or we may want to have different qualities of service depending on how close to the Infostation the mobiles are, establishing priorities but still trying to be fair. Also, we can date the messages such that the oldest messages get prioritized (regardless or in conjunction with channel conditions). The use of pricing mechanisms has also been proposed to limit the offered traffic [39]. The mechanism works by advertising access fares, and users decide based on these fares whether they will contend. If the system is overloaded, prices will be raised in order to reduce demand.

Performance evaluation, either analytical or by simulation, must be carried out to assess different access strategies.

7.2.3 Measurements and Estimation

In this dissertation, it was assumed that the mobile's location and channel quality were perfectly known at all times. Although this assumption simplifies greatly the analysis, we also want to study how the channel quality can be practically measured in an Infostation system. Furthermore, we would like to evaluate how measurement error reduces system capacity.

7.2.4 Registration and Random Access

The registration process will identify the presence of the user, so that this user can be taken into account in the resource allocation for data transmission. Registration has to use a random multiple access scheme because it has to be done through a common resource. Several random access algorithms exist in the literature and we can study which one could be more adequate for Infostations.

Appendix A
Derivation of the Optimum Average Capacity

We want to solve

$$C = \max_{g(x)} \int_0^r C(x)\pi(x)\,dx\,, \tag{A.1}$$

such that

$$\int_0^r g(x)\,\pi(x)\,dx = 1, \tag{A.2}$$

and

$$g(x) \geq 0, \tag{A.3}$$

where

$$C(x) = \frac{1}{2}\log_2\left[1 + g(x)\cdot\frac{\alpha h^2}{x^2+h^2}\right]. \tag{A.4}$$

As explained in [40], we can include the constraints by using Lagrange multipliers, find the Euler equation and solve the resulting differential equation. In addition, the inequality constraint (A.3) imposes a Kuhn-Tucker condition. Here follows the derivation.

First, we convert the inequality constraint into an equality

$$g(x) - \beta^2(x) = 0 \tag{A.5}$$

and introduce Lagrange multipliers

$$\int_0^r \left(\log\left[1 + g(x)\frac{\alpha h^2}{x^2+h^2}\right]\pi(x) - \lambda(g(x)-1)\pi(x) - \gamma(x)\left(g(x)-\beta^2(x)\right)\right)dx, \tag{A.6}$$

where $\gamma(x)$ depends on x because it corresponds to a non-integral constraint.

If we call the integrand $u(x)$, the Euler equation (see [40]) is

$$\frac{d}{dx}\left(\frac{\partial u}{\partial g'(x)}\right) - \frac{\partial u}{\partial g(x)} = 0 \tag{A.7}$$

and in this case the first term is null. Equation (A.7) becomes

$$-\frac{\partial u}{\partial g(x)} = \frac{1}{1+g(x)\frac{\alpha h^2}{x^2+h^2}} \frac{\pi(x)}{\ln(2)} \frac{\alpha h^2}{x^2+h^2} - \lambda\pi(x) - \gamma(x) = 0. \tag{A.8}$$

The Kuhn-Tucker condition is given by

$$-\frac{\partial u}{\partial \beta} = -2\gamma\beta = 0 \tag{A.9}$$

and multiplying by $\frac{\beta}{2}$

$$\gamma\beta^2 = 0. \tag{A.10}$$

Applying equation (A.5), we obtain

$$\gamma(x)g(x) = 0, \tag{A.11}$$

which means that either $\gamma(x) = 0$ or $g(x) = 0$ or both.

Taking $\gamma(x) = 0$, we have

$$\frac{1}{1+g(x)\frac{\alpha h^2}{x^2+h^2}} \cdot \frac{\pi(x)}{\ln(2)} \cdot \frac{\alpha h^2}{x^2+h^2} - \lambda\pi(x) = 0, \tag{A.12}$$

which gives

$$g(x) = \frac{\frac{\alpha h^2}{\lambda \ln(2)} + h^2 - x^2}{\alpha h^2} \qquad \text{for } g(x) > 0. \tag{A.13}$$

For $\gamma(x) \neq 0$, $g(x) = 0$. As we see, the shape of the $g(x)$ function is the same regardless of the distribution $\pi(x)$, which only affects the value of the adjusting parameter λ. Summarizing the result,

$$g(x) = \begin{cases} \dfrac{x_c^2 - x^2}{\alpha h^2} & \text{for } x \leq x_c, \\ 0 & \text{otherwise,} \end{cases} \tag{A.14}$$

where $x_c^2 \triangleq \frac{\alpha h^2}{\lambda \ln(2)} + h^2$ can be seen as a threshold distance beyond which no power is allocated and the transmitter just shuts off.

To determine x_c we apply the constraint

$$\int_0^{x_c} \left(\frac{x_c^2 - x^2}{\alpha h^2} \right) \pi(x) dx = 1, \tag{A.15}$$

which for a uniform probability distribution gives a closed-form solution, and in general can be solved by numerical methods. And once we know x_c, we have the average capacity

$$C = \int_0^{x_c} \frac{1}{2} \log \left(\frac{x_c^2 + h^2}{x^2 + h^2} \right) \pi(x) dx. \tag{A.16}$$

We can use now the uniform probability distribution of our model. We have two cases:

- When $x_c \leq r$, which is our case of interest, the active radius is x_c, and solving we get

$$x_c = \left(\frac{3}{2} \alpha h^2 r \right)^{1/3}, \tag{A.17}$$

$$C = \frac{x_c}{r \ln 2} - \frac{h}{r \ln 2} \arctan \left(\frac{x_c}{h} \right), \tag{A.18}$$

  and this happens when $r > r_{\min} = \sqrt{\frac{3}{2} \alpha h^2}$.

- When $x_c > r$ (that is, $r < r_{\min}$), then the active radius will only be the whole radius r, and x_c will not have a physical interpretation. The value for x_c is:

$$x_c = \left(\alpha h^2 + \frac{r^2}{3} \right)^{1/2}. \tag{A.19}$$

Appendix B
Distance to Cochannel Infostations

We give here the exact expressions for the distances D_i between a mobile (located at distance r from an Infostation) and the first ring of cochannel interfering Infostations (in two dimensions), as a function of the frequency-reuse cluster size N and for given cell radius R. These values can be derived using geometric arguments.

- For $N = 1$:

$$D_1^2 = D_2^2 = \left(\frac{\sqrt{3}}{2}R\right)^2 + \left(\frac{3}{2}R - r\right)^2, \tag{B.1}$$

$$D_3^2 = D_6^2 = \left(\sqrt{3}R\right)^2 + r^2, \tag{B.2}$$

$$D_4^2 = D_5^2 = \left(\frac{\sqrt{3}}{2}R\right)^2 + \left(\frac{3}{2}R + r\right)^2. \tag{B.3}$$

- For $N = 3$:

$$D_1^2 = (3R - r)^2, \tag{B.4}$$

$$D_2^2 = D_6^2 = \left(\frac{3\sqrt{3}}{2}R\right)^2 + \left(\frac{3}{2}R - r\right)^2, \tag{B.5}$$

$$D_3^2 = D_5^2 = \left(\frac{3\sqrt{3}}{2}R\right)^2 + \left(\frac{3}{2}R + r\right)^2, \tag{B.6}$$

$$D_4^2 = (3R + r)^2. \tag{B.7}$$

- For $N = 4$:

$$D_1^2 = D_2^2 = \left(\sqrt{3}R\right)^2 + (3R - r)^2, \tag{B.8}$$

$$D_3^2 = D_6^2 = \left(2\sqrt{3}R\right) R^2 + r^2, \tag{B.9}$$

$$D_4^2 = D_5^2 = \left(\sqrt{3}R\right)^2 + (3R + r)^2. \tag{B.10}$$

- For $N = 7$:

$$D_1^2 = \left(\frac{5\sqrt{3}}{2}R\right)^2 + \left(\frac{3}{2}R - r\right)^2, \tag{B.11}$$

$$D_2^2 = \left(\frac{\sqrt{3}}{2}R\right)^2 + \left(\frac{9}{2}R - r\right)^2, \tag{B.12}$$

$$D_3^2 = \left(2\sqrt{3}R\right)^2 + (3R - r)^2, \tag{B.13}$$

$$D_4^2 = \left(\frac{5\sqrt{3}}{2}R\right)^2 + \left(\frac{3}{2}R + r\right)^2, \tag{B.14}$$

$$D_5^2 = \left(\frac{\sqrt{3}}{2}R\right)^2 + \left(\frac{9}{2}R + r\right)^2, \tag{B.15}$$

$$D_6^2 = \left(2\sqrt{3}R\right)^2 + (3R + r)^2. \tag{B.16}$$

- For $N = 9$:

$$D_1^2 = D_2^2 = \left(\frac{3\sqrt{3}}{2}R\right)^2 + \left(\frac{9}{2}R - r\right)^2, \tag{B.17}$$

$$D_3^2 = D_6^2 = \left(3\sqrt{3}R\right) R^2 + r^2, \tag{B.18}$$

$$D_4^2 = D_5^2 = \left(\frac{3\sqrt{3}}{2}R\right)^2 + \left(\frac{9}{2}R + r\right)^2. \tag{B.19}$$

- For $N = 12$:

$$D_1^2 = (6R - r)^2, \tag{B.20}$$

$$D_2^2 = D_6^2 = \left(3\sqrt{3}R\right)^2 + (3R - r)^2, \tag{B.21}$$

$$D_3^2 = D_5^2 = \left(3\sqrt{3}R\right)^2 + (3R + r)^2, \tag{B.22}$$

$$D_4^2 = (6R + r)^2. \tag{B.23}$$

Appendix C
The M/M/1 Queue with Reneging

We analyze this system because it is used in Chapter 4 to model the behavior of an Infostation.

An M/M/1 queue is a queueing system with Poisson arrivals, exponential service time, a single server and infinite queue size [41]. An M/M/1 queue *with reneging* is a M/M/1 queue where units can be lost before completing service due to random time-out periods [28]. That is, every unit that joins the system may renege before completing service if its sojourn time extends beyond its time-out period.

We will assume that time-out (or reneging) periods are i.i.d. exponential random variables with rate ν. The arrival rate is λ and the service rate is μ. We will also use the respective ratios $\rho = \lambda/\mu$ and $\eta = \mu/\nu$ of the arrival rate to service rate and the service rate to the reneging rate.

C.1 Stationary State Distribution

This queueing system is a birth-death process, with the number of units in the system as state. The birth rate is λ and the death rate at state k is $\mu + k\nu$. From the birth-death equations, we can easily find the stationary state distribution p_k as [28]

$$p_k = \frac{\lambda^k}{\prod_{j=1}^{k}(\mu + j\nu)} p_0 = \frac{(\eta\rho)^k}{\prod_{j=1}^{k}(\eta + j)} p_0. \tag{C.1}$$

Alternatively, we can express equation (C.1) using gamma functions as

$$p_k = \frac{(\eta\rho)^k\Gamma(\eta+1)}{\Gamma(\eta+k+1)}p_0. \tag{C.2}$$

We can further elaborate using the beta function $\beta(x,y) = \Gamma(x)\Gamma(y)/\Gamma(x+y)$, resulting in

$$p_k = \frac{(\eta\rho)^k}{k!}\frac{\Gamma(\eta)\Gamma(k+1)}{\Gamma(\eta+k+1)}\eta p_0 = \frac{(\eta\rho)^k}{k!}\beta(\eta,k+1)\,\eta p_0. \tag{C.3}$$

This expression will help us find p_0 through the total probability theorem,

$$1 = \sum_{k=0}^{\infty} p_k = \sum_{k=0}^{\infty}\frac{(\eta\rho)^k}{k!}\beta(\eta,k+1)\,\eta p_0. \tag{C.4}$$

To solve the summation, we use the integral form of the beta function

$$\sum_{k=0}^{\infty}\frac{(\eta\rho)^k}{k!}\eta\,\beta(\eta,k+1) = \eta\sum_{k=0}^{\infty}\int_0^1\frac{(\eta\rho z)^k}{k!}(1-z)^{\eta-1}\,dz = \eta\int_0^1 e^{\eta\rho z}(1-z)^{\eta-1}\,dz, \tag{C.5}$$

where we have interchanged summation and integration. Then, we can use the incomplete gamma function $\gamma(x,y) = \int_0^y u^{x-1}e^{-u}du$ to express equation (C.5) as

$$\sum_{k=0}^{\infty}\frac{(\eta\rho)^k}{k!}\eta\,\beta(\eta,k+1) = \frac{\eta\,e^{\eta\rho}}{(\eta\rho)^\eta}\gamma(\eta,\eta\rho). \tag{C.6}$$

Hence, the expression for the null state probability is

$$p_0 = \frac{(\eta\rho)^\eta}{\eta\,e^{\eta\rho}\gamma(\eta,\eta\rho)}, \tag{C.7}$$

and the general expression for the stationary probabilities is

$$p_k = \frac{(\eta\rho)^k}{k!}\frac{(\eta\rho)^\eta\beta(\eta,k+1)}{e^{\eta\rho}\gamma(\eta,\eta\rho)}. \tag{C.8}$$

C.2 Reneging Probability

The reneging probability is the probability that an arriving unit will leave the system before finishing service because of reneging. Outage probability will be an alternative name for the reneging probability, and we will represent it as P_{out}. It is given by the average reneging rate normalized by the arrival rate,

$$P_{out} = \frac{1}{\lambda}\sum_{k=1}^{\infty} \nu k p_k. \tag{C.9}$$

In [28], it is shown that the reneging probability can be expressed as

$$P_{out} = 1 - \frac{\gamma(\eta+1, \eta\rho)}{\eta\rho\,\gamma(\eta, \eta\rho)}. \tag{C.10}$$

We have found an alternative expression that relates P_{out} with p_0, so that we can easily calculate P_{out} if we have already calculated p_0 from equation (C.7). From equation (C.9), we can get

$$P_{out} = \frac{1}{\lambda}\left[\sum_{k=1}^{\infty}(\mu + k\nu)p_k - \mu + \mu p_0\right], \tag{C.11}$$

and using the fact that the average number of departures $\sum_{k=1}^{\infty}(\mu + k\nu)p_k$ has to be equal to the average number of arrivals λ for a stationary state distribution to exist, the result is

$$P_{out} = 1 - \frac{\mu}{\lambda}(1 - p_0). \tag{C.12}$$

C.3 Reneging Probability for FCFS Queueing Policy

We find now the reneging probability of an arriving unit that finds k units already in the system, assuming an FCFS queueing policy. This value, which we will call $P_{out|k}$, is related to the reneging probability P_{out} through

$$P_{out} = \sum_{k=0}^{\infty} P_k P_{out|k}. \tag{C.13}$$

Keeping in mind that we are using an FCFS policy, we have that

$$(1 - P_{out|k}) = \left[\prod_{i=1}^{k} P(i|i+1)\right] Prob\{\text{Complete service if nobody in system}\}, \tag{C.14}$$

where $P(i|i+1)$ is the probability that a mobile in position $i+1$ in the queue moves to position i before it gets out of coverage. The mobile in position $i+1$ will advance if the remaining dwell time (or time within coverage) exceeds either 1) at least one of the remaining dwell times T_j, $j = 1, 2, \ldots i$ for any mobile ahead of it in the queue, or 2) the service time of the mobile being served. Thus we can find that

$$1 - P(i|i+1) = \frac{\nu}{(\mu+\nu) + i\,\nu} = \frac{\nu}{\mu + (i+1)\,\nu}. \tag{C.15}$$

Similarly

$$Prob\{\text{Complete service if nobody in system}\} = \frac{\mu}{\mu+\nu}, \tag{C.16}$$

which gives

$$P_{out|k} = 1 - \frac{\mu}{\mu+\nu} \prod_{i=1}^{k} \left(1 - \frac{\nu}{\mu + (i+1)\,\nu}\right) = \frac{(k+1)\,\nu}{\mu + (k+1)\,\nu}. \tag{C.17}$$

We have checked numerically that by using the results in equations (C.17) and (C.8), the value of P_{out} given in equation (C.13) coincides with the general one in equation (C.12).

This result also corrects an error in an often cited paper [22]. We contacted the authors of [22], and they released a correction [42] acknowledging our contribution.

C.4 Mean Queue Waiting Time for FCFS Queueing Policy

For a FCFS queue, the queue waiting time of a unit is independent of its service time. Therefore, we can calculate the mean queue waiting time without conditioning to service time.

One distinction we can make is to calculate the mean queue waiting time of units that finish service only or to do it for all units. The values are different.

C.4.1 Considering only Units that Finish Service.

We will call successful units those units that will finish service. A successful unit that finds k units in the system will occupy position $k+1$ in the queue. If we define t_k as the time until the next end of service or reneging among the first k units, we have that

$$\begin{aligned} P(t_k = t|(k+1) \text{ successful}) &= \frac{P((k+1) \text{ successful}|t_k = t)P(t_k = t)}{P((k+1) \text{ successful})} && \text{(C.18)} \\ &= \frac{e^{-\nu t}\frac{\mu}{\mu+k\,\nu}(\mu + k\,\nu)e^{-\left(\mu+k\,\nu\right)t}}{\frac{\mu}{\mu+(k+1)\,\nu}} && \text{(C.19)} \\ &= \left(\mu + (k+1)\,\nu\right)e^{-\left(\mu+(k+1)\,\nu\right)t}. && \text{(C.20)} \end{aligned}$$

Thus, the mean time for the successful unit in position $k+1$ to advance to position k is

$$\bar{t}_k = \frac{1}{\mu + (k+1)\,\nu}, \tag{C.21}$$

and the total mean time in queue for a successful unit that finds k units in the system is

$$W_{qs}^{(k)} = \sum_{i=1}^{k} \frac{1}{\mu + (i+1)\,\nu} = \frac{\Psi(k+2+\eta) - \Psi(2+\eta)}{\nu}, \tag{C.22}$$

where we have used the Digamma function $\Psi(x) = d\ln\Gamma(x)/dx$.

The probability of finding k units in the system for a successful unit is

$$Q_k = \frac{(1 - P_{out|k})P_k}{1 - P_{out}}. \tag{C.23}$$

And, with these, we can find the mean queue waiting time for successful units as the summation

$$W_{qs} = \sum_{k=1}^{\infty} Q_k W_{qs}^{(k)}. \tag{C.24}$$

C.4.2 Considering All Units.

A unit that finds k units already in the system will have to wait in queue for a mean time equal to

$$W_{qa}^{(k)} = \frac{1}{\mu + (k+1)\nu} + P(k|k+1)W_{qa}^{(k-1)} \tag{C.25}$$

where $P(k|k+1)$ is as defined in (C.15) and $W_{qa}^{(0)} = 0$. Solving this recursive equation, we obtain

$$W_{qa}^{(k)} = \frac{k}{\mu + (k+1)\nu} \tag{C.26}$$

Thus, the mean queue waiting time is

$$W_{qa} = \sum_{k=1}^{\infty} P_k W_{qa}^{(k)}. \tag{C.27}$$

Appendix D
Cycle Time

We find here the average time between Infostation visits in two dimensions. We can calculate this cycle time as the average of the time elapsed since we enter a cell area directed to its coverage area, until this event happens again (refer to Figure 4.6). When entering a cell, the mobile can take any direction from $-\pi/2$ to $\pi/2$ (with respect to the normal) with probability density function given by $f^*_\Theta(\theta)$ in (4.14), which we repeat here for convenience,

$$f^*_\Theta(\theta) = \begin{cases} \frac{1}{2}\cos\theta & -\frac{\pi}{2} < \theta < \frac{\pi}{2} \\ 0 & \text{otherwise.} \end{cases} \tag{D.1}$$

If the mobile direction happens to fall between $(-\phi, \phi)$, with $\phi = \arcsin(r/R)$, then the mobile will cross the coverage area.

After crossing a cell through the coverage area, the mobile will visit another cell. In the new cell, the mobile will not cross the coverage area with probability

$$p = 1 - \int_{-\phi}^{\phi} \frac{1}{2}\cos\theta \, d\theta = 1 - \frac{r}{R}. \tag{D.2}$$

We define the random variables T_I and T_O as the time to cross a cell through the coverage area and the time to cross a cell without passing through the coverage area. The cycle starts by crossing a cell through the coverage area, which means time T_I elapses. Next, with probability $1-p$ we are done (a new cycle starts), and with probability p the mobile crosses the cell without passing through the coverage area (adding T_{O_1} to the cycle time). In the second case, and after crossing the cell, we either are done, or again with probability p the mobile avoids the following coverage area (adding T_{O_2}). This process gives the following expression for the average cycle time

$$\begin{aligned}\tau_c &= E\left[T_I\right] + p(E\left[T_{O_1}\right] + p(E\left[T_{O_2}\right] + p(E\left[T_{O_3}\right] + \ldots \\ &= E[T_I] + \frac{p}{1-p} E[T_O]. \end{aligned} \tag{D.3}$$

Now we use a derivation similar to the one in [43] to find $E[T_I]$ and $E[T_O]$. We define W the random variable for the space traveled within a cell by a mobile that crosses the coverage area. Since $w = 2R\cos\theta$, the pdf of W can be found from $f^*_\Theta(\theta)$, albeit restricting θ to the interval $[-\phi, \phi]$ (such that the mobile crosses the coverage area). The new distribution for θ is then

$$f^\phi_\Theta(\theta) = \begin{cases} \frac{R}{2r} & -\phi < \theta < \phi \\ 0 & \text{otherwise,} \end{cases} \tag{D.4}$$

and from this distribution we get

$$f_W(w) = \frac{w}{2r\sqrt{4R^2 - w^2}}, \quad 2\sqrt{R^2 - r^2} < w < 2R. \tag{D.5}$$

Assuming that the mobile speed in a cell remains constant, the sojourn time is $T_I = W/V$. Using the speed distribution of boundary crossing mobiles $f^*_V(v)$ from equation (4.7), we find the pdf of T_I as

$$\begin{aligned} f_{T_I}(t) &= \int_0^\infty v f_W(tv) f^*_V(v)\, dv \\ &= \frac{1}{2rE[V]} \int_{\frac{2R\cos\theta}{t}}^{\frac{2R}{t}} \frac{v^3 t\, f(v)\, dv}{\sqrt{4R^2 - (tv)^2}}. \end{aligned} \tag{D.6}$$

The expected value of T_I is then

$$\begin{aligned} E[T_I] &= \int_0^\infty \frac{t}{2rE[V]} \int_{\frac{2R\cos\theta}{t}}^{\frac{2R}{t}} \frac{v^3 t\, f(v)\, dv}{\sqrt{4R^2 - (tv)^2}} dt \\ &= \frac{1}{2rE[V]} \int_0^\infty \int_{\frac{2R\cos\theta}{v}}^{\frac{2R}{v}} \frac{v^3 t^2\, f(v)\, dt}{\sqrt{4R^2 - (tv)^2}} dv \\ &= \frac{R^2}{rE[V]} \left\{ \frac{r}{R} \sqrt{1 - \left(\frac{r}{R}\right)^2} + \arcsin\frac{r}{R} \right\}. \end{aligned} \tag{D.7}$$

We proceed analogously with T_O. We call Y the random variable for the space traveled within a cell by a mobile that does not cross the coverage area. Since $y = 2R\cos\theta$, the pdf of Y can be found from $f^*_\Theta(\theta)$, albeit restricting θ to the intervals $[-\pi/2, -\phi)$ and $(\phi, \pi/2]$. The new distribution for θ is then

$$f_\Theta^{\pi/2}(\theta) = \begin{cases} \dfrac{R\cos\theta}{2(R-r)} & \phi < |\theta| < \frac{\pi}{2} \\ 0 & \text{otherwise.} \end{cases} \tag{D.8}$$

From this distribution we get

$$f_Y(y) = \frac{y}{2(R-r)\sqrt{4R^2 - y^2}}, \quad 0 < y < 2\sqrt{R^2 - r^2}. \tag{D.9}$$

Assuming that the mobile speed in a cell remains constant, the sojourn time is $T_O = Y/V$. Thus we find the pdf of T_O as

$$\begin{aligned} f_{T_O}(t) &= \int_0^\infty v f_Y(tv) f_V^*(v)\, dv \\ &= \frac{1}{2(R-r)E[V]} \int_0^{\frac{2R\cos\theta}{t}} \frac{v^3 t\, f(v)\, dv}{\sqrt{4R^2 - (tv)^2}}. \end{aligned} \tag{D.10}$$

The expected value of T_O is then

$$\begin{aligned} E[T_O] &= \int_0^\infty \frac{t}{2(R-r)E[V]} \int_0^{\frac{2R\cos\theta}{t}} \frac{v^3 t\, f(v)\, dv}{\sqrt{4R^2 - (tv)^2}}\, dt \\ &= \frac{1}{2(R-r)E[V]} \int_0^\infty \int_0^{\frac{2R\cos\theta}{v}} \frac{v^3 t^2\, f(v)\, dt}{\sqrt{4R^2 - (tv)^2}}\, dv \\ &= \frac{R^2}{(R-r)E[V]} \left\{ \frac{\pi}{2} - \frac{r}{R}\sqrt{1 - \left(\frac{r}{R}\right)^2} - \arcsin\frac{r}{R} \right\}. \end{aligned} \tag{D.11}$$

Substituting equations (D.7) and (D.11) into equation (D.3), we get the mean cycle time

$$\tau_c = \frac{\pi R^2}{2rE[V]}. \tag{D.12}$$

We next derive the mean dwell time τ_d. Let us call Z the random variable for the space traveled within the coverage area by a mobile that crosses the coverage area. Since $z = 2\sqrt{r^2 - R^2 \sin^2\theta}$ with θ in the interval $[-\phi, \phi]$, we can find the pdf of Z using the pdf of θ in equation (D.4), and we get

$$f_Z(z) = \frac{z}{2r\sqrt{4r^2 - z^2}}, \quad 0 < z < 2r. \tag{D.13}$$

Assuming that the mobile speed in the coverage area remains constant, the dwell time is $T_d = Z/V$. Thus we find the pdf of T_d as

$$f_{T_d}(t) = \int_0^\infty v f_Z(tv) f_V^*(v)\, dv \tag{D.14}$$

$$= \frac{1}{2rE[V]} \int_0^{\frac{2r}{t}} \frac{v^3 t\, f(v)\, dv}{\sqrt{4r^2 - (tv)^2}}. \tag{D.15}$$

The expected value of T_d is then

$$\begin{aligned}\tau_d &= \int_0^\infty \frac{t}{2rE[V]} \int_0^{\frac{2r}{t}} \frac{v^3 t\, f(v)\, dv}{\sqrt{4r^2 - (tv)^2}}\, dt \\ &= \frac{1}{2rE[V]} \int_0^\infty \int_0^{\frac{2r}{v}} \frac{v^3 t^2\, f(v)\, dt}{\sqrt{4r^2 - (tv)^2}}\, dv \\ &= \frac{\pi r}{2E[V]}. \end{aligned} \tag{D.16}$$

References

[1] R. H. Frenkiel and T. Imielinski, "Infostations: The joy of 'many-time, many-where' communications", Tech. Rep. TR-119, Wireless Information Networks Laboratory (WINLAB), Rutgers, the State University of New Jersey, Apr. 1996.

[2] M. Serizawa, "Broadband personal communication networks and services", in *Telecom 95*, Palexpo, Geneva, Oct. 1995.

[3] K. Take, Y. Mita, T. Oh-Ishi, and H. Tominaga, "Mobile packet communications with a chained isolated radio zone network system", *Electronics and Communications in Japan, Part 1*, vol. 79, no. 1, 1996.

[4] M. Flament et alii, "An approach to 4th Generation wireless infrastructures — scenarios and key research issues", in *Proceedings of the IEEE 49th Vehicular Technology Conference VTC'99*, May 1999.

[5] T. Sakamoto, K. Tsunoda, E. Kamagata, and M. Serizawa, "Network and protocol architectures of hybrid multimedia mobile access communication system", in *Proceedings of the IEEE 49th Vehicular Technology Conference VTC'99*, May 1999.

[6] G. Wu, C-W. Chu, K. Wine, J. Evans, and R. Frenkiel, "WINMAC: a novel transmission protocol for INFOSTATIONS", in *Proceedings of the IEEE 49th Vehicular Technology Conference VTC'99*, May 1999.

[7] H. Mao, G. Wu, J. Evans, and M. Caggiano, "An adaptive radio link protocol for Infostations", in *Proceedings of the IEEE 49th Vehicular Technology Conference VTC'99*, May 1999.

[8] A.L. Iacono and C. Rose, "Minimizing file delivery delay in an Infostations system", Tech. Rep. TR-167, Wireless Information Networks Laboratory (WINLAB), Rutgers, the State University of New Jersey, Aug. 1998.

[9] J. Irvine et alii, "Efficient UMTS data provision using INFOSTATIONS", in *Proceedings of the IEEE 48th Vehicular Technology Conference VTC'98*, 1998.

[10] J. D. Kraus, *Antennas*, McGraw-Hill, New York, second edition, 1989.

[11] J. Evans, "A low cost asymmetric radio for Infostations", Tech. Rep. TR-130, Wireless Information Networks Laboratory (WINLAB), Rutgers, the State University of New Jersey, Sept. 1996.

[12] R. J. King, *Microwave Homodyne Systems*, Peter Peregrinus Ltd., England, 1978.

[13] W.C. Jakes Jr., *Microwave Mobile Communications*, Wiley, New York, 1974.

[14] T. Ye, A. Jacobsen, and R.H. Katz, "Mobile awareness in a wide area wireless network of Info-stations", in *Proceedings of ACM MobiCom'98, Dallas*, Oct. 1998.

[15] T. Imielinski, S. Vishwanathan, and B. R. Badrinath, "Data on air - organization and access", *IEEE Trans. on Knowledge and Data Engineering*, Aug. 1996.

[16] Takaha, "Car traffic simulation", *Journal of Simulation Society*, vol. 1, no. 2, pp. 12–18, 1982.

[17] R.F. Benekohal and J. Treiterer, "CARSIM. CAR-following model for SIMulation of traffic in normal and stop-and-go conditions", *Transportation research record*, , no. 1194, pp. 99–111, 1988.

[18] J.G. Proakis, *Digital Communications*, McGraw Hill, 3rd edition, 1995.

[19] A.J. Goldsmith, *Design and Performance of High-Speed Communication Systems over Time-Varying Radio Channels*, PhD thesis, University of California at Berkeley, 1994.

[20] T.S. Rappaport, *Wireless communications, Principles and practice*, Prentice Hall, 1996.

[21] G.D. Forney, Jr., L. Brown, M.V. Eyuboglu, and J.L. Moran III, "The V.34 high-speed modem standard", *IEEE Communications Magazine*, pp. 28–33, Dec. 96.

[22] D. Hong and S.S. Rappaport, "Traffic model and performance analysis for cellular mobile radio telephone systems with prioritized and nonprioritized handoff procedures", *IEEE Transactions on Vehicular Technology*, vol. VT-35, no. 3, pp. 77–92, Aug. 1986.

[23] H. Xie and D.J. Goodman, "Mobility models and the biased sampling problem", in *2nd Int. Conf. Universal Personal Communications, Ottawa, Canada*, 1993.

[24] D. Bertsekas and R. Gallager, *Data Networks*, Prentice Hall, 2nd edition, 1992.

[25] S.S. Rappaport, "Blocking, hand-off and traffic performance for cellular communication systems with mixed platforms", *IEE Proceedings 1*, vol. 140, no. 5, pp. 389–401, Oct. 1993.

[26] E. Chlebus and W. Ludwin, "Is handoff traffic really Poissonian", in *IEEE ICUPC'95 Conf. Record*, Nov. 1995, pp. 348–353.

[27] P.V. Orlik and S.S. Rappaport, “On the hand-off arrival process in cellular communications”, submitted to *Wireless Networks*, ACM/Baltzer Science, 1999.

[28] E.G. Coffman Jr., A.A. Puhalski, M.I. Reiman, and P.E. Wright, “Processor-shared buffers with reneging”, *Performance Evaluation*, vol. 19, no. 1, pp. 25–46, 1994.

[29] B. Jabbari, Y. Zhou, and F. Hillier, “Random walk modeling of mobility in wireless networks”, in *Proceedings of the IEEE 48th Vehicular Technology Conference*, 1998, vol. 1, pp. 639–643.

[30] J.G. Kemeny and J.L. Snell, *Finite Markov Chains*, chapter III, D. Van Nostrand Company, 1960.

[31] K.G. Chen, “Integrated dynamic radio resource management of wireless communication systems”, Master’s thesis, Rutgers, the State University of New Jersey, May 1996.

[32] W.C.Y. Lee, *Mobile Communications Design Fundamentals*, chapter 4, pp. 186–191, John Wiley & Sons, 2nd edition, 1993.

[33] J.M. Hernándo Rábanos, *Comunicaciones Móviles*, Centro de Estudios Ramón Areces, 1997.

[34] S.C. Schwartz and Y.S. Yeh, “On the distribution function and moments of power sums with log-normal components”, *Bell System Technical Journal*, vol. 61, no. 7, pp. 1441–1462, Sept. 1982.

[35] N. Abramson, “The throughput of packet broadcasting channels”, *IEEE Transactions on Communications*, vol. COM-25, no. 1, pp. 117–128, Jan. 1977.

[36] M.J. Ferguson, “A study of unslotted Aloha with arbitrary message lengths”, in *Proceedings 4th Data Communications Symposium*, Oct. 1975, pp. 5.20–5.25.

[37] F.A. Tobagi and V.B. Hunt, “Performance analysis of carrier sense multiple access with collision detection”, *Computer Networks*, vol. 4, no. 5, pp. 245–259, Oct/Nov 1980.

[38] R. Mazumdar, L.G. Mason, and C. Douligeris, “Fairness in network optimal flow control: Optimality of product forms”, *IEEE Transactions on communications*, vol. 39, no. 5, pp. 775–782, May 1991.

[39] V. Shah, N. Mandayam, and D.J. Goodman, “Power control for wireless data based on utility and pricing”, Tech. Rep. 159, Wireless Information Networks Laboratory (WINLAB), Rutgers, the State University of New Jersey, Mar. 1998.

[40] D.M. Burley, *Studies in optimization*, chapter 6, New York, Wiley, 1974.

[41] L. Kleinrock, *Queueing Systems*, vol. II, Wiley-Interscience, 1975.

[42] D. Hong and S.S. Rappaport, "Comments on "Traffic model and performance analysis for cellular mobile radio telephone systems with prioritized and non-prioritized handoff procedures"", to appear *IEEE Transactions on Vehicular Technology*, submitted August 1999.

[43] K.L. Yeung and S. Nanda, "Channel management in microcell/macrocell cellular radio systems", *IEEE Transactions on Vehicular Technology*, vol. 45, no. 4, pp. 601–612, Nov. 1996.

Vita

Joan Borràs-Chia

1993 *Enginyer de Telecomunicació* degree (M.Sc.) from Universitat Politècnica de Catalunya, Barcelona, Spain

1994-95 Completion of the course requirements for the *Discrete Math and Telematics* doctorate program at Universitat Politècnica de Catalunya

1995-97 "la Caixa" fellowship, to study the Ph.D. program in Electrical and Computer Engineering at Rutgers, the State University of New Jersey

1997 D.J. Goodman, J. Borràs, N.B. Mandayam, and R.D. Yates, "INFOSTATIONS: A New System Model for Data and Messaging Services", *Proc. of the IEEE 47th Vehicular Technology Conference*, vol. 2, pp. 969-973

1997 Graduate Assistantship, Wireless Information Networks Laboratory, Department of Electrical and Computer Engineering, Rutgers, the State University of New Jersey

1998-99 Lecturer, Department of Applied Math and Telematics, Universitat Politècnica de Catalunya, Barcelona, Spain

1999 J. Borràs and R.D. Yates, "Infostation Overlays in Cellular Systems", *Proc. of WCNC'99*, New Orleans

1999 J. Borràs and R.D. Yates, "Cellular Excess Capacity for Infostations", *Proc. of EUNICE'99*, Barcelona, Spain

1999 J. Borràs and R.D. Yates, "Highway Infostations", *Proc of WPMC'99*, Amsterdam, the Netherlands

2000 Ph.D. in Electrical and Computer Engineering, Rutgers, the State University of New Jersey